Control of Stochastically Interacting Systems on Networks

by

Amith Somanath

Submitted to the Department of Aeronautics and Astronautics
in partial fulfillment of the requirements for the degree of
Doctor of Philosophy
at the
MASSACHUSETTS INSTITUTE OF TECHNOLOGY
June 2017

Signature redacted

Author .....
Department of Aeronautics and Astronautics
June 9, 2017

Signature redacted

Certified by .....
Sertac Karaman
Associate Professor of Aeronautics and Astronautics
Thesis Supervisor

Signature redacted

Certified by .....
Kamal Youcef-Toumi
Professor of Mechanical Engineering
Thesis Supervisor

Signature redacted

Certified by .....
Emilio Frazzoli
Professor of Aeronautics and Astronautics

Signature redacted

Certified by .....
Jonathan P. How
R. C. Maclaurin Professor of Aeronautics and Astronautics

Signature redacted

Accepted by .....
Youssef M. Marzouk
Associate Professor of Aeronautics and Astronautics
Chair, Graduate Program Committee

Control of Stochastically Interacting Systems on Networks

by

Amith Somanath

Submitted to the Department of Aeronautics and Astronautics
on June 9, 2017, in partial fulfillment of the
requirements for the degree of
Doctor of Philosophy

Abstract

The goal of this thesis is to develop control theoretic analysis and algorithms for characterizing and controlling stochastically interacting systems on networks. Such systems have three essential features - (i) they are stochastic processes, (ii) they are made up several individual components connected through a network, and (iii) the connected components influence one another through local interactions. This thesis presents analysis and control of three representative examples of such systems from the fields of spreading processes, smart manufacturing, and transport phenomena.

In the first part of the thesis, control of spreading processes on lattices is considered. Analysis and control of spreading processes is difficult because the dimensionality of state space is often large. A common approach to this issue is to use mean field approximations which completely average out the stochasticity inherent to these systems. Instead this thesis, using recently developed tools from nonequilibrium statistical physics, accurately characterizes open loop behavior of spreading processes in its stable, neutral and unstable regimes. Such a characterization is not possible using approximate models. Furthermore, for an unstable spreading process, a randomized control policy is proposed that is optimal in both resource allocation and control effort.

In the second part of the thesis, control of smart manufacturing processes is considered. Due to increased product customization and rapidly changing demands, the recent trend in manufacturing is to shift towards modular architectures. Such a shift presents scheduling challenges in a rapidly and dynamically changing environment. This thesis presents a queuing theory framework for modeling job flow, and a stochastic scheduling algorithm. Such an approach is amenable for fast implementation while achieving balanced load among operating agents.

In the last part of the thesis, control of transport phenomena is considered. Transport phenomena are systems that are in *nonequilibrium*. Even though study and analysis of systems exhibiting nonequilibrium phenomena have been considered in the past, there is no effective way to control or modify the behavior of these systems. This thesis presents control theoretic formulations for systems in nonequilibrium.

Starting from a paradigmatic model for traffic flow known as totally asymmetric simple exclusion process (TASEP), thesis presents routing policies to achieve maximum flow rate of traffic for all set of input traffic conditions. Extensions are also made to TASEP models on intersections and generic road networks.

Thesis Supervisor: Sertac Karaman
Title: Associate Professor of Aeronautics and Astronautics

Thesis Supervisor: Kamal Youcef–Toumi
Title: Professor of Mechanical Engineering

Acknowledgments

It is said that it takes a village to nurture a child. This thesis has been a long and arduous journey and it has benefited from a village of people. First and foremost, I would like to thank my advisors, Prof Kamal Youcef-Toumi and Prof Sertac Karaman for their support, advice and encouragement. I am grateful to them for believing in me and supporting me at difficult times. Kamal's emphasis on practical engineering and thinking about the bigger picture has helped me to a great extent. I am thankful to Sertac for his emphasis on mathematical rigorousness and attention to detail.

I would also like to thank my committee members, Prof Jon How and Prof Emilio Frazzoli for their critical comments and feedback. Prof How, who was also my academic advisor, has at times provided me with very useful academic advice. I thank Prof Frazzoli for being available for meetings even though he was away from MIT. I thank my thesis readers, Prof Hamsa Balakrishnan and Dr Ulas Ayaz for their time. I also thank Beth Marois and Catherine Hogan for their administrative help.

I am grateful to have had the company of many good friends and well wishers throughout the course of my program. I have also benefited tremendously from the members of both the Mechatronics Research Laboratory (MRL), and the Laboratory of Information and Decision Systems (LIDS) at MIT. I thank them for their camaraderie, support and help. They have provided me with an intellectually satisfying atmosphere and have lend me an ear when I needed them. I would like to thank (in no particular order) Bo Jiang, You Wu, Dimitris Chatzigeorgiou, Iman Soltani, Yoshiya Shibata, Liangjing Yang, Rajat Talak, Vinay Raman, Sourabh Saha, Pratik Chaudhari, Harshad Khadilkar, Jongho Lee, Narmada Herath, Sze Zheng Yong, Swarna Pandian, and Smitha Rao. I would also like to thank Venkatesh and Krishnamurthy families. Most of the work in this thesis is unfunded, but I gratefully acknowledge the financial support provided by Omron Corporation during the final stages of this thesis, without which it would have been very difficult to complete it.

I would like to express my sincere gratitude to my parents for their continuous support and encouragement, without which none of this would have been possible. This thesis is dedicated to them.

Contents

List of Figures

List of Tables

Chapter 1

Introduction

1.1 Objectives

In this thesis, we study dynamical models of complex systems involving a large number of interconnected components. There are numerous examples from the fields of natural sciences and engineering, such as spread of epidemic diseases or forest fires [1–3], operation of smart factories [4, 5], opinion dynamics [6, 7], flow of traffic on transportation networks [8–11], crystal growth on surfaces [12, 13], financial markets [14], and inter-cellular transport dynamics [15], that fall into this category of systems. Though seemingly disparate, these examples share several properties that allow us to study them under a common light, namely, (i) they are *stochastic processes*, *i.e.* the governing dynamics of these systems have an inherent randomness associated with them, (ii) they have a *networked connectivity*, *i.e.* the underlying connectivity architecture has a structure, and (iii) they have *local interactions*, which means that the agents/nodes/entities in these systems interact with each other locally through a set of predefined rules.

Stochastic process models can be utilized when the exact inner-workings of the process are unknown, but statistics are available. For example, the spread of an epidemic disease is random depending on the immunity of the individuals in a given population. The demands in a smart factory fluctuate dynamically as well as the health of machines on shop floor; machines can breakdown randomly. Similarly, the

topology of the forest in a wild fire determines the growth rate and extent of fire damage. People's opinions and ideologies are formed, influenced, and even changed by the opinions of their social circles. From a mathematical point of view, such systems can be formally modeled as Markov processes consisting of countably many jump processes that interact by modifying each others transition rates. These stochastic processes interact with one another based on the connectivity structure that is described by a graph. In addition, with every vertex of the graph, we associate a set of time varying random variables that evolve according to a set of stochastic local rules.

In most of the example applications considered above, control actions can be exerted to influence the evolution of these stochastically interacting systems. For instance, distributing (limited amount of) vaccines in a strategic manner may help stop an epidemic, aggressive advertising may influence opinion dynamics, routing policies can avoid congestion on transportation networks, and strategic capital injection may alleviate the systemic risk of a financial meltdown.

The central objective of this thesis is to develop a control theoretic framework for analyzing, characterizing, and stabilizing these complex systems. As such, the key research questions that are addressed in this thesis are fourfold - (i) how can we develop mathematically tractable models for such systems? (ii) what are the notions of stability for these models? (iii) how do we characterize typical (open loop) behavior for the models?, and (iv) how can we design control algorithms for the models that ensure stability while simultaneously optimizing desired performance objectives?

Using representative examples each from the fields of (i) spreading processes, (ii) smart manufacturing processes, and (iii) transport phenomena, this thesis shows how such a control theoretic framework can be developed. The models considered in the thesis should *not* be thought of as detailed models of complex phenomena, but as representative models that capture the essential behavior inherent in these complex systems. These models help to gain insights into understanding of these systems and aid in the development of control policies. With that said, the models do efficaciously capture the (global) macroscopic behavior that emerges from (local) microscopic interactions between nodes/agents; a feature that is a characteristic of such stochastically

interacting systems.

1.2 Related Literature and Technical Gaps

1.2.1 Control of Spreading Processes

Spreading processes can be defined as stochastic processes that spread or grow according to a set of local rules. As stated earlier, such processes are used for modeling various dynamic processes on social, economic, and political networks, such as the spread of epidemics, forest fires, opinion dynamics, and financial breakdowns [1, 3, 6, 7, 14, 16, 17]. Formally, a spreading process on a graph can be represented by a set of time-varying random variables, each of which is associated with a vertex of the graph and evolve according to stochastic local rules. As applications of spreading process encompass various domains, in the description below, we interchangeably use the terms person, agents, or nodes to address individual entities in the spreading process.

Depending on the context, the random variable associated with a given node (people, servers, banks etc.) takes one possible value from a predefined finite set of possible conditions. For instance in epidemiology [18–21], the two most popular models for disease spreading are the so called Susceptible-Infected-Susceptible (SIS) model (also known as the contact process) and the Susceptible-Infected-Recovered (SIR) model. In an SIS model, a person could be in two conditions namely, (i) is healthy but susceptible to infection, or (ii) is infected. Similarly in an SIR model, a person could either be (i) healthy but susceptible to infection, (ii) infected, or (iii) recovered and immune to infection. On the other hand, in an opinion model [6], an agent can have a positive, negative or neutral opinion about a popular ideology, and in a forest fire model, a tree in the forest could either be green, burning and on fire, or burnt. See [22–24] for detailed surveys.

In addition, the random variables change their values based on stochastic interactions within their connected neighborhood. For example, in disease spreading, a

healthy person has a higher chance of contracting the disease when s/he comes in contact with several infected people, as opposed to a single infected person. Technically these interactions are modeled as Markov jump processes, where the random variable associated with a node has a chance to change its value, depending on the values of the random variables of its neighbors, independently of all others nodes.

The complex system that emerges out of these interconnections between several such nodes is hard to analyze due to several reasons. The state space (or the possible configurations) that the system could be in has a dimensionality that is prohibitively large. In the example of the SIR model, if the random variable associated with a node i is denoted by X_i, then X_i can take upon one particular value in the finite set $\{0, 1, 2\}$, where the integers denote the conditions $\{S = 0, I = 1, R = 2\}$ respectively. For a total of N nodes in the underlying graph, a particular state of the process is the set $\{X_1, X_2, \cdots, X_N\}$, and thus the state space of the process (all possible realizations) has a cardinality 3^N, which is exponential in the total number of nodes N. For instance, when $N = 200$, this number is 3^{200}, which is more than the number of atoms in the universe. Furthermore, the time evolution of the state space that depends on interactions between states is easier to state as simple rules, but hard to express mathematically due to combinatorial complexity. For instance, in the SIR model, let the transitions between conditions $S \to I$ for any state i be a Poisson process with rate λ, and the transition between conditions $I \to R$ be Poisson with rate μ, then the evolution can be written as,

$$\text{If } X_i(t_0) = 0, \text{ then } X_i(t > t_0) = 1 \sim \text{ Poisson at rate } \lambda \cdot \sum_{j \in \mathcal{N}_\mathcal{I}} X_j$$

$$\text{If } X_i(t_0) = 1, \text{ then } X_i(t > t_0) = 2 \sim \text{ Poisson at rate } \mu$$

where $\mathcal{N}_\mathcal{I}$ denote the infected neighboring nodes ($X_j = 1$) of node i. As the neighborhood $\mathcal{N}_\mathcal{I}$ is a function of the network structure, the more complicated the network, harder it is to analyze the behavior of the process. In addition, spreading process models are usually heterogeneous. As opposed to homogeneous models, heterogeneous models [23] allow nodes and edges to have different spreading and recovery

rates. For example, for forest fires, heterogeneous descriptions provide a framework to incorporate topology of the forest, fuel (grass, wood, brushes), and wind effects into the forest fire model. Needless to say, such models of spreading process are more complicated to analyze accurately.

Various approaches have been considered in the literature to make this problem mathematically tractable. Prior work in spreading processes can be roughly categorized into classes depending on the degree of rigorousness and granularity considered in the models: (i) how do we model the state space of the spreading process? (ii) how do we consider stochastic interactions? (iii) how do we deal with (exponentially) growing dimensionality of state space, and (iv) how complex is the underlying network architecture?

The most common approach to deal with the large dimensionality of the state space of the spreading process is by utilizing a *mean field approximation.* Mean field approximation is a general term associated with many forms of approximations, but fundamentally the approximation ignores correlations between pairs of random variables. By using such an approximation, the evolution of the process is described in terms of a derived (and usually averaged) quantity that is a function of random variables associated with the nodes.

The simplest mean field approach utilizes a density based description of the spreading process (also known as population models) [20, 25–31]. Density based models consider the evolution of the fraction of the total population that are in a particular condition. For instance, a density description of SIR model has just three states; the fraction of population that is healthy, the fraction that is infected and the fraction that has recovered, thereby reducing the dimensionality of the state space to that of the number of conditions in which a node can be in. Population models also assume a "well mixed" population, which means that every node can interact with every other node and thus ignores the location information of the nodes. The rate at which infected population influences the healthy population is assumed to be proportional to the product of the healthy and infected populations. This approximation is known as the *law of mass action* [16,19] which is again a generalization of mean field approaches.

These assumptions allow the evolution of the spreading process to be described by a nonlinear ordinary differential equation whose solution can be obtained easily.

Another popular approach is the networked mean field approximation. In such an approximation, the value of the random variable at a given node is approximated to be weighted average of the values of random variables of its neighboring nodes [32–35]. This description allows the update equations to be written as ordinary differential equations in terms averaged probability at every node. The main advantages of networked mean field approximations are that it retains the underlying connectivity structure of the network and provides a means for controlling spreading process through spectral optimization. In addition it can also be applied to heterogeneous spreading process models (for instance [36–39]).

An approximation whose complexity is in between density based models and networked mean field models, are the so called meta-population models [40–42]. In a meta population model, individual nodes are clustered into a smaller subset of nodes, thereby reducing the size of the state space to a more suitable and tractable description. A classical well-mixed population model is assumed for the clusters, where as a networked mean field model is assumed in between the clusters. Such models are useful for instance to characterize spread of an epidemic disease between connected network of cities. Depending on the granularity of the approximation, mean field approximations yield different models. If approximated at the granularity of population of all nodes, it results in density models. If approximated at the granularity of individual nodes, it results in networked mean field approximation models. An approximation in between the two approaches results in meta-population models.

On the other hand, such descriptions obtained from approximations of spreading process have several drawbacks. By converting the evolution of the process into deterministic differential equations, the approximations average out the stochasticity that is inherent to these processes. The density based descriptions of the processes usually assume a well mixed interaction between the nodes, but in doing so ignore the underlying graph or connectivity structure. If the degree of the connectivity graph is low, it is well known that approximations based on mean field theories

are inaccurate. Also as approximate models describe the evolution of the process based on some derived quantity and do not deal with the random variables directly, there is a disconnect between what results based on approximations imply for the original stochastic spreading processes. For example, mean field approximations to disease spreading models describe the evolution of the disease in terms of the average infection probability of a particular person. This is very different from the original stochastic disease spreading process, in which either a person is infected with disease or is healthy. Furthermore, approximate models do not accurately predict the stability thresholds or the survival time of an infection.

Though the modeling and analysis of spreading processes have been a long standing area of research, there has been limited work on ways to effectively control (or contain) the growth of such processes. The goal in controlling such a process is to contain/stop/cure the process as quickly as possible, *i.e.* to minimize extinction time of the spreading process. However, such a problem is ill posed unless a cost (or weight) is imposed on the control effort (budget, fire retardant, vaccine, etc.), otherwise we can influence every node of the process and stop the spreading immediately which is usually not practical. Using the nonlinear differential equations obtained by mean field approximation and law of mass action as a starting point, several researchers have analyzed growth of stochastic processes on complex networks and have proposed various control algorithms to contain the growth of process based on spectral optimization [34, 43, 44], optimal control [45–47], geometric programming [42, 48–50], among other methods [45–47, 51–56].

For networked mean field approximations, it can be shown that the extinction time of the spreading process is characterized by the largest eigenvalue of the adjacency matrix of the graph [43]. As such, researchers have used spectral optimization methods to control the spreading process. Given a fixed budget C, the control problem considered in spectral optimization methods is to identify optimal set of nodes (at most C) to be removed from the graph A, such that the largest eigenvalue, $e_{max}(A)$ is minimized. It has been shown that this problem can be converted into a geometric optimization problem [44, 49] and can be solved efficiently. This method can also be

extended to handle heterogeneous models.

Unfortunately control algorithms used on approximated models have many disadvantages. At the core, the control strategy is a *static* one. It does not account for the current "state" (or configuration) of the spreading process, and minimizes the eigenvalue of adjacency matrix which is a time invariant property of the network. Even though networked mean field approximations account for graph structure, they do not predict exact stability thresholds for a graph. In fact, there has been no rigorous characterization of spreading process from a control theoretic framework, so as to what stability means for such processes, when does it exit, how does the system behave in stable, neutral and unstable regime and so on. Epidemic mean field models predict that if $e_{max}(A) < \frac{\mu}{\lambda}$ the expected time to extinction is sublinear, and is exponential otherwise [57, 58]. However, what effect this control strategy of node removal has on the original stochastic spreading process, and if this is indeed a necessary condition is unclear, although it appears that the result serves as a lower bound. For instance, approximate models do not accurately predict the long time survival of an infection, because the threshold goes to zero as number of nodes N becomes large. This is due to the fact that $e_{max}(A)$ grows unbounded as $N \to \infty$ [59].

In this thesis, we consider exact formulations of spreading processes and analyze stochastic interactions rigorously. For mathematical tractability, we consider homogeneous models of spreading processes on lattices. A lattice network is one where the vertices are arranged into a grid. This kind of structure arises in a number of applications in physics. As a result, mathematical physicists have long been working on stochastic processes on lattices [13,60–62]. In particular, such processes have been used to understand non-equilibrium statistical mechanics phenomena [63, 64]. There is now a rich and growing mathematical physics literature in this direction [12]. Many of these results identify *phase transitions*: slight variations in parameters of local interactions may have tremendous impact on global properties. We first characterize the notion of stability for spreading processes. Our definitions of stability is based on the phase transition phenomena, and our results utilize the tools developed in statistical mechanics. We then derive theoretical bounds on stability thresholds.

Using newly available tools from non-equilibrium statistical physics, we are able to characterize open loop behavior of the spreading processes in its stable, neutral, and unstable regimes accurately. This type of rigorous characterization is not possible by employing mean field models. Furthermore, given an unstable spreading process on a lattice, we develop an optimal control policy that stabilizes the process, almost surely. In order to develop a control policy, we first show that an insightful description of the spreading process can be obtained by analyzing the process in terms of the edges rather than nodes of the underlying graph. We then define a randomized preferential node treatment policy. To derive the properties of the aforementioned policy, we construct an equivalent tree description of the spreading process. Using tools from branching process and percolation on irregular trees [65,66], we show that this policy in indeed stabilizing and optimal, both in control effort and resource utilization.

1.2.2 Control of Smart Manufacturing Processes

Industry 4.0 is the new trend in manufacturing and data exchange that is being considered as the fourth industrial revolution [5, 67, 68]. Due to the need for strong product customization [69], the newer trend in industry is to shift towards a demand based production as opposed to an inventory based one. Such a manufacturing process envisions smart factories in which the shop floor would be modular, with individual machines or work stations operating independently from one another. The modular manufacturing units would be connected by automated guided vehicles (AGVs) which would transfer materials from one unit to another. These smart factories would enable humans and machines to communicate and work cooperatively in the same environment. In addition, the smart factory would have a virtual copy of physical world for monitoring, health diagnosis, and repair.

It has been envisioned that Industry 4.0 would have four features [4, 70] - (i) *Interoperability*: the ability of machines, devices, and sensors to communicate with each other and with people, (ii) *Information transparency*: ability of information systems to create a virtual copy of physical world using digital models of plant and sensor data, and to convert raw sensor data to higher value context information, (iii)

Technical assistance: cooperative working with humans including assistance in unsafe environments, and (iv) *Decentralization:* decentralized decision making at lower levels of operations and autonomous operation at all levels.

However, achieving the objectives envisioned by Industry 4.0 requires addressing few issues with the manufacturing process. The shop floor of a smart factory is a dynamic and changing environment, and is subject to machine failures and breakdowns. In addition, the machines (or work stations) could have multiple capabilities. For example, a CNC machine could perform one operation (such as cutting) from a variety of possible set of operations (for instance, cutting, welding, drilling, milling etc.) at a given time. As the manufacturing process is demand based, it is subject to changing demands in variety, customization and volume. In addition, different types of products might be in production. As such, scheduling of individual machines (or work stations) and that of transfer vehicles like AGVs is an issue. If a machine breaks down, the scheduler should be able to achieve a balanced operational load among the operating machines while maximizing the overall throughput of the factory.

Traditional scheduling problems in manufacturing are combinatorially hard [71] which make real time implementation difficult in dynamic environments. To deal with flexible scheduling in dynamic environments, several agent based manufacturing paradigms have been proposed in the literature [72–74]. Some of them include negotiation based architectures [75], reactive reinforcement learning [76], layered architectures [77], ontology based approaches [78, 79], capability based planning and model checking [80, 81], among others [82–84]. Unfortunately, no structured development methodology is used in industrial practice for the agent-based control systems specification, design, verification, implementation or reconfiguration of automation solution. The reason for this absence is the lack of proper reference models for control systems architectures that support formal analysis, verification, and real time code generation. As such, an important challenge is to develop formal and structured methodologies that will support the implementation of agent-based manufacturing control applications [73].

To overcome these issues with modeling, visualization and scheduling, a stochastic

scheduling approach is proposed in the thesis. Using queue theoretic formulations, entities on the factory floor - work stations with multiple capabilities and AGVs can be modeled effectively. We show that the connectivity structure of the machines can be elegantly captured in terms of the incidence matrix of the graph. In addition, stochastic scheduling techniques convert the original NP hard problem of scheduling machines and AGVs into an averaged cost problem, that be described by a linear program. This approximation is well suited for the smart factories as most operations are repetitive in nature. LP formulations achieve load balancing inherently and are also amenable for fast implementation in changing environments. The approach also provides a higher level virtual model of the factory floor and allows for monitoring the environment as required.

1.2.3 Control of Transport Processes

Transport processes describe physical phenomena in which there is an exchange of matter, momenta or energy in an observed system. Such processes could be used to model physical systems such as traffic flow, chemical systems, cell rolling, among many others. Fundamentally, transport phenomena are irreversible processes that are said to be operating in a state that is in *non-equilibrium* [64, 85, 86]. A system in non-equilibrium steady state is characterized by observables that do not change with time, yet exhibit an irreversible exchange of heat, particles or volume with its environment. For example, when a battery is connected to a resistor, a chemical potential drives the constant current that flows through the circuit. Though there is a steady current flowing out of the battery, the voltage drained from the battery is an irreversible process. Traffic flow on a highway is in similar vein, where a steady flow of traffic flows from one direction to another. As opposed to systems that are in thermodynamic equilibrium, non-equilibrium systems are operating far from their equilibrium conditions.

Based on the pioneering work by Maxwell, Boltzmann, Gibbs and many others, systems at thermodynamic equilibrium enjoy a well developed theory of statistical mechanics [87]. On the other hand, there is no such unified theory for non-equilibrium

statistical mechanics. In fact, developing a fundamental understanding of systems driven by non-equilibrium statistical mechanics is considered to be one of the grand challenges of our times, both by the U.S Department of Energy [88, 89] and the U.S National Academy of Sciences [90]. This emphasis has created a tremendous momentum, leading to a large literature aimed towards understanding this scientific phenomena [91, 92].

Even though these works have improved our understanding into the behavior of systems in non-equilibrium, there is no systematic approach to "control", govern or modify the behavior of these systems. Such approaches would improve the efficiency of existing systems, and might also aid in engineering new applications. For example, analysis and control of non-equilibrium phenomena in transportation networks might lead to better organization of urban transportation systems, thereby reducing delays and enhancing safety.

With the aforementioned goal in mind, in this thesis we take initial steps towards the overarching goal of developing control algorithms for plants governed by non-equilibrium statistical mechanics. A characteristic feature of systems in non-equilibrium is the existence of phases in its operating regime. A phase is a region in which a macroscopic (global) property of the system takes a common value for a large range of microscopic (local) parameters. Across these phases, the system shows a *phase transition*, in which slight variations in local parameters result in an abrupt change on global properties. Thus, the aim of exerting control actions on systems in non-equilibrium is to achieve one or more of the following behaviors - (i) maintain the system in a desired phase, (ii) move the system from one phase to another, (iii) change the boundaries of the phase diagram, and (iv) introduce new phases in the phase diagram.

In this thesis, we study models of traffic flow on transportation networks as a prototypical example of non-equilibrium behavior in transport processes. In the past, traffic flows on transportation networks have been modeled using several ways based on the granularity [8, 11, 93–95]. However, it is widely believed that physical mechanisms at microscopic level which give rise to synchronized traffic behavior are not

well understood [8]. Towards this end, a model known as the *totally asymmetric simple exclusion process* (TASEP) has been proposed in the literature [9, 10]. Similar to the role that the Ising model has played in equilibrium statistical physics, TASEP is believed to be a paradigmatic model for systems in non-equilibrium. A single lane of traffic can be modeled as a TASEP with open boundaries, with the entry and exit rates of traffic as model parameters. It has been shown through exact calculations that the model shows phase transitions in the *current* (or the rate of flow of traffic) according to the different values of model parameters [96–98]. The model exists in three regimes - a low density regime in which the lane is relatively empty, a high density regime in which the lane is heavily occupied, and a maximum current regime in which the current reaches its maximum possible value.

In this thesis, using TASEP as the model for single lane of traffic, we develop control policies to maximize the traffic flow rate. Our first result it to develop an exit rate control policy wherein the exit rate of the model is varied according to the average occupancy of the road. We show that such a policy achieves maximum current for all possible entry traffic rates. We also study control policies for automated gated intersections and other generic transportation networks.

1.3 Thesis Contributions and Outline

This goal of this thesis is to (i) develop mathematically tractable yet realistic models for stochastically interacting systems, (ii) perform control theoretic analysis of the models and characterize stability and open loop behavior of the these models, and (iii) develop control algorithms to stabilize unstable behavior and optimize performance objectives. Towards this end, the contributions of this thesis to three representative examples of stochastically interacting systems are listed below.

1.3.1 Control of Spreading Processes

The contributions in this section are towards accurate characterization of stochastic spreading processes without ignoring or approximating the stochasticity that is inher-

ent to such processes. Towards this end, we consider homogeneous models of spreading processes on lattices, define notions of stability, derive exact stability thresholds, characterize open loop behavior and develop control algorithms for stabilizing unstable spreading processes.

Stochastic modeling and control theoretic stability characterization: Chapter 2 of the thesis considers discrete and continuous time models for spreading processes on lattices. In the literature there are no clear notions of stability for spreading processes. Towards this end, notions of stability for spreading process are developed in this thesis. Mean field approaches in the literature characterize stability based on eigenvalue of Adjacency matrix of the connectivity graph. However, it is known that approximate models don't predict stability thresholds well. Furthermore, when the number of nodes become large (or in the case of infinite graphs), the eigenvalue of the matrix also grows unboundedly, poorly predicting the stability thresholds. This thesis develops the notion of stability of spreading processes using critical probability p_c of a given graph. This formulation allows one to derive accurate bounds on stability thresholds, as opposed to mean field approaches. The tightness of the bounds derived are validated using Monte-Carlo simulations. For example in the disease spreading, accurate predictions of stability thresholds are important as they tell us how much vaccine should be distributed to stop an epidemic. In addition, the critical probability p_c could be a new way of looking at networked systems in which spreading is an important criteria. Formulations in the thesis could be extended to many other graphs structures for which the value of p_c is known.

Analysis of open loop behavior of spreading processes: In second part of Chapter 2, the behavior of spreading process on lattices are characterized using rigorous results available from mathematical physics literature. Previous approaches characterize the behavior using linear models obtained by mean-field approaches. The linear models thus obtained, predict incorrectly an exponential behavior for the growth of the spreading processes. Clearly, this is not true in general for all graphs.

Using different tools from mathematical physics, this thesis characterizes the behavior of the spreading process in stable, neutral and unstable regimes. The characterizations are validated through extensive simulations. In the unstable regime, the spreading processes on lattices shows a linear growth, a fractal behavior near threshold, and exponential decay in the stable regime. Such characterizations are not possible using mean field models. Again using the example of disease spreading, such characterizations help us to answer queries like - at what rate does the disease spread? How does the *strength* of the disease influence its spread?, and when is the disease containable?

Randomized optimal control policy for unstable spreading processes: Chapter 3 of the thesis develops an optimal control policy that stabilizes a given unstable spreading process almost surely, *i.e.* with probability one. Previous approaches in literature use optimal control formulations on approximated model developed using mean field approximations. However the accuracy of such control strategies are questionable. As such, the this thesis proposes optimal control policy for stochastic spreading processes using the notions of critical probability developed before. In order to develop a control policy, an insightful description of the spreading processes can be obtained by considering the growth of the processes along the edges rather than nodes of the underlying graph. A randomized preferential node treatment policy is then described in the thesis. Using tools from mathematical physics such as branching process and percolation on irregular trees, it is shown that this policy in indeed stabilizing and optimal.

1.3.2 Control of Smart Manufacturing Processes

The contributions in this section are towards developing a design methodology for agent-based control systems architectures for smart manufacturing processes, that are suitable for formal analysis, simulation, and real time scheduling in dynamic environments.

Stochastic modeling and scheduling for manufacturing processes: Chapter 4 of the thesis develops a queue theoretic model for smart manufacturing processes. It is shown that the connectivity structure of the machines can be elegantly captured in terms of the incidence matrix of the graph. We consider an averaged cost optimization criteria for the model developed and show how the optimization can be solved using a linear program. Such an approach allows one to achieve real time scheduling in fast and changing environments. In addition, this approach achieves load balancing among operating machines under changing work flow. The proposed approach is validated using representative examples.

1.3.3 Control of Transport Processes

The contributions in this section are towards control of systems in non-equilibrium which haven't been considered before. Towards this end, we consider prototypical examples of non-equilibrium phenomena with applications in transportation.

Analysis and control policy for auto-gated single lane traffic: In Chapter 5, the thesis describes the totally asymmetric simple exclusion process model for transport phenomena, and identifies phase transitions. This thesis is one of the first attempts to control TASEP models. Our first result develops an exit rate control policy wherein the exit rate of the model is varied according to the average occupancy of the road. It is shown that such a policy achieves maximum current for all possible input rates.

Analysis and control policies for road intersections and networks: The analysis and control of systems in non-equilibrium is extended to other network architectures. In particular, TASEP models on automated gated intersections, and other generic transportation networks are considered.

Chapter 2

Control of Spreading Processes I

The goal of this chapter is to provide accurate characterization of typical behavior of spreading processes on lattices. From a control theoretic perspective, this characterization could be regarded as an open loop analysis of the spreading processes. Specifically, we are interested in answering the following questions: (i) what are the notions of stability for spreading processes? (ii) When is the process stable? and (iii) How does the process behave in its stable, neutral and unstable regimes? In the literature, spreading processes have usually been studied using a specific application (spread of epidemic diseases, computer malware, opinion dynamics, etc.) that serves as an aid towards the understanding of these processes, and helps us understand what "control" means in the context. As such, we too motivate the analysis and control of spreading processes through the problem of spread of wild fires in forests. Every year forest fires cause significant social and economic damage. It is estimated that in 2012 alone, more than 3 million acres of land were effected by forest fires [99] and these numbers are expected to grow in the near future due to the adverse effects of climate change and rapid urbanization [100]. Even though majority of fire fighting is still done on the ground, over the last decade, aerial vehicles have been adopted as an important fire-fighting resource [101–103]. Throughout this thesis, we use the example of forest fire synonymously with spreading processes.

In Section 2.1, we introduce discrete time and continuous time models of spreading processes on lattices. We call the mathematical models of spreading process of

wild fires in the forest as the *forest fire process*. Though such models of forest fires have been introduced in the past [2], we emphasize that choosing right models is crucial for mathematical tractability and analysis of the spreading process. Also, the control models introduced in this chapter are simplified models of firefighting robotic vehicles that control the spread of fire by spraying fire retardants. However, it should be noted that these models are widely applicable. For instance, similar models may apply towards understanding the spread of congestion through a Manhattan-like transportation network, where additional infrastructure can be controlled to alleviate congestion.

In the next section, we introduce control theoretic notions of stability for spreading processes, and then characterize stability of the forest fire process by providing a lower bound on stability. For characterizing the open loop behavior of fire process in stable, neutral and unstable regimes, different tools from mathematical physics are needed. Towards this end, Section 2.3 provides a succinct introduction to theory of bond percolation, first passage percolation, SLE curves and the KPZ growth model. By using coupling arguments, we show in subsequent section how spreading processes can be mapped to the known models in mathematical physics, thereby enabling us to characterize open loop behavior of the spreading processes. The typical behavior of the spreading processes have also been validated using Monte Carlo simulations. These simulations have been carried out on a lattice of size 500×500, and the numerical results have been obtained by averaging over 200 realizations of the fire process.

2.1 Modeling

2.1.1 Plant Model

We model the forest fire process as a set of trees represented by nodes on a d dimensional square lattice $\mathbb{Z}^d$ (where $\mathbb{Z}$ is the set of integers). The trees can be in three states - green (healthy or not burning), red (infected or on fire) or black (removed or burnt). In a *discrete time* model, if a green tree catches fire, it burns for

a time that is a geometrically distributed random variable with parameter $1-\beta$, $\mathbb{P}(k) = \beta^{k-1}(1-\beta), k = 1, 2, \cdots$. After this time, the tree is considered burnt (black). During each discrete time step a tree is burning, the tree spreads the fire with a probability α, to all its healthy neighbors independently of all other nodes. At $t = 0$, without loss of generality we assume that the fire starts at the origin (see Figure 2-1). In the *continuous time* description of the process, a green tree burns for a time that is an exponentially distributed random variable with parameter μ. During this time, the burning node tries to spread fire to each of its green neighbors independently after a time that is an exponentially distributed random variable with parameter λ. In both discrete and continuous time descriptions, the statistics of the burning process are independent from that of the fire spreading process.

2.1.2 Control Model

We now assume that two types of robotic agents are available for fighting fire - (i) one that reduce the propagation probability of a node, and (ii) one that reduce the burning time of a node. Specifically, if a particular node is treated by a robotic agent of first type, the fire propagation probability α (or λ in continuous time model) of the node is reduced by an amount $\Delta\alpha$ (or $\Delta\lambda$). Roughly speaking these type of agents have similar effect of that of using fire retardants on the burning trees. On the other hand, if a particular node is treated by the robotic agent of the second type, the parameter β is reduced by an amount $\Delta\beta$ (or μ is increased by an amount $\Delta\mu$ which reduces the mean burn time of the exponential random variable). Again, roughly speaking, these type of agents have similar effect of creating a fire wall that is accomplished by burning trees in the path of the forest fire.

For mathematical simplicity, we assume that one vehicle can treat one node at a given time. However, it should be noted that results for a model in which the number of nodes that can be treated by a robotic agent are more than one, are different only by a constant scaling. We also assume that the speeds of the robotic vehicles are much faster than that of the fire process, and thus the vehicles can act instantly on the nodes if available, with the delay being only due to the time taken for refilling

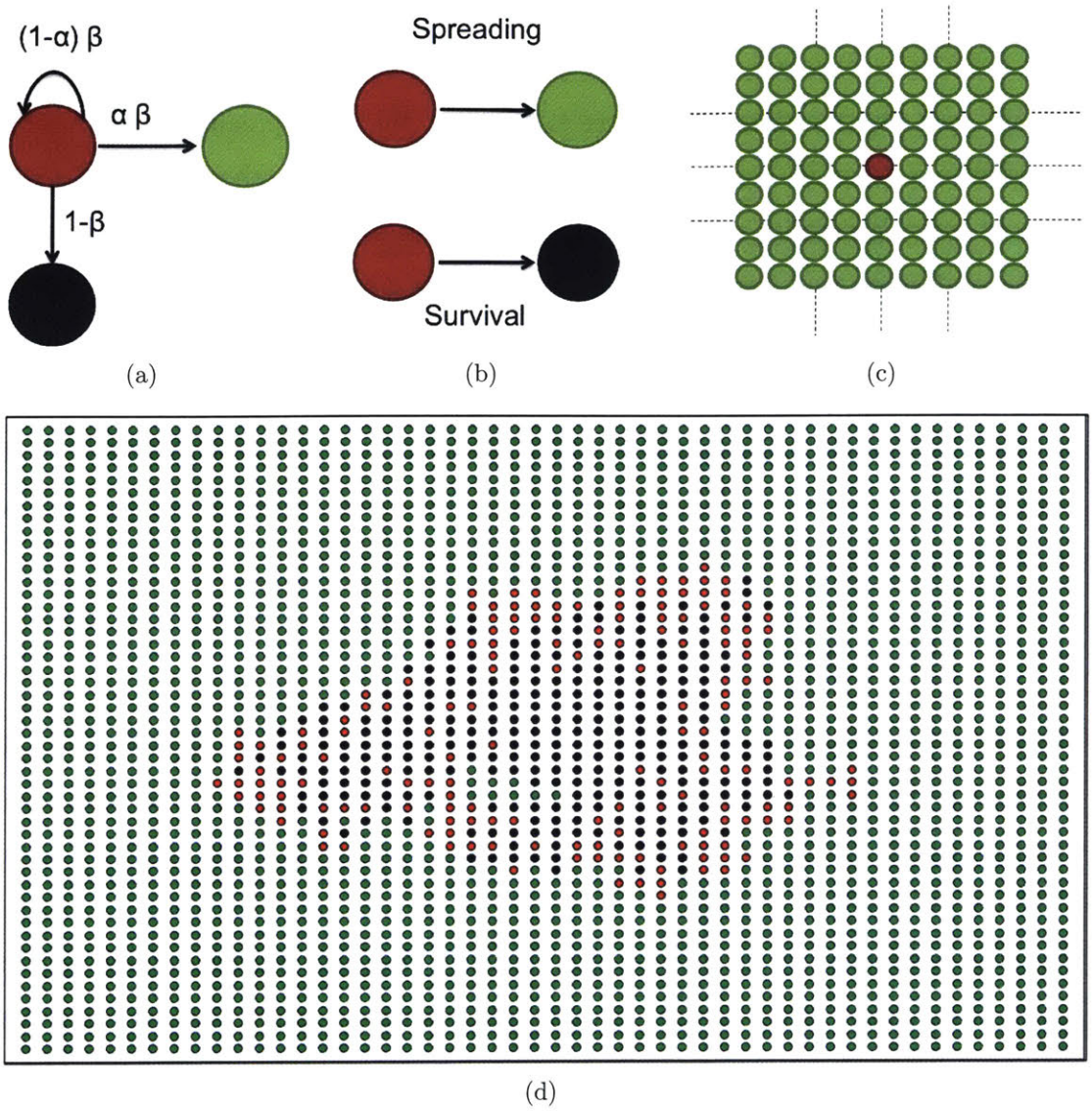

Figure 2-1: The mathematical model of the spreading process on lattices. (a) The Markov chain of possible transitions for the discrete time model of the process. (b) The two competing processes of spreading and survival phenomena. (c) At $t = 0$, the spreading process starts at origin and only the origin has been affected. (d) A typical realization of the spreading phenomena as obtained by a numerical simulation.

the retardant. However, we also analyze the case in which the robotic agents have a finite retardant carrying capacity and model the delay in filling up retardant in the following way. If an agent is utilized at $t = t_0$, it is reusable only after time $t = t_0 + \tau$, where τ is the time interval required to refill the retardant.

2.2 Stability

We begin by answering the following question - *how does the fire process behave for different values of system parameters?* Figure 2-6 shows results from numerical simulation for a fire process simulated for various values of system parameters α and β. The figure shows the fraction of the forest that has been affected for a fire starting at origin as the parameters are varied. It can be readily seen that there exists a certain threshold for the parameters beyond which there is large scale destruction of the forest. This leads us to the notion of stability for the fire process which is made precise by the following definitions.

Definition 2.1. *(Phase transition) Suppose p is a parameter of the fire process. Let $X_t = X_t(p)$ be the number of infected/burning nodes at time instant t. A fire process is said to be stable or sub-critical if,*

$$\limsup_{t\to\infty} X_t = 0 \quad \textit{almost surely.}$$

A fire process is said to be unstable or super-critical if,

$$\liminf_{t\to\infty} X_t = \infty \quad \textit{almost surely.}$$

Definition 2.2. *(Critical probability) There exists a critical probability p_c such that,*

$$\lim_{t\to\infty} X_t(p) = \begin{cases} 0 & \textit{almost surely,} \quad p \leq p_c \\ \infty & \textit{almost surely,} \quad p > p_c \end{cases}$$

Remark: We note that from a control theoretic perspective, the critical probability p_c plays the role of the imaginary axis (in particular the origin) in the analysis of dynamical systems. When $p < p_c$, the fire process is equivalent to a dynamical system with its eigenvalue in the left half plane, and the system is stable. On the other hand, when $p > p_c$, the system is unstable. When $p = p_c$, the fire process is equivalent to a dynamical system that is neutrally stable.

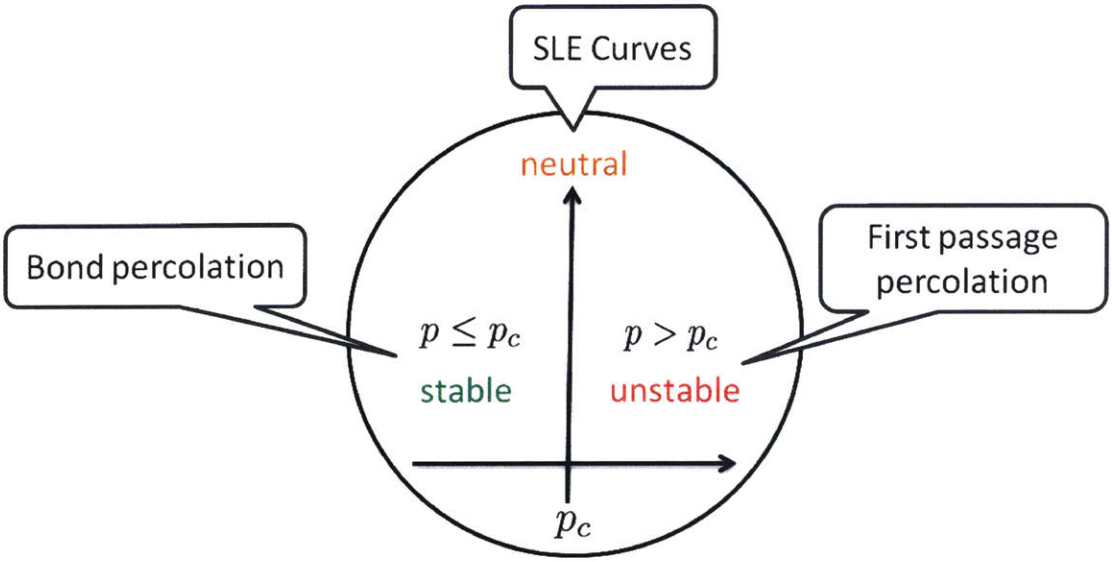

Figure 2-2: The critical probability p_c plays the role of origin in the definitions of stability of the spreading processes. Different tools from mathematical physics are used to characterize the spreading process in different stability regimes. The spreading process is characterized in its stable and neutral regime by comparing it with an equivalent Bond percolation model. The results from SLE curves are applicable when $p \approx p_c$. In the unstable regime, the first passage percolation model is used to characterize the spreading process by the use of a coupling argument.

2.3 Background

This section provides a succinct introduction to different tools from mathematical physics that would help us to characterize spreading processes on lattices.

2.3.1 Bond Percolation

Percolation theory describes the behavior of connected clusters in a random graph. The most studied model in percolation theory is the bond percolation model which was first introduced by Broadbent and Hammersley to model wetting of a dry stone immersed in liquid. Bond percolation model is usually described on infinite lattices; a lattice is a uniformly spaced set of points. Consider a square lattice, denoted by $\mathbb{Z}^d$, where the set of nodes are arranged to form a uniform grid. Here, $d = 1, 2, \ldots$ denotes the dimension of the lattice and $\mathbb{Z}$ indicates the set of integers. The edge set

of the lattice is denoted by $\mathcal{E}$,

$$\mathcal{E} = \{e_{xy} : |x - y| = 1, x, y \in \mathbb{Z}^d\}$$

For every two neighbors in $\mathbb{Z}^d$, there exist an edge (or bond) between the nodes with probability p and does not exist with probability $1 - p$, independently of all other edges (see Figure 2-3). One of the fundamental questions that bond percolation theory tries to answer is at what probability p does the entire lattice becomes connected, i.e, what is the probability at which there is a connected path between any two randomly chosen points on the lattice. This connectivity function is called percolation probability denoted by $\theta(p)$ and is clearly an increasing function of p. Let C denote the connected cluster around the origin, which is the set of all nodes that can be reached through connected paths from the origin. Then,

$$\theta(p) = \mathbb{P}(|C| = \infty) \tag{2.1}$$

$$p_c = \sup\{p : \theta(p) = 0\} \tag{2.2}$$

$$\chi(p) = \mathbb{E}[|C|, |C| < \infty] \tag{2.3}$$

$$\zeta(p) = \sqrt{\frac{\sum_{x \in C, |C| < \infty} \mathbb{E}[x^2]}{\chi(p)}} \tag{2.4}$$

where $|C|$ denotes the cardinality of connected cluster, and $\mathbb{E}(\cdot)$ denotes the expectation operator. The quantity p_c is called the critical probability. It implies that there exists a critical threshold for the connectivity of lattice; when $p > p_c$ the lattice gets connected and when $p \leq p_c$ the lattice is disconnected. $\chi(p)$ is the average size of the cluster when $p < p_c$ and $\zeta(p)$, known as the correlation length, is the typical radius of this cluster.

Even though the behavior of bond percolation model across p_c is well understood in the literature, the exact threshold p_c is hard to calculate analytically and as such is known exactly for few lattice structures and dimensions. For the rest of cases, the threshold has been calculated only through extensive numerical simulations. For a square lattice in 2D, the critical value, $p_c(\mathbb{Z}^2)$ has been calculated exactly after more

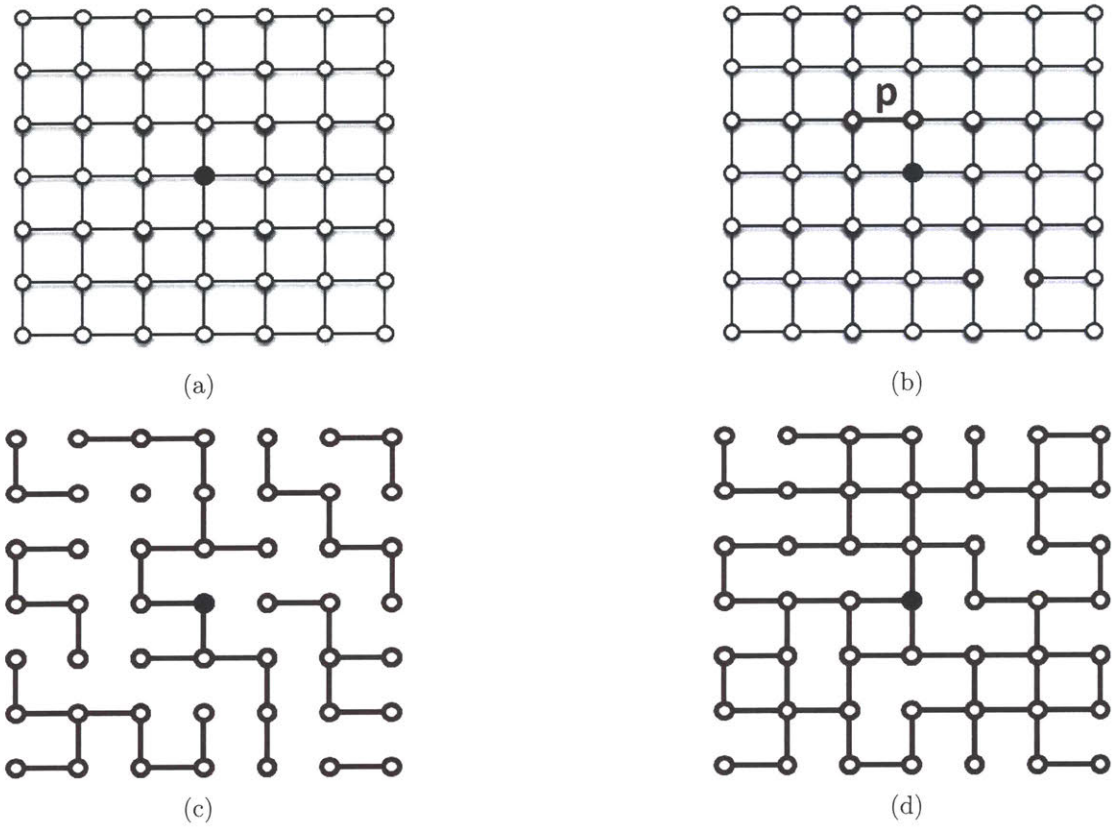

Figure 2-3: (a) Bond percolation model on a two dimensional lattice. The origin is shown in bold. (b) An edge (bond) is present with probability p and absent with probability $1 - p$, independent of all other edges on the lattice. (c) A particular realization of the model when $p < p_c$ and the lattice is disconnected, and (d) a realization of the model when $p > p_c$ and the lattice gets connected.

than 10 years of rigorous efforts by mathematicians, and has been shown to be equal to 1/2 [104].

When $p < p_c$, there is an exponential decay in the number of nodes. Specifically, the probability that the origin is connected to a node located at radius r decays exponentially with r. Furthermore, the probability that cluster contains n nodes also decays exponentially with increasing n. These statements are made precise by following theorems.

Theorem 2.1. *(Exponential decay of cluster radius) [105] Let $S(r)$ be a ball of radius r around the origin and let $\partial S(r)$ denote its boundary. Then, the probability (as a function of p) that the origin is connected to some node in $\partial S(r)$ decays exponentially*

fast if $p < p_c$,

$$\mathbb{P}(0 \text{ is connected to } \partial S(r)) < e^{-\frac{n}{\zeta(p)}}, \quad \forall r \geq 1$$

Theorem 2.2. *(Exponential decay of cluster size) [105] Let* $|C|$ *denote number of nodes in the connected cluster around the origin. If* $0 < p < p_c$, *there exists* $\lambda(p) > 0$ *such that,*

$$\mathbb{P}(|C| \geq n) \leq e^{-n\lambda(p)}, \quad \forall n \geq 1$$

A slightly different model is the *site percolation model* in which a particular site is occupied or unoccupied with probability p. The site percolation model is a broader model than the bond percolation model, and any bond percolation model can be transformed into a site percolation model but not otherwise. As with bond percolation, the critical question is at what probability does the lattice become connected? For a two dimensional square lattice, the critical value for percolation threshold is known to be $p_c^s(\mathbb{Z}^2) = 0.5927$ [105].

2.3.2 SLE Curves

Schramm Loewner Evolution (SLE), first discovered by Oded Schramm, has been shown to be the scaling limit of a variety of two dimensional lattice models in statistical physics [106, 107]. SLE is the stochastic version of the Lowner differential equation, which describes the evolution of the complement of a curve under a conformal mapping in the complex plane (Figure 2-4). In particular, let $\gamma : \mathbb{R}^+ \to \mathbb{H}$ be a simple curve in the upper half plane $\mathbb{H} \subset \mathbb{C}$ starting in $\mathbb{R}$. Let $\mathbb{H}_t$ be the unbounded connected component of $\mathbb{H} \setminus \gamma[0,t]$, *i.e.* the component formed by removing the curve $\gamma[0,t]$ from $\mathbb{H}$. Then for each t, there exists a conformal, bijective and analytic map $g_t : \mathbb{H}_t \to \mathbb{H}$ that satisfies the Loewner equation,

$$\frac{\partial g_t}{\partial t} = \frac{2}{g_t - U_t}, \quad g_0(z) = z, \tag{2.5}$$

where $U_t = g_t(\gamma(t))$, the mapping of the end of curve under g_t. Thus the Loewner equation describes how the map g_t evolves as the curve $\gamma[0,t]$ grows. It can be

Figure 2-4: Conformal mapping for the SLE cuvres. Half plane $\mathbb{H}$ with the curve $\gamma[0,t]$, complement of the curve $\mathbb{H}_t : \mathbb{H} \setminus \gamma[0,t]$, and the image of the complement under conformal mapping $g_t : \mathbb{H}_t \to \mathbb{H}$

shown that g_t is unique if few technicalities are satisfied, namely $g_t(z) - z \to 0$ and $g_t'(\infty) = \infty$ as $|z| \to \infty$. Under these assumptions, Laurent series expansion of $g_t(z)$ becomes, $g_t(z) = z + \frac{a}{z} + \mathcal{O}(|z|^{-2})$, where the term $a(\gamma[0,t])$ is known as the half plane capacity of $\gamma[0,t]$. It can be shown that $a(\gamma[0,t])$ is additive, *i.e.* $a(\gamma[0,t+s]) = a(\gamma[0,t]) + a(\gamma[t,t+s])$, which results in coefficient 2 in (2.5). It should be noted that, as g_t is a unique map, equation (2.5) can also be used to determine the evolution of curve γ given the driving function U_t.

Schramm Loewner Evolution or SLE_κ, parameterized by quantity $\kappa > 0$, is the evolution of curve γ when the driving function U_t is chosen to be a scaled Brownian motion, $U_t = \sqrt{\kappa}B_t$. Depending on the value of parameter $\kappa \in (0,8)$, SLE_κ has different properties [108]; if $\kappa < 4$, the curve is simple, for $4 < \kappa < 8$, the curve can intersect itself but does not cross and remains simple, and for $\kappa > 8$, the curve is space filling. Furthermore, for all values of $\kappa > 0$, the curve is a fractal. The trace of the curve has a Hausdorff dimension of $\min(1 + \frac{\kappa}{8}, 2)$, and the outer boundary of the curve has a Hausdorff dimension of $1 + \frac{2}{\kappa}$ [109].

Of particular relevance is the seminal result proved by Stanislav Smirnov [110], which shows that SLE_6 corresponds to critical percolation, *i.e.* the interface of the connected cluster of bond percolation at criticality when $p \approx p_c$. This is the only result known to date for $\kappa = 6$, which was proved for bond percolation model on a triangular lattices, earning Smirnov the Fields Medal in Mathematics in 2010 [111]. Once this

equivalence was established, it was shown that the properties of the connected cluster around origin in bond percolation behave as power laws. Furthermore, the fractal exponents of the boundary can be estimated precisely. These results are stated in the following theorems.

Theorem 2.3. *(Dimension of percolation boundary) [110, 112, 113] The scaling limit of the perimeter of the critical percolation is identical to that of SLE_6. The Hausdorff dimension of the boundary of SLE_6 is $4/3$ almost surely.*

Theorem 2.4. *(Critical exponents) [110] Let $S(r)$ be a ball of radius r around the origin and let $\partial S(r)$ denote its boundary. Let $|C|$ be the cardinality of the connected cluster around origin. Then,*

$$\mathbb{P}(0 \text{ is connected to } \partial S(r)) = r^{-5/24} \quad \text{as } r \to \infty$$
$$\mathbb{P}(n \leq |C| < \infty) = n^{-5/91} \quad \text{as } n \to \infty$$

2.3.3 First Passage Percolation

The bond percolation model described in previous section is a static model in which the connectivity of every bond is determined for the entire lattice in one time step. On the other hand, first passage percolation, first introduced by Hammersley and Welsh, can be used to model dynamical processes on lattices [114, 115]. Consider as before, a set of nodes on infinite square lattice $\mathbb{Z}^2$. We associate with every edge e of the lattice an i.i.d. random variable $\tau(e)$, which can be interpreted as the time taken to traverse along the edge e. Given any two nodes a and b on the lattice, let γ be a connected path on the lattice from a to b. We define the *passage time* $T(\gamma)$ as,

$$T(\gamma) = \sum_{e \in \gamma} \tau(e)$$

for any connected path γ from node a to node b (Figure 2-5). The random variable $T(\gamma)$ is the time taken to traverse from node a to b along the path γ. The first passage

time $T(a,b)$ is defined to be the minimum among all such paths.

$$T(a,b) = \inf_{\gamma} \{T(\gamma) : \gamma \text{ is a path from a to b}\}$$

The first passage time has the simple interpretation as the shortest time to reach node b starting from a while traversing along the edges with random times $\tau(e)$. If the distribution of passages times, $\tau(e)$ is an exponential distribution, the first passage percolation process is known as the Eden growth model in the literature [60].

Most of the research effort in first passage percolation theory is towards characterization of random variable $T(0,n)$, which is first passage time from origin to a node at distance n. Towards this end, a fundamental result in ergodic theory known as the subadditive theorem [116] provides technical conditions for the existence of a limit for the first passage times.

Theorem 2.5. *(Subadditive Ergodic Theorem) [116] Suppose $X_{m,n}$, $0 \leq m < n$ is a family of random variables satisfying,*

- $X_{0,n} \leq X_{0,m} + X_{m,n}$, *for all* $0 \leq m < n$.
- *For each* $k > 1$, *the sequence* $\{X_{nk,(n+1)k}\}_{n\geq 0}$ *is stationary.*
- *The distribution of the sequence* $\{X_{m,m+k}\}_{k\geq 1}$ *does not depend on* m.
- $E[X_{0,1}] < \infty$.

Then,

- $\lim_{n\to\infty} \frac{E[X_{0,n}]}{n} = \inf_n \frac{E[X_{0,n}]}{n} = \gamma$.
- *The limit* $X = \lim_{n\to\infty} \frac{X_{0,n}}{n}$ *exists and is finite almost surely.*
- *If the stationary sequences* $\{X_{nk,(n+1)k}\}_{n\geq 0}$ *are also ergodic, then* $X = \gamma$ *almost surely.*

The first passage percolation process satisfies the subadditive property which is similar to the stochastic version of the triangular inequality. It follows from the

ergodic theorem that the time taken to reach a particular node n starting from origin is a constant, which is usually called the time constant.

Theorem 2.6. *(Time constant) [117] Let $\hat{e}$ denote a unit vector in $\mathbb{Z}^d$. There exists a constant $\mu(\hat{e}) \in [0, \infty)$ called the time constant such that,*

$$\lim_{n\to\infty} \frac{T(0, n\hat{e})}{n} = \mu(\hat{e}) \quad \textit{almost surely and in } L^1.$$

The implication of existence of the limit is that the time taken to reach a particular node located at distance n is linear in n, even though the constant μ might be direction dependent. The exact value of the time constant is not known analytically and is usually estimated through numerical simulations. However, some bounds on the time constant are known.

Theorem 2.7. *(Bound on time constant) [117] For first passage percolation on $\mathbb{Z}^d$ with iid passage times $\tau(e)$, let $\mathcal{F}$ be the distribution of random variables τ. If $\mathcal{F}$ has a non trivial distribution, then $\mu(\hat{e}) < E[\tau(e)]$.*

As opposed to the expected value $E[T(0, n)]$, only limited results are available regarding the variance $var[T(0, n)]$. The results mainly consist of bounds on the variance, but do not predict exact behavior.

Theorem 2.8. *[118] Let $E[\tau(e)^2] < \infty$ and let F be a non-trivial distribution, then there exist constants C_1 and C_2, such that,*

$$C_1 \leq var[T(0, n\hat{e})] \leq C_2 n.$$

Another major result for variance is the lower bound for first passage percolation in 2D which indicates that the variance in fact grows unboundedly with n.

Theorem 2.9. *(Logarithmic lower bound) [119,120] For $d = 2$, there exists a constant B such that,*

$$var[T(0, n\hat{e})] \geq B \log n$$

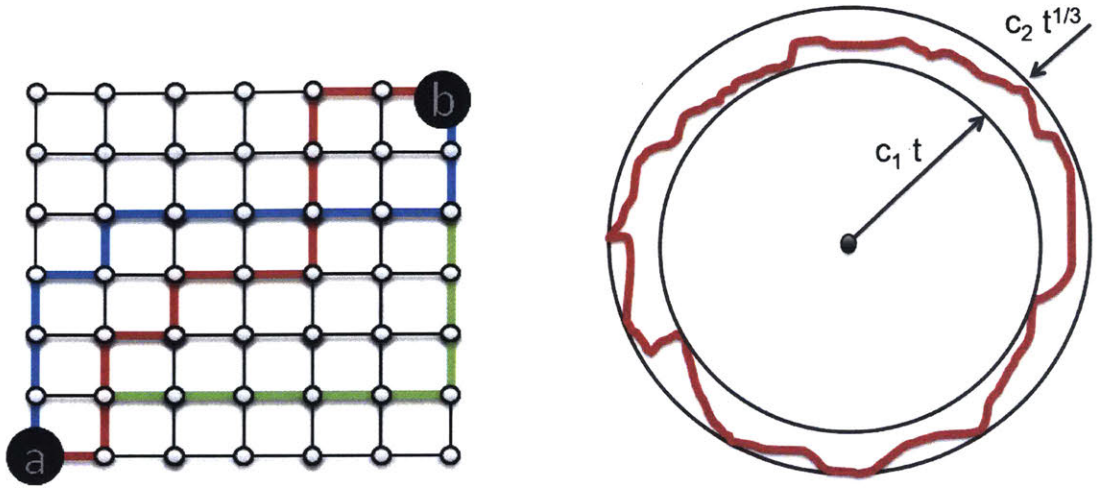

(a) (b)

Figure 2-5: (a) A schematic showing the first passage percolation model on a two dimensional lattice. Time to move along any edge is a random variable drawn from a distribution $\mathcal{F}$. There are multiple paths (and times) to reach from point a to b. The first passage time $T(a, b)$ is the minimum among all these times. (b) Long time behavior of a growth process as predicted by the KPZ growth model. The growth rate is linear in time but has a variance that also grows sublinearly. The first passage percolation can be thought of a growth process if we denote the growth set at time t as all the points reached by time t starting from origin.

Another quantity of interest is the shape of the process asymptotically. Even though the exact shape of the process is unknown, it has been shown that the shape can be bounded inside a convex and deterministic shape.

Theorem 2.10. *(Shape theorem) [121] There exists a deterministic, convex, compact set $\mathcal{B} \in \mathbb{R}^d$, such that for every $\epsilon > 0$,*

$$\mathbb{P}\big((1-\epsilon)\mathcal{B} \subset \frac{B(t)}{t} \subset (1+\epsilon)\mathcal{B} \text{ for large } t\big) = 1.$$

Furthermore, $\mathcal{B}$ has a non-empty interior and is symmetric about the axis of $\mathbb{R}^d$.

2.3.4 KPZ Growth Model

A different view point on the *stochastic growth processes* was described in the seminal work of Kardar, Parisi, and Zhang (KPZ) [62]. Stochastic growth processes gener-

alize the ideas of spreading processes and are models of spatial growth. They have been used to model formation of crystals, facet boundaries, bacteria growth, paper wetting, crack formation, and moving fronts among many others [12]. Using heuristic arguments, KPZ predicted that all growth processes should belong to a common universality class that can be described by the following stochastic partial differential equation (known as the KPZ equation),

$$\frac{\partial h}{dt}(t,x) = \nu\frac{\partial^2 h}{dx^2} + \frac{1}{2}\lambda\left(\frac{\partial h}{dx}\right)^2 + \sqrt{D}\,w, \tag{2.6}$$

where the parameters ν, λ, and D are non zero. The first term on the right hand side is the Laplacian which results in smoothing of the solution. The second term is a slope dependent growth rate term, that forces a faster growth rate whenever the slope is higher. The third term is the space-time Gaussian white noise that adds stochasticity to the equation. Based on the PDE model, KPZ predicted that fluctuations of growth rate of *any* growth process has an exponent of 1/3, *i.e.* the variance of the growth processes behaves as $t^{1/3}$ (see Figure 2-5). A growth model is said to be in KPZ universality class if its long term behavior is similar to that of the KPZ equation (2.6). Several growth models have been shown to belong to the KPZ universality class through extensive numerical simulations, and indeed have fluctuation exponent of 1/3.

Unfortunately, complete understanding of the KPZ equation is unknown and rigorous mathematical solutions for few instances of the KPZ equation have been obtained only recently [122–125]. In addition, the solutions are available only in one dimension and are limited to few growth models under specific boundary conditions. The major mathematical difficulty in solving KPZ equation directly is that the stochastic PDE is ill-posed in its original form as it involves taking a derivative of white noise. The approach taken by mathematicians is to start with parameter values $\nu = \frac{1}{2}, \lambda = -1, D = 1$ and transform the KPZ equation to a closely related stochastic version of Burger's equation (also known as stochastic heat equation) using Hopf-Cole transformation $h(t,x) = -\log z(t,x)$. This transformation converts the KPZ

equation to the stochastic heat equation (SHE),

$$\frac{\partial z}{dt} = \frac{1}{2}\frac{\partial^2 z}{dx^2} - z\ w. \tag{2.7}$$

The choice of (ν, λ, D) is inconsequential as any non zero choice can be transformed into one another. In this sense, the KPZ equation is also self-similar. The only model for which solution is known is called the corner growth model [124]. Few other models such as totally asymmetric simple exclusion process (TASEP) and the so called last passage percolation process can be shown to be equivalent to the corner growth model under specific transformations. The solution approach to the KPZ equation involves three steps: (i) seek solutions to SHE equation (2.7), (ii) apply Hopf-Cole transformation to the corner growth model to obtain a discrete version of SHE, and (iii) show convergence of discrete SHE to continuum SHE under weak symmetry [124]. For the corner growth model, the KPZ equation can be solved explicitly to obtain the probability distribution of the growth function as stated by the following theorem.

Theorem 2.11. *[124] The growth function $h(t,0)$ satisfies,*

$$\lim_{t\to\infty} \mathbb{P}\left(\frac{h(t,0) - t/2}{2^{-1/3}\ t^{1/3}} \geq -s\right) = F_{GUE}(s)$$

where $F_{GUE}(s)$ is the Tracy-Widom distribution.

It is important to note the appearance of the $t^{1/3}$ scaling in the variance of the corner growth model, and contrast it with the scaling of $t^{1/2}$ obtained using the central limit theorem. Such observations have led to the prediction of existence of a new universality class (KPZ) for correlated random variables, similar to the Gaussian universality class for independent random variables. It was also predicted in [62] that the space correlations have fluctuations of order $t^{2/3}$, though no mathematical rigorous results for the same are available. For his seminal work for finding analytical solutions to KPZ equation, mathematician Martin Hairer was awarded the Field's Medal in 2014 [111]. We summarize the KPZ prediction explicitly by the following conjecture,

Conjecture 2.12. *(Kardar, Parisi, and Zhang (KPZ)) [62] A stochastic growth process is said to belong to the KPZ universality class if its long term behavior is similar to the KPZ equation, i.e. there exists constants C_1, C_2 such that the growth process $h(x,t)$ behaves as, $h(t,t) \sim C_1 t + C_2 t^{1/3}$ for large t.*

2.4 Characterization of Spreading Processes

2.4.1 Stability

In this section we summarize the behavior of the stochastic growth process in different stability regimes using various tools that were described previously. We state our first result and provide a lower bound on critical probabilities of the forest fire process by comparing it to an equivalent bond percolation model [104] on a lattice in 2D. As it can be seen from Figure 2-6, simulation results confirm that the lower bound is tight. We note that obtaining a tight analytical bound for the phase transition threshold is important, as it allows us to develop control policies in the next chapter.

Theorem 2.13 (Lower bound on critical probability). *For the forest fire process, let (α_c, β_c) and (μ_c, λ_c) denote the critical probabilities for the discrete and continuous time models respectively, then the critical probabilities satisfy,*

(i) $(1+\alpha_c)\beta_c \geq 1$

(ii) $\frac{\lambda_c}{\mu_c} \geq 1$

Proof. To prove item (i), for the discrete time model, let A denote the event that a burning tree spreads fire to its healthy neighbor. Then

$$\begin{aligned}\mathbb{P}(A) &= \beta\alpha + \beta(1-\alpha)\beta\alpha + \beta^2(1-\alpha)^2\beta\alpha + \cdots \\ &= \frac{\beta\alpha}{1-\beta(1-\alpha)}\end{aligned}$$

At the critical threshold for $\mathbb{Z}^2$, this probability should be greater than the critical probability for bond percolation $p_c(\mathbb{Z}^2) = 1/2$ which gives the desired result. The

inequality is true because the fire process has more than one attempt (possibly infinite) to infect the neighboring node as compared to a single chance in the bond percolation model.

To prove item (ii), let U be a random variable such that, $U = \min\{X, Y\}$, where X and Y are exponential distributed random variable with parameters λ and μ respectively. For the continuous time model, the fire spreads to the neighboring node if $U = X$ or $X \leq Y$. This event happens with probability

$$\frac{\lambda}{\lambda + \mu},$$

which should be greater than $p_c(\mathbb{Z}^2) = 1/2$ as earlier, which in turn yields the desired result. □

Theorem 2.14. *(Upper bound on critical probability) For the forest fire process, let* (α_c, β_c) *and* (μ_c, λ_c) *denote the critical probabilities for the discrete and continuous time models respectively, then the critical probabilities satisfy, (i)* $\alpha_c\beta_c \leq p_{sc}$ *(ii)* $\frac{\lambda_c}{\lambda_c+\mu_c} \leq p_{sc}$ *where* p_{sc} *is the critical probability of the site percolation model.*

Proof. The result follow by the following observation. For the discrete model, if we assume that when the fire doesn't burn out in the first time step, it spreads to all its neighbors. This process is equivalent to the site percolation model. For a 2D lattice, $p_{sc}(\mathbb{Z}^2) = 0.5927$. The argument for the continuous time model follows similarly. □

2.4.2 Open Loop Behavior

In the previous sections, it was shown using a coupling argument that the spreading process on lattices in 2D is equivalent to a bond percolation model, under a suitable transformation of probability parameter. This equivalence allows one to use known results in bond percolation theory to characterize spreading process in it stable and neutral regime.

When $p < p_c$, the spreading process is in its stable regime and the number of affected nodes is finite almost surely. Furthermore the number of affected nodes

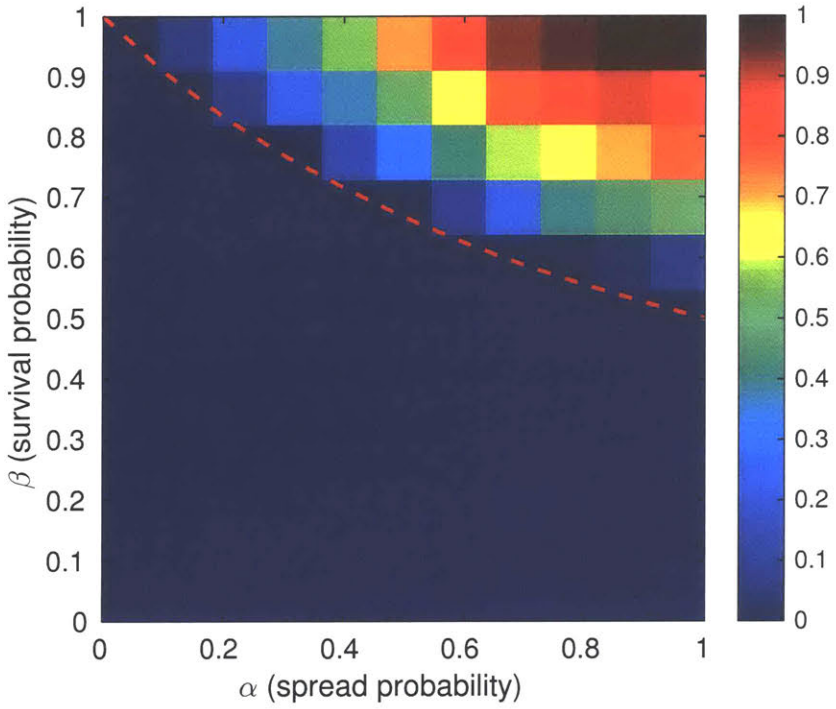

(a)

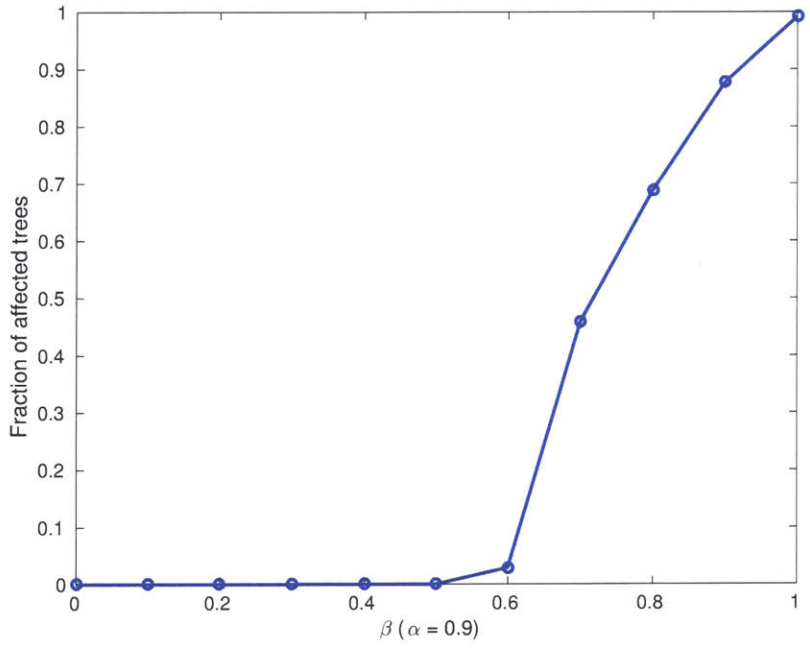

(b)

Figure 2-6: (a) The phase transition diagram for the fire process computed numerically. The plot shows the fraction of affected trees as a function of parameters α and β. The dotted line shows the theoretical threshold calculated in Theorem 2.13. Below the line the fire process is stable and above it is unstable. (b) A particular slice of phase diagram for $\alpha = 0.9$ and varying β. The phase transition occurs at $\beta_c \approx 0.52$ as predicted by Theorem 2.13.

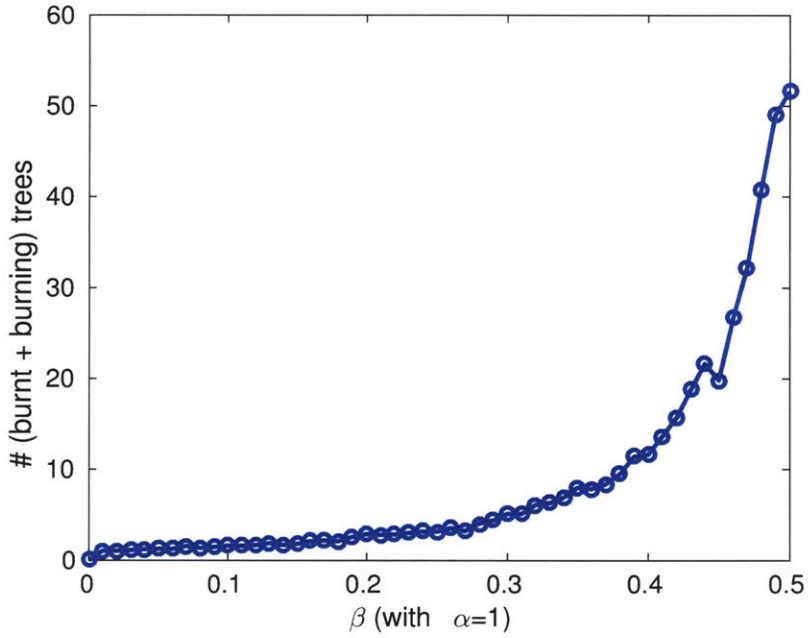

(a)

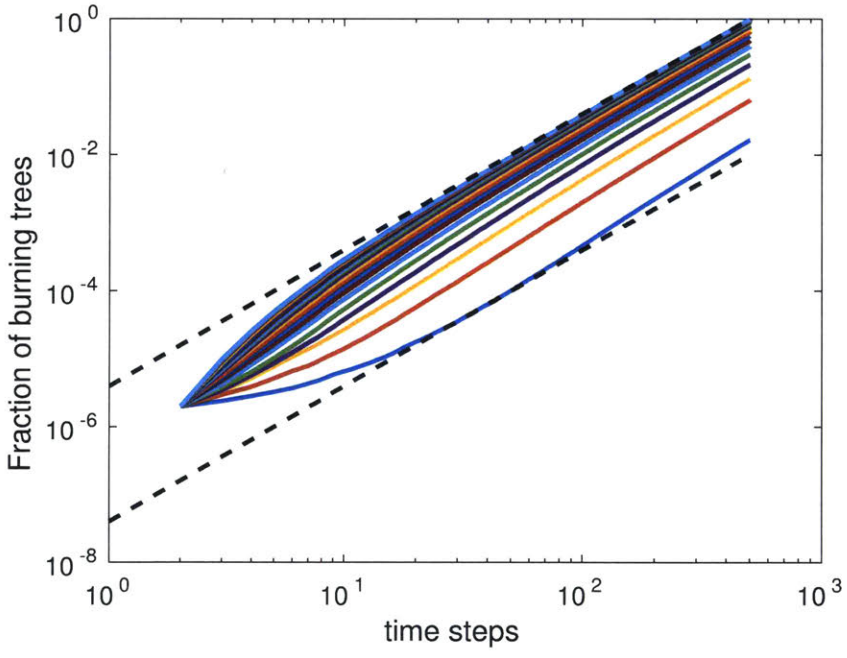

(b)

Figure 2-7: Numerical simulations of the spreading process in its stable and unstable regimes. (a) Exponential decay of number of affected nodes with probability parameter β in the stable regime, and (b) Log-log plot of growth of the spreading process in unstable regime for increasing values of probability parameter (from $\alpha \approx \alpha_c$ to $\alpha = 1$, with $\beta = 1$). The vertical axis is the fraction of the total number of nodes that have been affected. The two dotted lines indicate linear slope. Near the critical threshold the slope is super-linear indicating that the behavior is fractal. The slope becomes increasing linear as $\alpha \to 1$.

decay at a rate that is exponential in time (as shown in Figure 2-7) starting from any initial condition.

When $p \approx p_c$, the spreading process is in its neutral regime, and similar to the bond percolation model it shows a fractal behavior. A fractal behavior is characterized by a growth exponent that is super linear, and growth distributions that behave as power laws. Roughly speaking, a fractal is one that has a large perimeter for a given included area as opposed to a regular shape. For a geometry that has a regular shape, the ratio of the area to its perimeter is linear in its characteristic length. For a fractal shape, this ratio is super-linear function of the length. The super-linearity exponent is known as the growth exponent of the fractal. It can be seen from Fig 2-7 that the growth exponent of the spreading process near criticality is around 1.3. Numerical simulations are close to the growth exponent of 4/3 predicted by the rigorous analysis available in literature using SLE curves. This exponent approaches 1 as the probability parameter $p \to 1$, indicating that the geometry of the spreading process approaches regularity as we move away from the neutral regime.

In the unstable regime, when $p > p_c$, bond percolation model is not helpful to characterize the behavior of the spreading process. This is because the bond percolation model is a static model in which the state of the entire lattice is decided at one instance. On the contrary, numerical simulations show that there is growth in the number of affected nodes in the unstable regime for a spreading process. This behav-

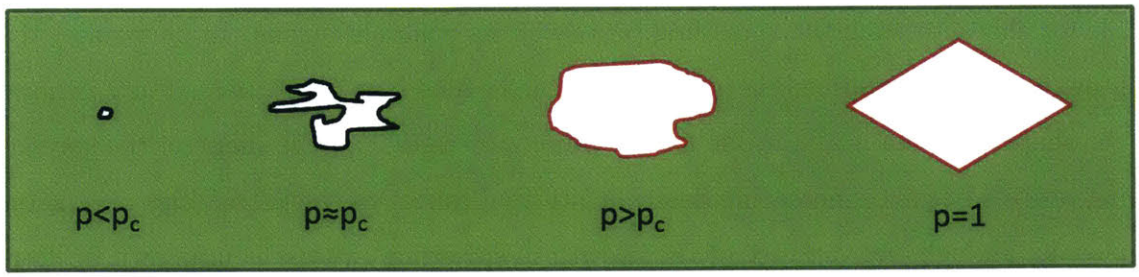

Figure 2-8: The shape of the spreading process for different values of probability parameter p. When $p < p_c$, the number of affected nodes is finite and the growth cluster is negligible. At $p \approx p_c$, the spreading process has a fractal shape; the perimeter of the geometry is superlinear in the characteristic length. For $p > p_c$, the shape becomes increasingly convex and deterministic as $p \to 1$.

ior is captured by the first passage percolation model and the predictions made using the KPZ equation. In this regime, we use the continuous time model of the spreading process and show its equivalence to the first passage percolation model. Let X and Y be exponential distributed random variable with parameters λ and μ respectively. Recall that λ is the probability parameter associated with spreading, and μ is the parameter associated with survival of the process. Define the passage time τ to be equal to X whenever $X < Y$, and equal to infinity when $X > Y$, i.e. $\tau = X$, with probability $\frac{\lambda}{\lambda+\mu}$, and $\tau = \infty$ with probability $\frac{\mu}{\lambda+\mu}$. Thus, the equivalence between the continuous time model of the spreading process and the first passage percolation can be shown by choosing the distribution $\mathcal{F}$ of the passage times τ as follows,

$$\tau = \begin{cases} \text{Exp}(\lambda), & \text{with probability } \frac{\lambda}{\lambda+\mu} \\ \infty, & \text{with probability } \frac{\mu}{\lambda+\mu} \end{cases}$$

where $Exp(\lambda)$ denotes exponential random variable with parameter λ.

Once this equivalence between the spreading process and first passage percolation is established, using the coupling argument, known results from the latter are applicable for characterizing the spreading process in its unstable regime. In particular, the growth rate of the spreading process is linear in time (see Figure 2-7). Furthermore, the shape theorem is applicable for spreading processes, and the shape of the spreading process becomes increasing deterministic and convex as the probability parameter $p \to 1$. Though the variance of the growth of spreading process is unknown in literature, we can conjecture using the KPZ model that the variances is not a constant but rather grows with time, and behaves as $t^{1/3}$. Table 2.1 and Figure 2-8 summarize the open loop behavior and the shape of the spreading process in its stable, neutral and unstable regimes.

Table 2.1: A summary of open loop behavior of the spreading process

	Stable	Neutral	Unstable
Affected Nodes	Finite	Finite Eventually	Infinite
Growth	Exponential decay	Power law decay	Linear growth/growing variance
Cluster shape	Negligible	Fractal	Convex and deterministic
Universality	Bond percolation	SLE Curves	First passage percolation/KPZ

2.5 Flooding Time Analysis

In the previous sections we provided exact characterization for spreading processes on lattices by coupling them with other well studied stochastic processes. For spreading processes on general graphs, such an accurate characterization might not be possible. However, in few cases we could still exploit the structure of the underlying graph to characterize the spread of the process asymptotically. This section provides the characterization for the same using the notion of *flooding time*. Flooding time $\mathcal{T}(N)$ is defined as the expected time it takes for the spreading process to spread to all N nodes for a given graph. For a finite graph, the flooding time is equivalent to the longest path in the graph. The behavior of $\mathcal{T}(N)$ provides an indication of how easy or difficult is it for the process to spread. We assume the unstable operating regime for the spreading process and use the continuous time model. In addition, we assume that $\lambda \gg \mu$ and for simplicity assume $\lambda = 1$.

Let $\partial B(t)$ denote the boundary of the spreading process at time t, which denotes the set of all burning nodes that are connected to a neighboring healthy node. Let n denote the cardinality of this set. Let $\partial E(n(t))$ denote the set of edges connecting the nodes in $\partial B(t)$ to their healthy neighborhood,

$$\partial E(n(t)) = \{u : u \text{ is an edge to a healthy neighbor of } v, v \in \partial B\}$$

Let $e(n(t))$ denote the cardinality of $\partial E(n(t))$. We note that ∂E is a function of $n(t)$, and depends on the arrangement of the burning nodes. For the same value of n, different arrangements of the nodes might give rise different edge set $\partial E(t)$. For

instance, on a square lattice in 2D, if at $t = 0$, $n = 1$, then $e(1) = 4$, $e(2) = 6$, $e(3) = 7$ or 8, $e(4) = 8, 9$ or 10 and so on. The main goal in the analysis that follows is to get an accurate bound on the number of edges $e(n)$ for a given structure of a graph. This would in turn result in an estimate of the flooding time.

Given the current state of the boundary $\partial B(t)$ at time instant t, let $t + \Delta t$ denote the first spreading time, *i.e.* the first time instant one of the nodes in $\partial B(t)$ spread fire through one of the edges in $\partial E(t)$.

Lemma 2.15. *Δt is an exponential random variable with parameter $e(n)$.*

Proof. The time it takes to spread fire to a healthy neighbor through an edge in $\partial E(t)$ is an exponential random variable with parameter $\lambda = 1$. Let X_i denote i.i.d exponential random variable with parameter 1. The time gap Δt is a random variable such that,

$$\Delta t = \min\{X_1, X_2, \cdots, X_{e(n)}\}$$

which is also an exponential random variable with parameter $e(n)$. Due to memoryless property of the exponential random variable spreading process through any edge, X_i are independent for all i. □

Lemma 2.16. *If at time $t = 0$, $n(0) = 1$, then the flooding time $\mathcal{T}(N)$, satisfies the following relation for all $N \geq 2$,*

$$\mathcal{T}(N) = \sum_{i=1}^{N-1} \frac{1}{e(n)}$$

Proof. Note that $T_1 = 0$ and for any $i \geq 2$, $(T_n - T_{n-1})$ is exponential distributed random variable with parameter $e(n-1)$ from Lemma 2.15, which has an expected value of $\frac{1}{e(n)}$. Thus, $E[T_N] = \mathcal{T}(N) = \sum_{i=1}^{N-1} \frac{1}{e(n)}$. □

If we know the growth behavior of edge set cardinality $e(n)$, we can obtain a bound on flooding time as follows.

Lemma 2.17. *Let $e(n) = cn^{\alpha}$, where $c, \alpha > 0$ are constants, then for large N,*

$$\mathcal{T}(N) = \begin{cases} \mathcal{O}(N^{1-\alpha}) & \alpha < 1 \\ \mathcal{O}(\log N) & \alpha = 1 \\ \mathcal{O}(1) & \alpha > 1 \end{cases}$$

Proof. We note that, $\mathcal{T}(N) = \sum_{i=1}^{N-1} \frac{1}{e(n)} \approx \int_1^N \frac{1}{c}\, n^{-\alpha}\, dn$ for large N. It follows that,

$$\mathcal{T}(N) \approx \begin{cases} \frac{1}{c(1-\alpha)}\, N^{1-\alpha} & \alpha < 1 \\ \frac{1}{c}\, \log N & \alpha = 1 \\ \frac{1}{c(\alpha-1)} & \alpha > 1 \end{cases}$$

Here $\mathcal{O}$ denotes order notation. If $f(x) = \mathcal{O}(g(x))$, then $\exists\ x_0$ and $M > 0$, such that $\left|\frac{f(x)}{g(x)}\right| \leq M, \forall x \geq x_0$. □

In the following theorem, we characterize the behavior of spreading process using flooding time for a line graph, square lattice, star graph and a complete graph.

Theorem 2.18. *(i) For a line graph, $\mathcal{T}(N) = \mathcal{O}(N)$.*

(ii) For a square lattice on $\mathbb{Z}^2$, there exist constants c_1, c_2, such that,
$c_1 \log N \leq \mathcal{T}(N) \leq c_2\sqrt{N}$.

(iii) For a star graph, $\mathcal{T}(N) = \mathcal{O}(\log N)$.

(iv) For a complete graph, $\mathcal{T}(N) = \mathcal{O}(\frac{\log N}{N})$.

Proof. (i) For a line graph, $e(n) = 2$, for all $1 \leq n \leq N$ and result follows.

(ii) For a lattice in $\mathbb{Z}^2$, $2(1 + \sqrt{2(n-1)+1}) \leq e(n) \leq 2n + 2, \forall n \geq 1$. The upper bound is obtained if we assume that nodes always increase along a straight line in which case they have n neighbors on two sides of the line and one neighbor on each front. To obtain the lower bound, we observe that the best packing for the nodes is achieved when they grow in the shape of a diamond. In this case if the

interior of the diamond has n infected nodes, then for any $k \geq 1$, $n = 2k^2-2k+1$, and the number of edges to the neighboring nodes are $e(n) = 4k$. Using linearity of expectation, $\sum_{i=1}^{N-1} \frac{1}{2n+2} \leq E[T_N] \leq \sum_{i=1}^{N-1} \frac{1}{2(1+\sqrt{2(n-1)+1}}$ which gives the desired result for large N.

(iii) For a star graph, if the hub is infected at $t = 0$, then $e(n) = N - n, 1 \leq n \leq N - 1$, and if a node other than hub is infected at $t = 0$, then $e(1) = 1$ till the hub gets infected after which $e(n) = N - n, 2 \leq n \leq N - 2$. In both cases, $E[T_N] = \sum_{i=1}^{N-1} \frac{1}{e(n)} \approx \log N$ for large N

(iv) For a complete graph $e(1) = N-1, e(2) = 2(N-2), \cdots, e(n) = n(N-n)$. This is true because if n out of N nodes are infected, then for every infected node there are n edges to infected nodes (that are not counted) and $N-n$ edges to the healthy nodes, thus a total of $n(N-n)$ edges. Thus $\mathcal{T}(N) = \sum_{i=1}^{N-1} \frac{1}{n(N-n)} = \frac{1}{N} \sum_{i=1}^{N-1} \frac{1}{n} + \frac{1}{(N-n)} = \frac{2 \log N}{N}$ for large N.

□

We note that for a lattice graph, the bound obtained by the flooding time analysis is weak as the results are asymptotic in nature. If $N = ct^2$, then the flooding time analysis suggests that the time to cover an area of N nodes is upper bounded by a time that is linear in t, and lower bounded by time that is logarithmic in t. This result should be compared with that obtained by first passage percolation and KPZ growth models, that accurately predict linear growth rate for spreading processes on lattices.

2.6 Summary

In this chapter we defined notions of stability for the spreading process on lattices and characterized its behavior in its stable, neutral and unstable regime. We also accurately characterized stability of the process using a coupling argument with the bond percolation model. A summary of the behavior of spreading process is provided in Table 2.1.

Chapter 3

Control of Spreading Processes II

In the previous chapter, we defined notions of stability for the spreading processes and using various tools from mathematical physics characterized the open loop behavior of the spreading processes in its stable, neutral and unstable regimes. This chapter characterizes the closed loop behavior of the spreading processes. In particular, we consider an unstable spreading process and develop randomized node treatment policies that guarantee the stability of the spreading process. As spreading processes are stochastic processes, a stabilizing policy is one which ensures that the number of burning (infected) nodes go to zero almost surely (with probability 1) for all possible realizations of the spreading process.

In the first part of this chapter, in Section 3.1, we consider two randomized heuristic policies - (i) a Random Node Treatment (RNT) policy that treats only a fraction of burning nodes at any given time, and (ii) a Finite Time Interval (FTI) policy that treats all the burning nodes at finite time intervals. We show that a finite number of robotic vehicles (bounded control) cannot stabilize an unstable spreading process in all its possible realizations. As such, when a growing number of vehicles are available, we provide technical conditions for stability of the spreading process. Even though the RNT policy is not optimal, it serves as a bound on the FTI policy; whenever an equivalent RNT policy is stabilizing, the corresponding FTI policy is also stabilizing.

The second part of this chapter, Section 3.2, is concerned with development of an optimal policy for stabilizing an unstable fire process on a 2D lattice. In order to

develop the control policy, we first show that an insightful description of the growth process can be obtained by analyzing the spreading of the process in terms of the edges, rather than the nodes of the underlying graph. We then define a randomized preferential node treatment policy that is optimal in both resource allocation and control effort. To derive the properties of the aforementioned policy, we construct an equivalent tree description of the growth of fire process. Using tools from branching process and percolation on irregular trees, we prove that this policy in indeed stabilizing and optimal.

In all our further discussions in this chapter, we assume that the spreading process is in its unstable regime with $p > p_c$. To avoid the difficulties associated with large parameter space of $(\alpha, \beta, \lambda, \mu, \Delta p, \tau)$, and for notational ease, whenever possible, we state all our results with regard to the probability parameter p, while noting that all results can be mapped back to the model parameters.

3.1 Heuristic Policies

The aim of this section is to develop control policies that stabilize an unstable fire process. The simplest policy one can consider is a policy in which all the boundary nodes are treated uniformly at random. For such a policy, few natural questions one would like to consider are (i) Is such a policy stabilizing?, (ii) If so, how many nodes need to be treated?, and (iii) Can treating a finite number of nodes stabilize the fire process? We start with defining the RNT policy,

Definition 3.1. *Random node treatment (RNT) policy: Given $Z(t)$ burning (red) boundary nodes of the fire process at time t, treat a fraction f of the nodes by selecting them uniformly at random.*

As a large number of robotic vehicles might not be available in practice, we ask if a finite number of vehicles can stabilize an unstable fire process? The result turns out to be negative as formalized by the following theorem.

Theorem 3.1. *A constant number of vehicles cannot stabilize an unstable fire process*

using the Random Node Treatment (RNT) policy. Let $n(t)$ be the number of available vehicles and let $Z(t)$ be the number of burning boundary nodes at time t. A fire process is unstable if

$$\lim_{t\to\infty} \frac{n(t)}{Z(t)} = 0$$

Proof. To prove the theorem, we show that the probability for the spreading process to reach any particular state s is non-zero. For instance, the probability for a fire starting from origin and propagating along a straight line to m nodes is at least p^m, which is non zero. Let at time $t = 0$, the initial state of the process have Z burning nodes on the boundary and let $Z > n$. Let r be the growth or spreading rate of an infected/burning node. At $t = 1$, $(Z - n)$ nodes are still burning, and continue to burn at $t = 2$ if $r(Z - n) > n$, which implies $\frac{n}{Z} < \frac{r}{r+1}$. Thus at any time $t > 0$, $\frac{n}{Z(t)} < \frac{r^t}{r^t+r^{t-1}+\ldots+r+1}$, which is non-zero for any $r > 0$. In particular, if $\frac{n(t)}{Z(t)} = 0$, then fixed number of vehicles $n(t)$ cannot stop the spreading process from reaching any state s and thus the spreading process is unstable. □

The above theorem leads to the natural question that suppose we can supply a growing number of vehicles, then at what rate should the vehicles be available in order to stabilize the fire process? The following theorem answers this question.

Theorem 3.2. *A random node treatment policy stabilizes an unstable fire process if $q < p_c$ where $q = p - f\Delta p$.*

Proof. At any given time t, let the number of vehicles be $n(t)$ and let the number of burning (red) boundary nodes be $Z(t)$. Let A denote the event that a particular node is treated by a robotic vehicle. Then, $\mathbb{P}(A) = \frac{\binom{Z-1}{n-1}}{\binom{Z}{n}} = \frac{n}{Z} = f$. Further, the propagation probability of any node is $q = (p - \Delta p)\ \mathbb{P}(A) + p\ \mathbb{P}(A^c) = p - f\Delta p$. The result follows from the fact that the fire process is stable if $q < p_c$. □

We have shown that treating only a fraction of burning nodes at random at every time step achieves stability for the fire process. However, in practice, vehicles might not be available at every time due to their finite retardant carrying capacity; it takes finite time to refill the vehicle before it is available for use. As such, we now consider the FTI policy in which the robotic vehicles are available only at finite time intervals.

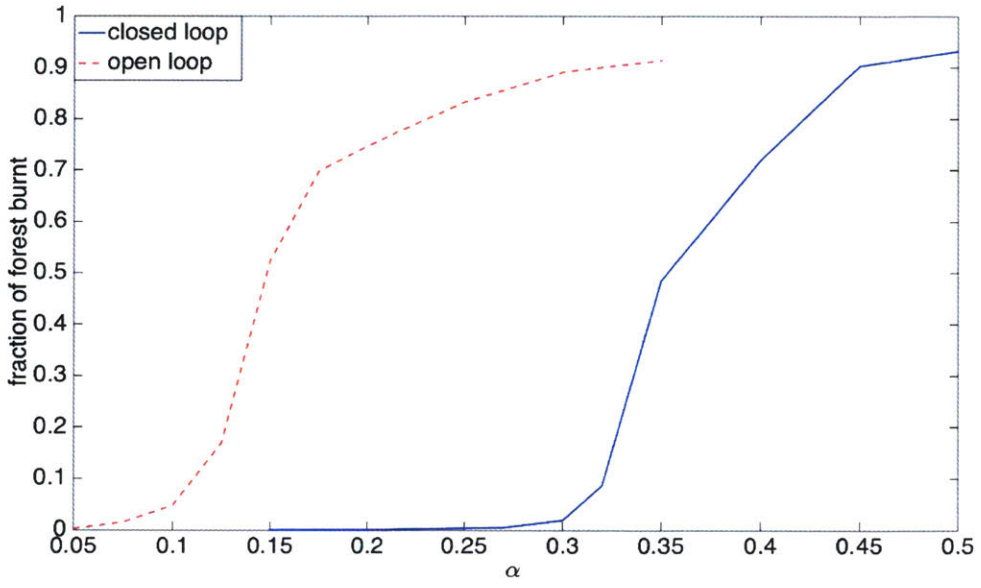

Figure 3-1: The behavior of fire process with and without control for $\beta = 0.99$. Note that the use of control results in a shift in the critical probability threshold to the right. The closed loop control has been simulated for $\Delta\alpha = 0.1$ and vehicle inter arrival times $\tau = 3$.

Definition 3.2. *Finite time interval (FTI) policy: Treat all burning boundary nodes of the spreading process at finite time intervals τ.*

It turns out that the stabilizing properties of the FTI policy could be easily analyzed by comparing it to an equivalent RNT policy. The equivalence is stated in the following theorem.

Theorem 3.3. *A finite time interval policy is equivalent to the random node policy with $f = \frac{1}{\tau}$. In particular, if the RNT policy is stable for some f, then the FTI policy is also stable if $\tau \leq 1/f$.*

Proof. We prove the argument by construction. Let $\{Z_r(0), Z_r(1), Z_r(2), \ldots, Z_r(t), \ldots\}$ be the sequence that denotes the number of red boundary nodes at time t when the RNT policy is applied and let $\{Z_f(0), Z_f(1), Z_f(2), \ldots, Z_f(t), \ldots\}$ be the sequence when the FTI policy is applied. A burning node can propagate fire to at most 3 nodes on a 2D lattice and thus from a branching process argument, we note that for the RNT policy $E[Z_r(t)] \leq (3q)^t E[Z_r(0)]$. Here $q = p - p_c$. For the FTI

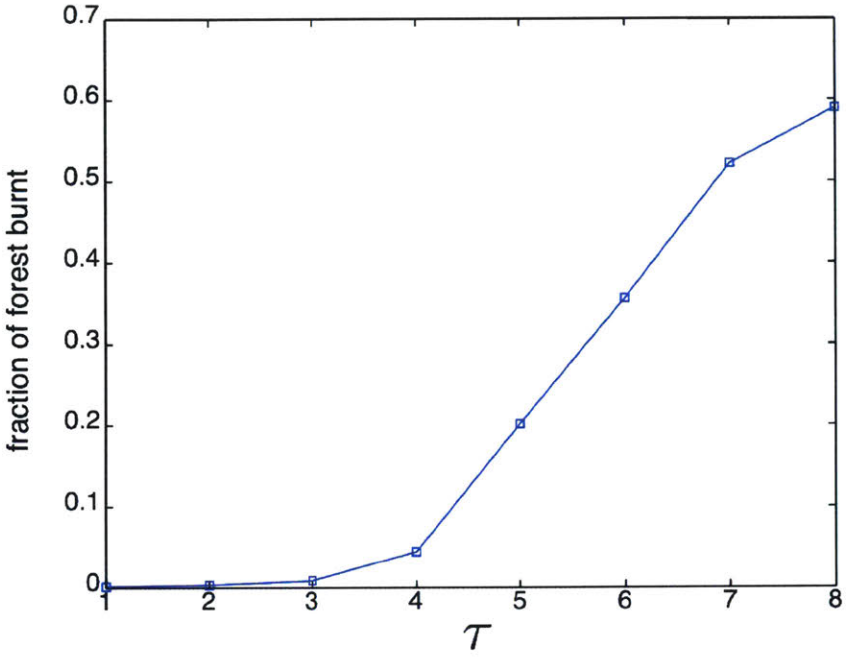

(a)

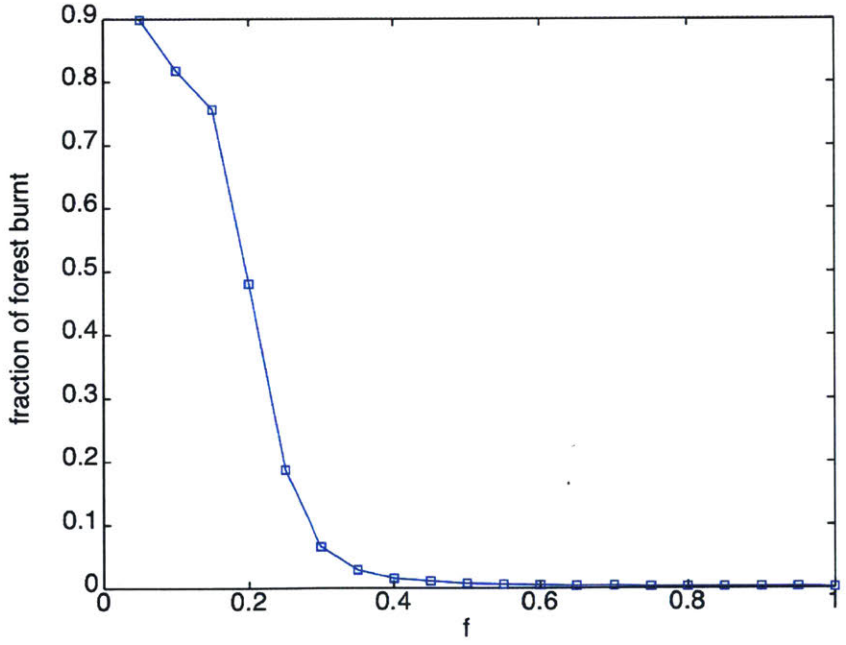

(b)

Figure 3-2: The fraction of the forest burnt under FTI and RNT policies for a discrete time model of fire process with $\alpha = 0.1, \beta = 0.99$. (a) FTI policy as a function inter arrival times τ. The process is unstable for $\tau > 4$. (b) RNT policy as a function of fraction f of boundary nodes treated by robotic vehicles. The graph shows a sharp transition from unstable to stable regimes around $f = 0.3$

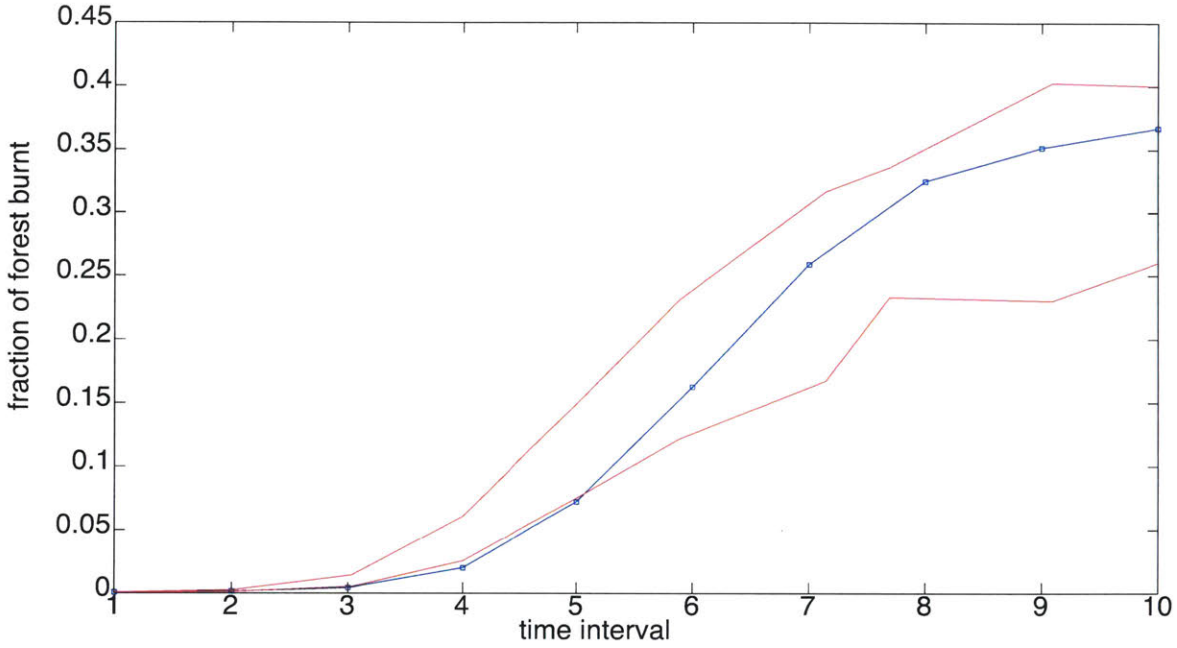

Figure 3-3: Comparison between the RNT and the FTI policies when $f = 1/\tau$ for the discrete time model of fire process with $\alpha = 0.1, \beta = 0.99$. The FTI policy (blue) for different time intervals τs is bounded above and below by the RNT policy (dashed) with number of vehicles $n = [Z/\tau]$ and $n = [Z/\tau]+1$. As τ is an integer variable in the discrete time model, $[\cdot]$ denotes the greatest integer function. Z is the total number of burning boundary nodes. Stability under the RNT policy ensures the stability under the equivalent FTI policy.

policy, the expected number of boundary nodes after m treatments is bounded by $E[Z_f(m\tau)] \leq (3p)^{m\tau-m}[3(p-\Delta p)]^m E[Z_r(0)]$. This bound has been obtained by noting that the boundary grows at rate proportional to p when no vehicles are present, and at rate $p - \Delta p$ otherwise. Let $E[Z_r(t)]_{max}$ denote the maximum expected value of sequence $\{Z_r(t)\}$ and let $E[Z_f(t)]_{max}$ be the corresponding maximum for the sequence $\{Z_f(t)\}$. At time $t = m\tau$, if we want $E[Z_f(t)]_{max} \leq E[Z_r(t)]_{max}$ starting with the same initial condition, then $(3p)^{m\tau-m}[3(p-\Delta p)]^m \leq [3(p - f\Delta p)]^{m\tau}$. The result follows by taking the limit $m \to \infty$ and using the fact that $(1-x)^y \geq 1 - xy$ when $0 < x, y < 1$. In particular, because $E[Z_f(t)] \leq E[Z_r(t)]_{max}$, the boundedness of the RNT policy ensures the boundedness of the FTI policy if $\tau \leq 1/f$ □

It is possible to define a policy that is a combination of the RNT and the FTI policies, and does not utilize all the vehicles at a given time, but instead uses a fraction of available vehicles for treatment at a particular time, while reserving the rest to be used at a later time. The following corollary gives technical condition when such a combined policy is stabilizing.

Corollary 3.4. *An unstable spreading process can be stabilized by a random node treatment policy in conjunction with finite time interval policy if* $q = p - \frac{f}{\tau}\ \Delta p < p_c$

3.2 Optimal policy

In the previous section, we described heuristic control policies that could stabilize an unstable fire process when certain technical conditions were satisfied. However, the policies were not optimal. In this section we are interested in developing optimal control policies for stabilizing the fire process. The key quantities of interest for defining optimality are (i) the number of nodes that should be treated by a control policy, and (ii) the location of the nodes that should be treated. We define the number of nodes to be treated as the *resource* or the *control effort* used by the control policy at every time step. In addition, if the resource available is finite, then the policy might allocate the resource to certain nodes *preferentially*; *i.e.* treat certain nodes with preference as opposed to treating all nodes uniformly. This leads us to a Preferential Node Treatment (PNT) policy that is defined below.

Definition 3.3 (Preferential node treatment (PNT) policy). *Given an unstable fire process with parameter* $p \geq p_c$*, select each node for treatment at time instant* t *with a Bernoulli probability,*

$$q_t = \min\{(1 - \frac{p_c}{p})\frac{d_i Z_t}{\sum_{i=1}^{Z_t} d_i}, 1\}$$

where, Z_t *are the number of boundary nodes at time instant* t*, and* d_i *is the outgoing degree of node* i*, with* $1 \leq i \leq Z_t$*.*

At every time step t, the PNT policy defined above treats nodes with unequal probability q_t proportional to their *outgoing degree*. The outgoing degree, d_i, for a

given burning node is the total number of healthy (green) nodes connected to it. It should be noted that if $d_i = 0$, then the node is not a boundary node. Figure 3-4 shows one particular realization of the fire process, and provides an example for node treatments under the PNT policy. The properties of the PNT policy are formalized below.

Theorem 3.5 (Stability and optimality of the PNT policy). *For an unstable fire process with parameter $p > p_c$, a preferential node treatment policy stabilizes the fire process almost surely. Further more, the policy is optimal in resource allocation and control effort.*

Remark: The PNT policy has three features - (i) Higher the value of p, larger are the expected number of nodes that are treated. As $p \to p_c$, the expected number of nodes that are treated go to zero (ii) a node with higher outgoing degree has a higher chance of getting treated as compared to one with a lower degree, and (iii) p_c encapsulates the structure of the graph on which the fire process is defined. For $\mathbb{Z}^2$, $p_c = 1/2$. Thus if $p = 1$, then at least half the total number of boundary red nodes need to be treated for achieving stability.

The rest of the chapter is concerned with proving that the PNT policy is indeed stabilizing and optimal. The proof consists of two parts. In the first part, in Subsection 3.2.1, we consider the resource allocation question: *given any finite amount of fire fighting resource, R, how should it be allocated among the burning nodes?* In the second part, in Subsection 3.2.2, we consider the control effort question: *what is the minimum value of this resource, R^*, that guarantees stability of the fire process?* The proof of Theorem 3.5 is then completed in Subsection 3.2.3 by combining the results obtained from the earlier two subsections.

In the discussion to follow, we switch between the continuous and discrete time models as required based on ease of description of the results for the fire process, while noting that the results derived in one regime easily extends into the other. Whenever we use the continuous time description, without the loss of generality we assume that $\lambda = 1$. We also ignore the effect of competition between spreading and

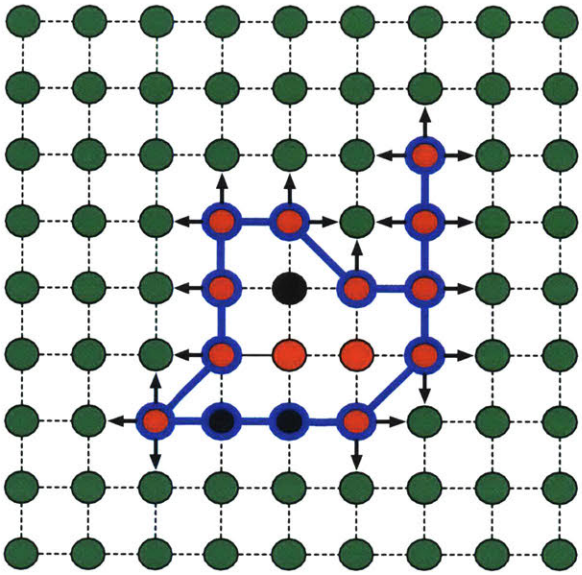

Figure 3-4: A particular realization of fire process and the PNT control policy. The blue polygon denotes the boundary of the fire process at some particular time instant t. The red boundary nodes are capable of spreading fire to neighboring green nodes, thus $Z_t = 11$. The directed arrows from red to green nodes show the edges along which the fire process propagates, thus $\sum_{i=1}^{Z_t} d_i = 20$. If $p = 0.75$, the (bottom) left most red boundary node is selected for treatment by the PNT policy with probability $q_t = \frac{1}{3} \times 3 \times \frac{11}{20} = 0.55$.

burning times by assuming that $\lambda \gg \mu$, which implies that the all the boundary nodes are burning (red). It should be noted that this assumption does not affect the optimality properties of the policy; it only simplifies the description of the policy.

3.2.1 Optimal Resource Allocation

We first state few properties of the exponential random variables which we later utilize for developing policies for the fire process. Due to memoryless property of the exponential random variable, if we observe the fire process at any time instant, the time for which a particular node has been burning is independent of the time for which it will burn in the future. Furthermore, the time for which a burning node continues to burn is also an exponential random variable with the same distribution. We also use the following properties for a set of independent exponential random

variables.

Lemma 3.6. *If $X_1, X_2, \cdots, X_n$ are independent and identically distributed exponential random variables with rate 1. Let $Y = \min\{X_1, X_2, \cdots, X_n\}$. Then,*

(i) Y is exponential random variable with rate n.

(ii) $\mathbb{P}(Y = X_i) = \frac{1}{n}$, for all i.

Proof. Let $P_1, P_2, \cdots P_n$ be n independent Poisson processes each with rate 1. In a Poisson process, the inter arrival times are exponentially distributed with rate 1. Then, the merged process $P = \sum_i^n P_i$ is also a Poisson process whose rate is n. The quantity Y is equivalent to the first arrival in the merged process which is exponential distributed with rate n. Similarly, the probability that the first arrival in the merged process occurs from process P_i is $1/n$. Alternatively,

$$\begin{aligned}\mathbb{P}(Y = X_i, Y \geq x) &= \int_x^\infty \mathbb{P}(Y \geq z | Y = X_i)\ f_{X_i}(z)\ dz \\ &= \int_x^\infty \prod_{j \neq i} \mathbb{P}(Y \geq z)\ e^{-z}\ dz = \int_x^\infty e^{-nz}\ dz = \frac{1}{n}\ e^{-nx}\end{aligned}$$

Summing $\dfrac{e^{-nx}}{n}$ over all i yields $\mathbb{P}(Y \geq x) = e^{-nx}$ which is density function of an exponential with rate n. If we integrate over the entire support of the density function by substituting $x = 0$, it follows that $\mathbb{P}(Y = X_i) = \int_0^\infty e^{-nz}\ dz = \frac{1}{n}$. □

We now apply the above results to the fire process. We observe that the red nodes are capable of spreading fire along their outgoing edges to the green nodes that are connected to them. Along every such edge, the time it requires to spread fire has an exponential distribution. Using Lemma 3.6, it follows that the first edge along which fire spreads has a uniform distribution among all the edges; spreading along any edge is equally likely. Thus, at any given time instant t, if we have a resource of strength R_t that can be used to reduce the spread of fire, the optimal policy that minimizes the variance of the fire spread is to distribute the resource R_t uniformly along all the edges of the boundary nodes of the fire process.

Lemma 3.7. *Given fire fighting resource R_t, the optimal policy (that minimizes variance of spreading) is one that distributes the resource uniformly to all the edges along which the fire can spread. In particular, every edge receives resource R_t/E_t, where E_t are the number of outgoing edges from the burning boundary nodes at time t.*

Proof. Let I_i be the indicator random variable that takes value 1 if a particular edge i propagates fire and 0 otherwise. The total number of edges that propagate fire in the next time step are $S = \sum_{i=1}^{E_t} I_i$. We know that I_i are i.i.d Bernoulli random variables with parameter p. Let u_i be the resource given to each edge which results in reduction of the spread probability to $\bar{p}_i = p - u_i$. We are interested in finding resource allocation u_i that minimizes variance of S with a bounded resource constraint $u_1 + u_2 + \cdots + u_{E_t} \leq R_t$. Minimizing variance is same as minimizing second moment of S, thus the optimization problem is to

$$\min_u \sum_{i=1}^{E_t} \bar{p}^2 \quad \text{such that} \quad \sum_{i=1}^{E_t} u_i \leq R_t$$

Solution of the optimization problem can be found by introducing a Lagrange multiplier λ,

$$\mathcal{J} = \sum_{i=1}^{E_t} \bar{p}^2 + \lambda(\sum_{i=1}^{E_t} u_i - R_t)$$
$$\min \mathcal{J} \implies \frac{\partial J}{\partial u} = 0,\ \lambda \frac{\partial J}{\partial \lambda} = 0 \implies u_i = \frac{R_t}{E_t}, \forall i$$

□

There are two issues in implementing the above policy directly for the fire process- (i) Even though the fire process spreads along the edges that are connected to the burning nodes at the boundary, the edges cannot be treated. We can only treat (or delete) a burning node, and thereby control the fire process. (ii) The robotic vehicles might not be able to reduce the parameters (α, β) of the fire process continuously. This leads us to define a modified policy as follows. If a particular node has a outgoing degree d_i, then an equivalent policy is to allocate a resource of $\frac{d_i R_t}{E_t}$ to that particular

node. If Z_t are the boundary red nodes at time t, then number of outgoing edges is equal to the sum of degrees of all boundary red nodes, *i.e.* $E_t = \sum_{i=1}^{Z_t} d_i$. To account for the discrete action of the robotic vehicles, we assume that if we choose to treat a particular node, it is deleted (or burnt) at the next time step. With these two modifications, we can define a randomized node treatment policy that allocates the same expected amount of resource as compared to the policy described in Lemma 3.7 as follows,

Lemma 3.8. *The expected amount of resource allocated by a randomized policy that treats every node with Bernoulli probability*

$$q = \min\{\frac{Rd_i}{\sum_{i=1}^{Z_t} d_i}, 1\}$$

is upper bounded by that allocated by policy described in Lemma 3.7.

Proof. Let I_i be an indicator random variable that takes value 1 if a particular node is treated and 0 otherwise. Then, the total resource allocated or the number of nodes that get treated are $\sum_{i=1}^{Z_t} I_i$ whose expectation is less than $\sum_{i=1}^{Z_t} \frac{Rd_i}{\sum_{i=1}^{Z_t} d_i} = R$. We have used the fact that $E[\min\{X, Y\}] \leq \min\{E[X], E[Y]\}$ for any two random variables X, Y. □

As the randomized policy is upper bounded, at optimality, the net resource allocated by the two policies described in Lemmas 3.7 and 3.8 are the same. The intuition behind the randomized policy is that if any of the edges of a burning boundary node is selected for treatment, then the corresponding node is also assumed to be treated. Clearly, under such a policy a node with higher outgoing degree has a higher chance of getting selected. The $\min(\cdot)$ is due to the fact that probability parameter p is positive, and it is not possible to allocate a resource to a node to drive this parameter below 0.

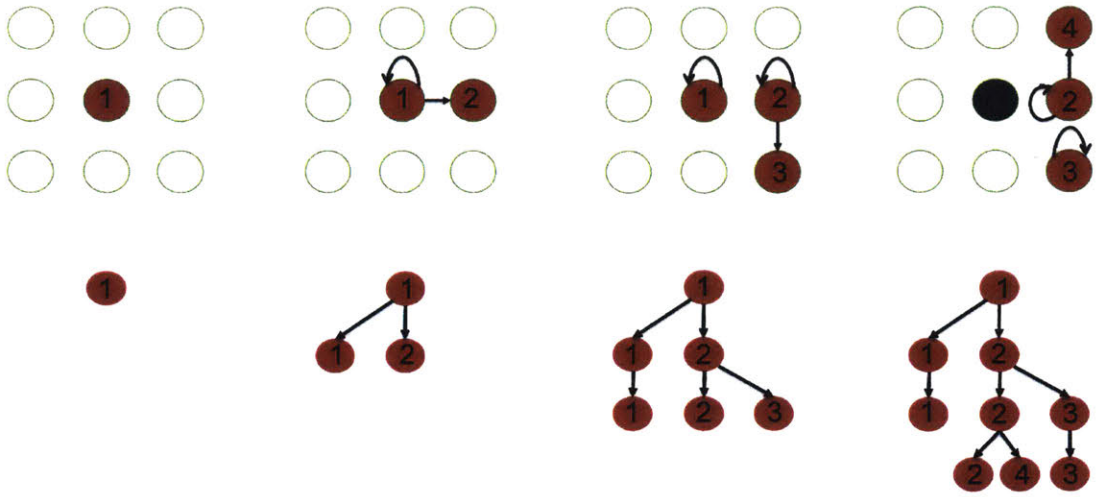

Figure 3-5: The mapping of the fire process to an equivalent tree description on a 2D lattice. At $t = 0$, there is one red node. At $t = 1$, the red node remains burning and propagates fire to a neighboring green node, thus giving birth to two children in the tree description. At $t = 3$, the red node at origin remains burning giving birth to itself while the other burning node gives rise to two children. At $t = 4$, the node at the origin burns out and thus there is no further progeny for the left most branch in the tree description.

3.2.2 Optimal Control Effort

In the previous subsection, we discussed how to optimally distribute any given resource R. In this subsection, we discuss the minimum amount of this resource, R^*, that is needed to stabilize the fire process almost surely. To do so we use several concepts from branching processes and percolation on irregular trees - (i) We construct an equivalent tree description of the fire process on a 2D lattice. (ii) We observe that the generated tree could be obtained from the progeny of a branching process, and that branching process and percolation on a tree are equivalent concepts. (iii) We use the notion of branching number for an irregular tree, which is the counterpart of the degree of a regular tree, and observe that branching number is related to the percolation threshold. (iv) We provide technical conditions for the extinction of the branching process constructed from the fire process under a control policy.

Before we begin with constructing an equivalent tree description of the fire process, we provide few definitions. A *tree* is a connected graph with no cycles. The topmost

node of the tree is called the *root* of the tree. The number of leafs (or children) of a particular node of the tree is called the degree of the node. If the degree of every node of the tree is the same it is called a *regular* tree, otherwise the tree is *irregular*. The vertical distance from the root is called the *generation or depth* of the tree.

Figure 3-5 shows the procedure for tree construction starting with one burning node. The construction uses two notions - (i) if a burning node at the current time step continues to burn at the next time step, it gives birth to itself, and (ii) the number of additional children the burning node produces at next time step is the number of healthy (green) nodes that caught fire through this node. The key point is that we keep track of the path through which a healthy (green) node caught fire from a burning (red) node. On the other hand, if the burning node burns out at the next time step, no additional nodes are added along that path. It should be noted that the number of nodes at any given generation in the tree description are precisely the boundary burning nodes in the graph description of fire process. In addition, it can be easily seen that such a construction produces an irregular tree. We note that such an irregular tree can also be obtained as a result of a branching process, a short background for which is provided below.

Branching Process: A branching process (also known as Galton-Watson branching process) is a stochastic process that models population growth. The setting of the process is as follows. At time $t = 0$, there is $Z_0 = 1$ individual (or node) which gives birth to a random number of children Z_1 at time $t = 1$, according to a known probability distribution $\mathcal{F}$. Similarly at $t = 2$, each individual among Z_1 gives birth to a random number of children according to the same probability distribution $\mathcal{F}$. The (level or) time t is known as the generation of the process. A key question that one is concerned with is whether the progeny of the process dies out, *i.e.* after a generation the population becomes extinct and no more children are produced (an inherent assumption that is made is that at each generation, the individuals at that generation can produce children only once).

In particular, let $\mathcal{B}$ be a branching process with children distribution $\mathcal{F} = \mathbb{P}_k$ for

$k = 0, 1, 2, \ldots$ (number of children produced are k with probability $\mathbb{P}_k$). Let Z_t be the progeny of the process at generation t. Define η to be the extinction probability of the process with $\eta = \lim_{t\to\infty} \mathbb{P}(Z_t = 0)$. Let $g(x) = \sum_k x^k \mathbb{P}_k$ be the moment generating function of $\mathcal{B}$, and let $\zeta = \sum_k k\mathbb{P}_k$ be the expectation of the children distribution. We state the key result from the theory of branching process below.

Theorem 3.9 (Branching process [65]). *The extinction probability η of the process $\mathcal{B}$ is the smallest non-negative root of the equation $x = g(x)$. If $\zeta < 1$, then $\eta = 1$.*

Proof. Let A_t denote the event that $Z_t = 0$, and let $\mathbb{P}(A_t) = \eta_t$. Clearly, $A_t \subset A_{t+1}$, and thus A_t is an increasing event. Thus by continuity of probabilities, if $A = \cup_{t=1}^{\infty} A_t$, then $\mathbb{P}(A)$ exits and $\mathbb{P}(A) = \lim_{t\to\infty} \eta_t = \eta$. We first show if $\zeta < 1$, then $\eta = 1$. Note that $E[Z_t] = \zeta^t$. Then, by Markov inequality, $\mathbb{P}(Z_t \geq 1) \leq \zeta^t$. It follows that,

$$\sum_{t=1}^{\infty} \mathbb{P}(Z_t \geq 1) \leq \sum_{t=1}^{\infty} \zeta^t = \frac{1}{1-\zeta} < \infty$$

if $\zeta < 1$. Thus, by Borel-Cantelli lemma probability that the event $\{Z_t \geq 1\}$ happens infinity often is 0. For every ω, the event $Z_t(\omega) \geq 1$ occurs only finitely, which implies $\exists T(\omega)$ such that $\forall t > T(\omega), Z_t(\omega) = 0$. □

Theorem 3.9 states that the branching process dies out almost surely (with probability 1) is the expected number of children of an individual/node is less than one, $\zeta < 1$. If $\zeta > 1$, then there is a non-zero probability that the branching process never dies out and continues for ever (see Figure 3-6).

We also define a branching process with deletion, $\mathcal{B}_{\mathcal{D}}$, as follows. Let $\mathcal{B}_{\mathcal{D}}$ be a branching process with the expected value of the children distribution, $E[\mathcal{F}] = \zeta_D$. In addition, at every generation, we retain each node with probability r and delete it with probability $1 - r$. Let η_D be the extinction probability and $g_D(x)$ the moment generating function of process $\mathcal{B}_{\mathcal{D}}$ respectively. The following corollary follows from Theorem 3.9 that gives technical conditions for extinction of $\mathcal{B}_{\mathcal{D}}$.

Corollary 3.10 (Branching process with deletion). *The extinction probability η_D of the process $\mathcal{B}_{\mathcal{D}}$ is the smallest non-negative root of the equation $x = g_D(x^r)$. If*

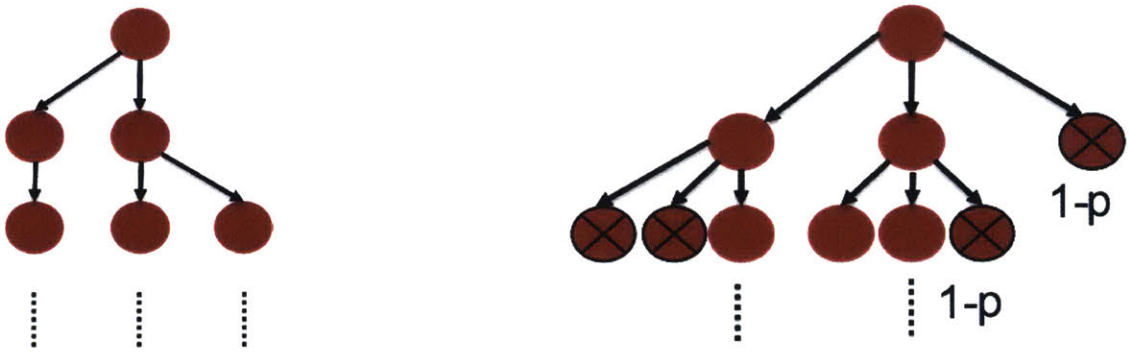

(a) (b)

Figure 3-6: A schematic of branching process and percolation on a tree. (a) Starting from the parent node, the progeny of the branching process dies out almost surely (with probability 1) if expected value of the number of children produced at each generation is less than one. (b) A percolation on a regular tree is equivalent to the branching processes in which nodes are retained with probability p and deleted with probability $1-p$. If the degree of regular tree is 3, then the tree does not percolate almost surely if $p < 1/3$.

$r\ \zeta_D < 1$, *then* $\eta_D = 1$.

It should be noted that in the branching process $\mathcal{B}_{\mathcal{D}}$, it could be possible that $\zeta_D > 1$, and the process would continue to branch for ever. However, by choosing an appropriate deletion probability r, the expected number of children for every node $r\zeta_D$ could be driven below one, thereby making the process die out almost surely.

Percolation on Trees: We now provide a short introduction to the theory of percolation on irregular trees and define the notion of *branching number*, which would be applied later in the chapter to characterize the fire process. We saw earlier that a regular tree is one in which every node has a constant degree. Consequently, the knowledge of the degree is sufficient to specify a regular tree. For example, a binary tree is one in which every node has degree equal to two. *Branching number* (denoted as B_r), generalizes this notion of a constant degree for any tree, in particular an irregular tree. Roughly speaking, the branching number of an irregular tree is the average or the constant degree for the entire tree. We provide a short background to the available results on the branching number of the tree below, based on the

interpretation of random walks on the tree. However, it should be noted that there are several interpretations of the branching number of a tree and we refer the reader to [66, 126] for details.

Let $\mathbb{T}$ be an infinite irregular tree, *i.e.* its children extend to infinity. Consider a random walk on $\mathbb{T}$, starting at the root with the following property. Given any node with m children, the random walk returns to its parent node with probability $\frac{b}{m+b}$ and jumps to any of the m children with probability $\frac{1}{m+b}$, where b is a parameter. There exists a critical value of parameter $b_c = b_c(\mathbb{T})$ such that for $b > b_c$, the walk is recurrent, *i.e.* returns to the root infinitely often and for $b < b_c$, the random walk is transient, *i.e.* it has a finite probability of never returning to the root. This critical threshold b_c is same as the branching number of the irregular tree.

Theorem 3.11 (Theorem 4.3 in [126]). *The critical threshold b_c is the branching number of irregular tree $\mathbb{T}$, $B_r(\mathbb{T}) = b_c$.*

We now define the notion of percolation on an irregular tree as follows.

Definition 3.4 (Percolation on tree). *Given an irregular tree $\mathbb{T}$, consider a process in which at every generation, a node is retained with probability p and deleted with probability $1 - p$. Then, there exists a critical threshold $p_c = p_c(\mathbb{T})$, such that if $p > p_c(\mathbb{T})$, the tree percolates, i.e. the root is connected to a node at infinity. On the other hand, if $p < p_c(\mathbb{T})$, the root gets disconnected from the node at infinity almost surely.*

Furthermore, it turns out that the critical threshold for percolation p_c for an irregular tree and its branching number are closely related.

Theorem 3.12 (Theorem 6.2 in [126]). *The critical threshold p_c satisfies the relation,*

$$p_c(\mathbb{T}) = \frac{1}{B_r(\mathbb{T})}.$$

As a final remark it should be noted that all results for irregular trees are also applicable for regular trees.

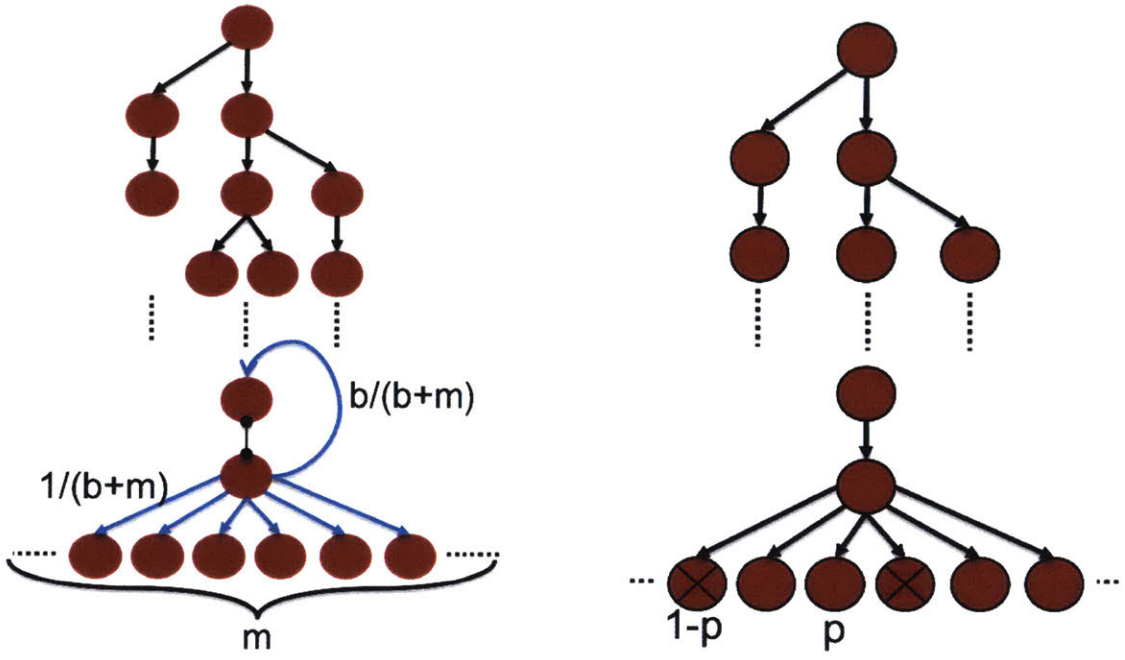

(a) (b)

Figure 3-7: Graphical representations of Theorems 3.11 and 3.12. (a) Notion of branching number of irregular trees. Starting from the any node, a random walk jumps to any of its m children with probability $\frac{1}{b+m}$, or returns to the its parent node with probability $\frac{b}{b+m}$. There exists a critical threshold b_c, such that if $b < b_c$, the random walk escapes to infinity, and if $b > b_c$, it returns to the root node infinitely often. b_c is defined as the branching number for the irregular tree. (b) Percolation on trees. At each generation, let a node be retained with probability p and deleted with probability $1-p$. As we increase p, there exists a critical threshold p_c such that, if $p < p_c$, the tree is disconnected almost surely and if $p > p_c$, the tree percolates, *i.e.* there exists a path from the root node to infinity almost surely. This critical probability and the branching number are closely related: $p_c = \frac{1}{b_c}$.

Application to fire process: We now apply the concepts described thus far from the theory of branching process and percolation on trees to characterize the fire process. Recall that earlier we converted the fire process to an equivalent tree description. However, the key issue in directly applying the results from theory of branching process is that, in the case of fire process, the children distribution of the constructed irregular tree is unknown. However, we could use the notion of branching number of irregular trees to estimate the expected children distribution.

We first note that the irregular tree generated by a branching process $\mathcal{B}$ is equiva-

lent to the tree that generated by percolation on a regular tree $\mathcal{T}_{\mathcal{R}}$. In particular, let the expected value of the children distribution for $\mathcal{B}$ be ζ, and let the degree of the $\mathcal{T}_{\mathcal{R}}$ be d. For percolation on $\mathcal{T}_{\mathcal{R}}$, we delete nodes with probability $1-p$ (and retain with probability p). The two processes are equivalent if $\zeta = dp$, because both the processes produce the same expected number of nodes in every generation.

We could extend the note above to irregular trees as well. In particular, consider percolation on an irregular tree with branching number B_r, in which a node is retained with probability p and deleted with probability $1-p$. The percolation condition for this process is equivalent to the extinction probability threshold for a tree that is generated by a branching process $\mathcal{B}$, if the expected children distribution, $\zeta = pB_r$. In particular, if $\zeta = pB_r < 1$, the branching process dies out almost surely and the tree does not percolate. It should be noted that as $B_r = \frac{1}{p_c}$, this equivalence just follows from definition of percolation, *i.e.* if $p < p_c$, there is no path from the root node to infinity.

Finally, consider two processes, (i) percolation on an irregular tree with branching number pB_r, with a retainment probability of every node with probability r and deletion with probability $1-r$, and (ii) a branching process with deletion $\mathcal{B}_{\mathcal{D}}$, with an expected number of children $\zeta = pB_r$ for every node, along with a node retainment probability of r. From Corollary 3.10, the branching process $\mathcal{B}_{\mathcal{D}}$ dies out almost surely if $prB_r < 1$. The process (i) has a simple interpretation for the control of fire process; for the irregular tree constructed from the fire process, the burning nodes spread fire to their healthy neighbors with probability p, the irregular tree itself has a branching number B_r, and an independent control policy deletes nodes at every generation (independently of other nodes) with probability r. Thus, we can find a control policy that stabilizes an unstable fire process almost surely, if we can find a bound on the branching number.

Let $\mathcal{T}_{\mathcal{F}}$ be the irregular tree constructed from the fire process. Recall from Chapter 2 that for the fire process on a 2D lattice, its stability threshold is lower bounded by the percolation threshold for the 2D lattice; $p_c(\mathcal{T}_{\mathcal{F}}) \geq p_c(\mathbb{Z}^2)$. Also, the relation $B_r(\mathcal{T}_{\mathcal{F}}) = \frac{1}{p_c(\mathcal{T}_{\mathcal{F}})}$ implies that $B_r(\mathcal{T}_{\mathcal{F}}) \leq p_c(\mathbb{Z}^2)$. Therefore, an unstable fire process

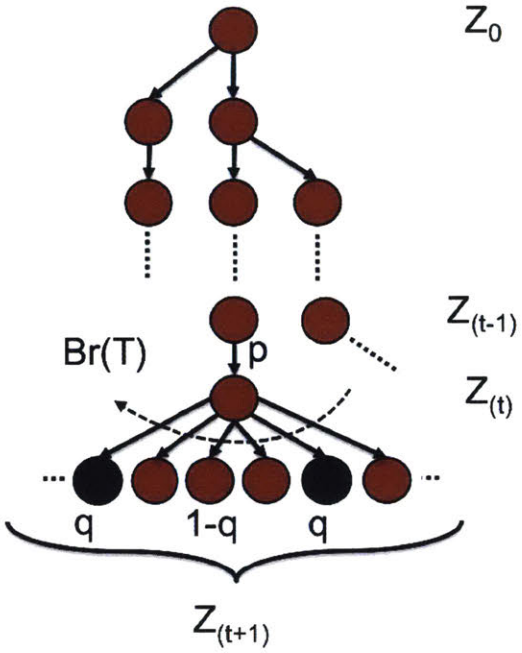

Figure 3-8: An equivalent branching process description for the fire spreading process on lattices. A node spreads fire to its neighbors with probability p. The equivalent number of neighbor a node is attached to is given by the branching number $Br(\mathcal{T}_{\mathcal{F}})$. The PNT policy removes every affected node with Bernoulli probability q.

with $\frac{p}{p_c(\mathbb{Z}^2)} > 1$, can be stabilized almost surely by a control policy that retains nodes with probability r and deletes with probability $1-r$ if the quantity $r\frac{p}{p_c(\mathbb{Z}^2)} \leq 1$, *i.e.* $r \leq \frac{p_c(\mathbb{Z}^2)}{p}$. Furthermore, total the number of nodes that get deleted at a generation t in the control policy is equal to $(1-r)Z_t$. Consequently, the resource R_t, that is needed at generation t to guarantee stability of an unstable fire process is minimized when $r = \frac{p_c}{p}$, implying that the minimum resource needed to stabilize an unstable fire process is $R_t^* = (1 - \frac{p_c}{p})Z_t$.

3.2.3 Proof of Optimality of PNT policy

We summarize the arguments presented in the previous subsections and complete the proof of Theorem 3.5.

Proof. Starting from the fire process on the 2D lattice, we constructed an equivalent

irregular tree description in which the nodes at a generation t, represent all the boundary burning nodes of the fire process (Z_t). Then, we argued that the tree description is equivalent to a branching process description with same number of expected nodes at each generation. We also showed that a policy that deletes nodes at each generation for this branching process, and ensures that the branching process dies out almost surely, uses a minimum resource $R_t^* = (1 - \frac{p_c}{p})Z_t$.

We first claim that the PNT policy uses the same amount of resource R_t^* at every generation t. From Lemma 3.8, it follows that the resource used by the PNT policy at every generation is at most R_t^*. Furthermore, the PNT policy distributes this resource among all burning boundary nodes, proportional to their outgoing degree d_i, which is optimal. As the irregular tree and the branching process description are constructed from the fire process, almost sure extinction of the branching process implies that the fire process is stable, *i.e.* $\limsup_{t\to\infty} X_t(p) = 0$ almost surely. □

3.3 Summary

In this chapter, we considered closed loop control of spreading processes. In the first part of the chapter, we characterized heuristic control policies to gain insights. The effect of control on the spreading process results in a shift in critical probability threshold. In the second part of the chapter, we developed a randomized node treatment policy that stabilizes an unstable fire process almost surely. Using tools from the theory of branching process and percolation on trees, we showed that this policy is indeed stabilizing and optimal.

Chapter 4

Control of Smart Manufacturing Processes

This chapter discusses stochastic scheduling techniques for throughput maximization in smart factories. Industry 4.0, considered as the new industrial revolution envisions smart factories with modular architectures, consisting of several individual work stations that are served by automated guided vehicles (AGVs). The work stations consist of machines with multiple capabilities. In manufacturing terminology, a capability is the ability of the machine to perform a specific manufacturing process (for instance cutting, welding, soldering, milling etc.). The work order required for a particular product determines the network or connectivity structure between individual work stations. In addition to work stations and AGVs, the shop floor also consists of multiple supply and shipping units to aid the manufacturing process. Figure 4-1 shows one such layout of the smart factory. The problem that is addressed in this chapter is how (when or at what rate) to schedule individual machines and the AGVs in order to maximize the overall throughput of the smart factory.

Towards this end, the modeling aspects of the smart factory are described in Section 4.1. In the Section 4.2, the inherent *structure* of the problem formulation is discussed and it is shown how this structure leads to a stochastic scheduling algorithm. The application of the scheduling methodology to two prototypical examples is also presented.

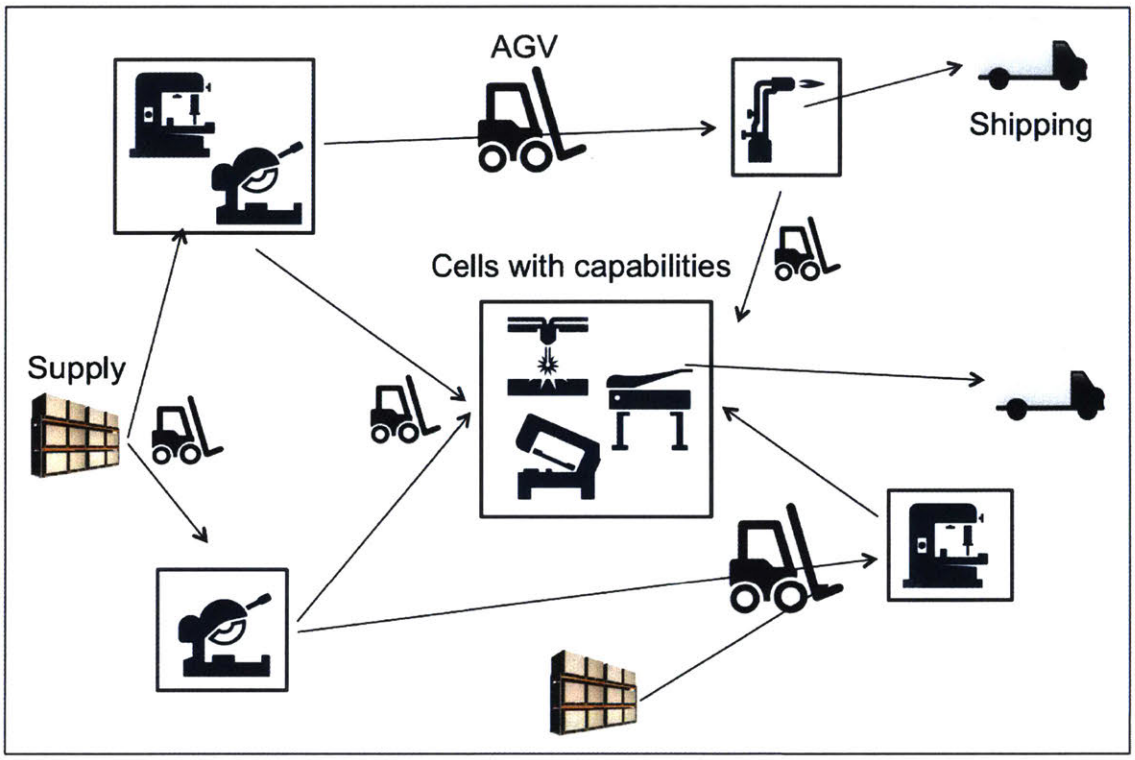

Figure 4-1: A schematic of the modern factory floor. The factory floor consists of modular cells with multiple capabilities (such as cutting, welding, drilling, etc.). The cells are connected by automated guided vehicles that transfer processed products from one cell to another. In addition, the floor consists of multiple supply and shipping units.

4.1 Modeling

We model the shop floor of the modern factory as a directed graph $G(N, E)$, where the nodes N represent the set of machines on the factory floor. We associate with every machine $i \in N$, (i) a set of capabilities $j \in \mathcal{J}$ (eg. soldering, welding etc.) that the machine is capable of performing, (ii) a set of input queues of preprocessed products Q_{ij}^{in} and, (iii) a set of output queues Q_{ij}^{out} of finished products. For a given machine with a particular capability, we also associate a time varying maximum service rate, $\mu_{ij}^{max}(t)$, defined as the maximum rate at which the machine is capable of processing an input product. Depending on operation capabilities of the machine, this quantity can change with time dynamically. The input and output queues have finite capacity that we denote by B_{ij}. Without loss of generality, we assume that

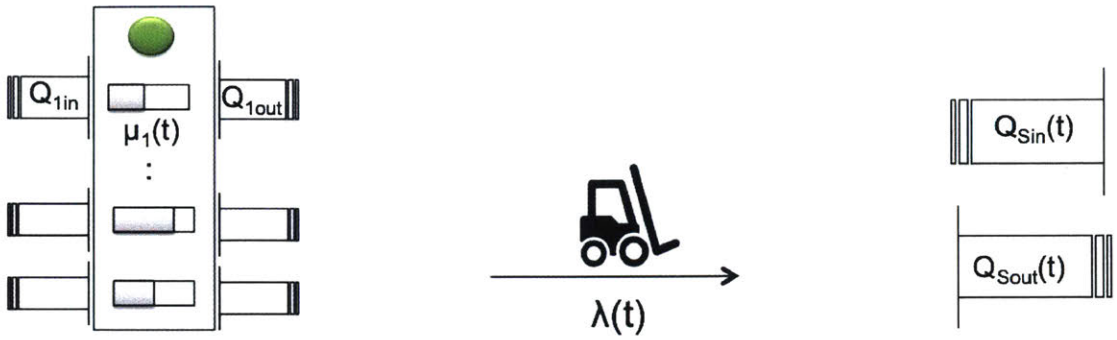

(a) (b) (c)

Figure 4-2: Building units of the smart factory shop floor. (a) Machines or Cells with multiple capabilities modeled as input-output queues with a finite service rate, (b) an AGV with a finite transfer rate, and (c) supply and shipping queues

a machine with multiple capabilities can service at most one product from the set of input queues. It should be noted that if a machine is capable of processing more than one queue simultaneously, it is equivalent to increasing the count of machines and thereby increasing the node set N. In this context, the individual work stations should be thought of as smart CNC machines, which perform one task at a given time even though they are capable of processing many tasks.

The edge set E in the graph represents the connectivity between individual machines and denotes the type of products individual machines can accept and produce. We assume that the product transfers between the output and input queues of individual machines are performed by automated guided vehicles (AGVs). As the AGVs have limited capacity and finite speed, we associate with every edge $e \in E$, a maximum service rate, $\lambda_e^{max}(t)$, that represents the maximum rate at which jobs could be transferred from an output queue to an input queue by an AGV along an edge e. We note that there could be regions on the factory floor where a single AGV could be operating between several edges in the edge set E.

In addition, the factory floor also consists of supply and shipping units. The supply units are modeled as *sources* or input queues Q_{Sin}. Similarly, the shipping units are modeled as *sinks* or output queues Q_{Sout}. We assume that there are no processing times associated with input and output queues.

4.2 Stochastic Scheduling Formulation

Given the aforementioned model of the factory floor, the problem is to develop a scheduling algorithm for machines and the AGVs. For the queue theoretic formulation we define stability as the following.

Definition 4.1 (Stability). *A queue theoretic system is stable if all the queues are bounded,* $\exists M > 0$ *such that* $Q_{ij}(t) < M, \forall i, j$ *and* $\forall t > 0$.

Problem Statement: Given a connected graph $G(V, E)$, and associated maximum service rates μ_{ij}^{max} and maximum transfer rates $\lambda_e^{max}(t)$, develop a scheduling algorithm for individual machine operations and transfers, such that the overall system is stable and the throughput is maximized.

We propose a stochastic scheduling algorithm for the problem. For the ease of understanding the problem structure, consider a very simple example shown in Figure 4-3, which consists of machine with a single capability. The equivalent graph structure for this simple factory can be obtained by replacing the machine with two nodes as shown. There are four queues which form the state space of the system. The control parameters are the three service rates of the machine ($\mu_2(t)$) and that of the AGVs ($\lambda_{12}(t), \lambda_{23}(t)$) respectively. Using a fluid limit formulation of this queue theoretic model, the evolution of the states can be described by the following dynamical equations,

$$\dot{Q}_{Sin}(t) = -\lambda_{12}(t) \tag{4.1}$$

$$\dot{Q}_{in}(t) = \lambda_{12}(t) - \mu_2(t) \tag{4.2}$$

$$\dot{Q}_{out}(t) = \mu_2(t) - \lambda_{23}(t) \tag{4.3}$$

$$\dot{Q}_{Sout}(t) = \lambda_{23}(t) \tag{4.4}$$

which can be conveniently written as,

$$\underbrace{\begin{bmatrix} \dot{Q}_1 \\ \dot{Q}_{2i} \\ \dot{Q}_{2o} \\ \dot{Q}_3 \end{bmatrix}}_{\dot{\mathbf{x}}} = \underbrace{\begin{bmatrix} -1 & 0 & 0 \\ 1 & -1 & 0 \\ 0 & 1 & -1 \\ 0 & 0 & 1 \end{bmatrix}}_{\mathbf{I}} \underbrace{\begin{bmatrix} \lambda_{12} \\ \mu_2 \\ \lambda_{23} \end{bmatrix}}_{\mathbf{u}} \tag{4.5}$$

where I is the incidence matrix of the equivalent graph, which is the matrix that describes connectivity from the nodes to the edges of a graph. $I_{xy} = 1$ and $I_{yx} = -1$ if there is a directed edge from node x to node y in the graph G, and $I_{xy} = 0$, if the nodes x and y are disconnected.

Linear programing formulation: The structure of the smart factory can be conveniently expressed in terms of the incidence matrix of the underlying connectivity graph. This enables us to solve the scheduling problem as an optimization problem by converting it to a Linear Program (LP).

$$\max \sum_{t=0}^{T} c' u(t) \quad \text{(throughput)} \tag{4.6}$$

$$x(t+1) = x(t) + \mathbf{I}\, u(t), \quad \text{(update equations)} \tag{4.7}$$

$$0 \leq x(t) \leq B \quad \text{(max queue size)} \tag{4.8}$$

$$0 \leq u(t) \leq u_{max} \quad \text{(max service rates)} \tag{4.9}$$

$\ldots$ additional linear constraints, if any

Here, T denotes the time horizon and B denotes the maximum operating capacity at a machine or work station. Depending on the context, the objective function optimizes the desired version of the throughput, which could be the averaged throughput over time horizon T, final throughput at time T, specific service or transfer rates. As we will see in the next example, additional constraints might be added depending on the operating conditions and layout of the factory.

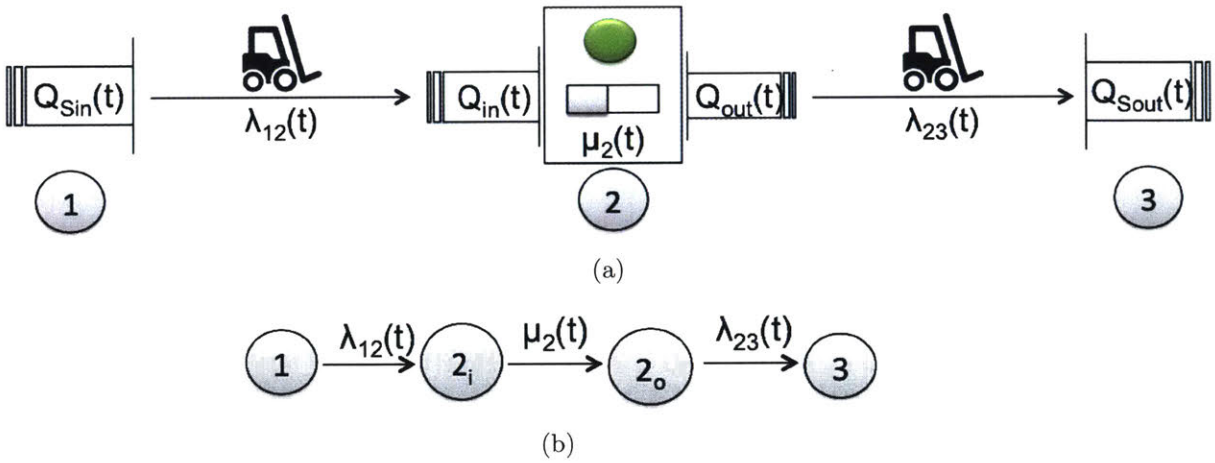

Figure 4-3: (a) A layout of a simple factory consisting of one machine with single capability operating between a supply and shipping unit, and (b) the equivalent graph description. Two independent AGVs operate on two transfer routes.

A feasible solution to the LP implies stability of the overall system as a feasible solution implies the boundedness of all queues. Given a solution to the LP, the scheduling scheme is to schedule individual work stations and AGVs at time instances t with Bernoulli probabilities $p(t)$ as follows,

$$p(t) = \left\{ \frac{\mu_2(t)}{\mu_{2,max}}, \frac{\lambda_{12}(t)}{\lambda_{12,max}}, \frac{\lambda_{23}(t)}{\lambda_{23,max}} \right\} \tag{4.10}$$

Figure 4-4 shows the implementation of the algorithm on the simplest factory layout. The figure shows four test scenarios (a) ($\lambda_{12} = 0.1, \mu_2 = 1, \lambda_{23} = 1$), (b) ($\lambda_{12} = 1, \mu_2 = 0.1, \lambda_{23} = 1$), (c) ($\lambda_{12} = 1, \mu_2 = 1, \lambda_{23} = 0.1$), and (d) ($\lambda_{12} = 1, \mu_2 = 0.2, \lambda_{23} = 0.5$). All cases have been simulated for $T = 10, B = 10$ and initial queue size $Q_1(0) = 100$. In case (a), the machine service rate μ_2 drops because it cannot produce faster than input rate λ_{12}. In case (b), the stability requirement forces λ_{23} to drop because queue lengths cannot become negative. λ_{12} remains high until the buffer is full, after which it starts dropping as well. In case (c), the machine is operating at a reduced rate, but is getting served by a fast AGV. The buffer sizes of the queues allow the system to remain operative even at higher service rates. Case (d) is a random test case, the behavior of which could be understood from cases (a-c). In (d), the

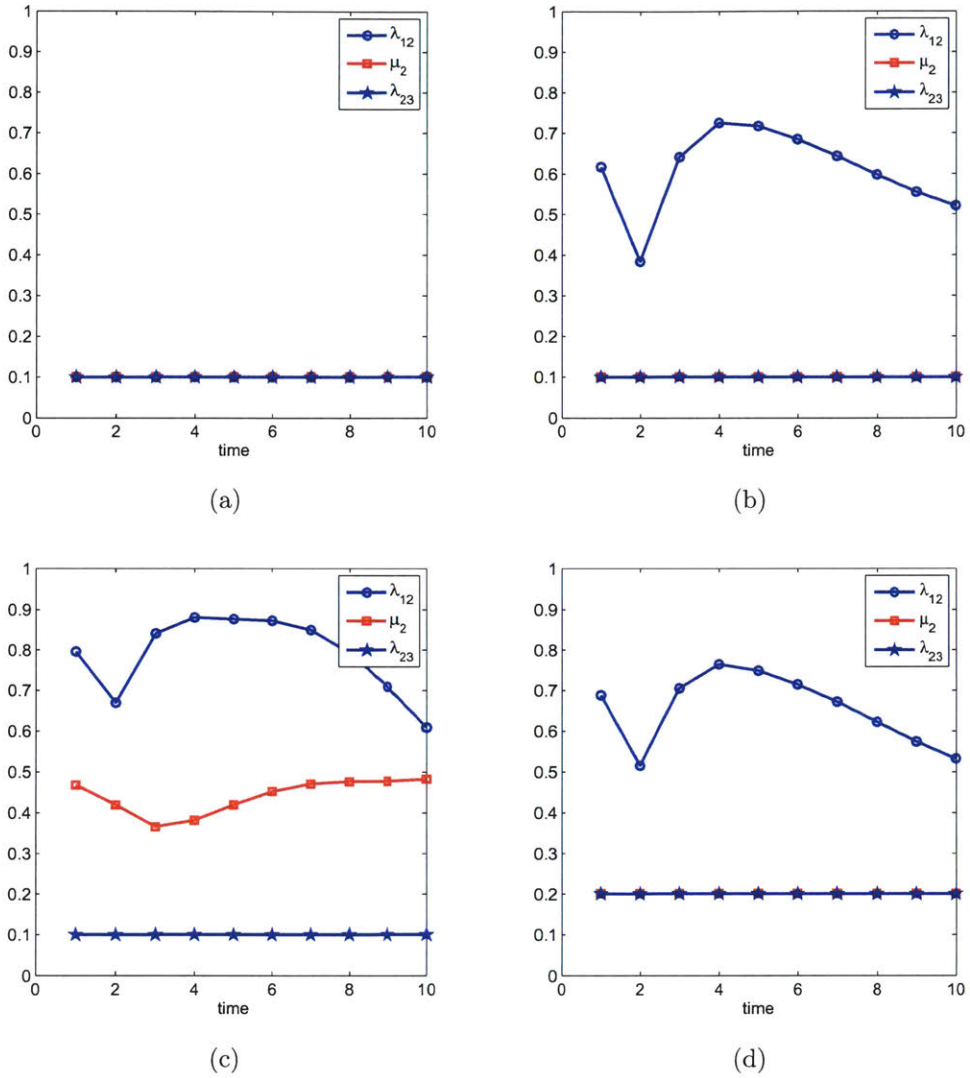

Figure 4-4: Four simulation scenarios for (a)($\lambda_{12} = 0.1, \mu_2 = 1, \lambda_{23} = 1$), (b) ($\lambda_{12} = 1, \mu_2 = 0.1, \lambda_{23} = 1$), (c) ($\lambda_{12} = 1, \mu_2 = 1, \lambda_{23} = 0.1$), and (d) ($\lambda_{12} = 1, \mu_2 = 0.2, \lambda_{23} = 0.5$). In case (a) the machine service rate μ_2 drops because it cannot produce faster than input rate λ_{12}. In case (b) the stability requirement forces λ_{23} to drop because queues cannot go negative. λ_{12} remains high till the buffer is full, after which it starts dropping as well. In case (c) the machine is operating at reduced rate, but is getting served by a fast AGV λ_{12}. The buffer size of queues, allows the system to remain operative at higher service rates. Case (d) is a random test case, which can be narrowed to cases (a-c). In (d) the machine service rate is the bottleneck, so it behaves similar to case(b)

machine service rate is the bottleneck, so it behaves similar to scenario in case (b). In all cases the queue sizes are always bounded, and system is stable. In addition, the system continues to operate at maximum possible flow rate given constraints.

Intuitively speaking, stochastic scheduling procedure discussed above avoids the NP hardness of general scheduling problems by converting exact formulations into an average cost formulation thereby making the problem mathematically tractable. Such a procedure is well suited in an industrial set ups which are subject to repetitive operations. In addition, LP formulations allow for fast implementation of the algorithm in a changing environment. As we will see in the next example, load balancing between operating agents in case of agent failure is also achieved automatically under the formulation.

Once the structure of the problem is well understood, it can be applied to any complex layout of the factory floor. Figure 4-5 shows a more complex layout of a factory floor. The factory has a work station with two capabilities, but the machine can process any one of the two input queues at a given time. In addition, there are only limited AGVs available on multiple routes as shown. The scheduling problem in this scenario can also be formulated as an LP with the state update equations expressed in terms of the incidence matrix as before,

$$\dot{\mathrm{x}} = \mathbf{I}\,\mathrm{u} \quad I \in \mathbb{R}^{11\times 10} \tag{4.11}$$

where $x \in \mathbb{R}^{11\times 1}$ is the state vector and $u =\in \mathbb{R}^{10\times 1}$. In this case few additional constraints need to be included in the LP formulation,

$$\frac{\lambda_{12}(t)}{\lambda_{12,max}} + \frac{\lambda_{13}}{\lambda_{13,max}} \leq 1, \tag{4.12}$$

$$\frac{\lambda_{24}(t)}{\lambda_{24,max}} + \frac{\lambda_{34}(t)}{\lambda_{34,max}} \leq 1, \tag{4.13}$$

$$\frac{\mu_{41}(t)}{\mu_{41,max}} + \frac{\mu_{42}(t)}{\mu_{42,max}} \leq 1, \tag{4.14}$$

which correspond to the constraints on the AGVs and the machine 4 respectively. The stochastic schedule for machine 4 in this case can be generated by sampling from

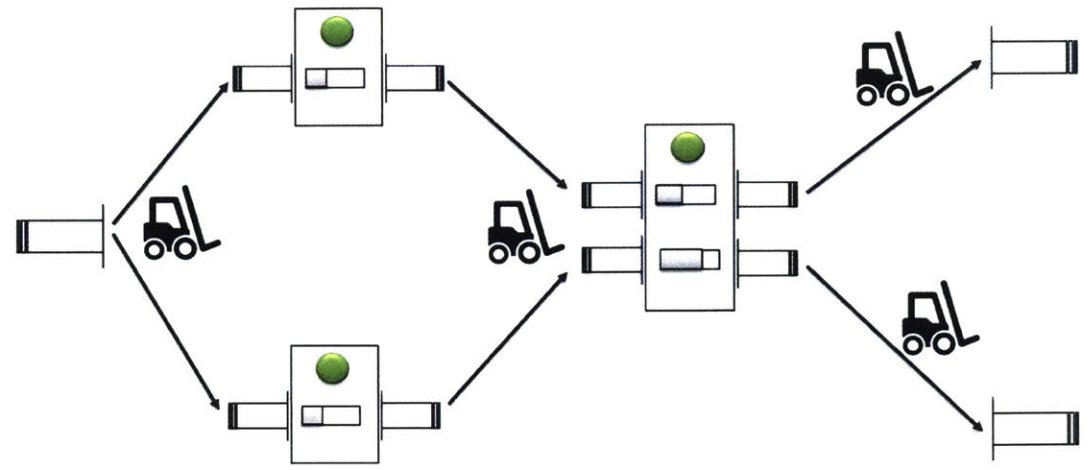

(a)

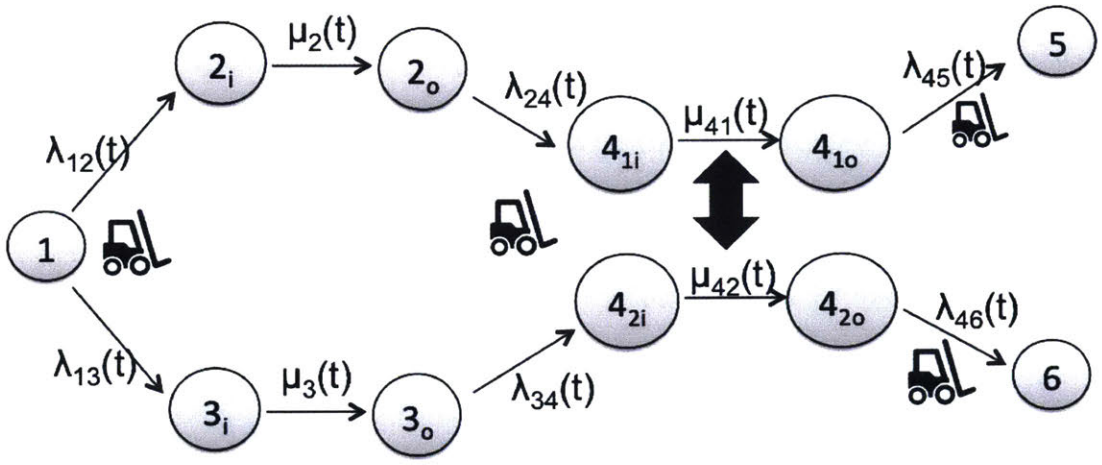

(b)

Figure 4-5: (a) A layout of a complex factory consisting of two machines with one capability and one machine with two capabilities. On the left part of the factory, each AGV need to serve two routes (b) Equivalent graph description.

discrete probability distribution,

$$p_{41}(t) = \frac{\mu_{41}(t)}{\mu_{41,max}}, \quad p_{42}(t) = \frac{\mu_{42}(t)}{\mu_{42,max}} \tag{4.15}$$

4.3 Summary

In this chapter we developed queue theoretic formulation for throughput optimization in smart factories. Using stochastic scheduling techniques, we converted hard scheduling problems to average cost formulations. This allowed us to utilize the scheduling problem as a linear program. The formulations were applied to representative examples.

Chapter 5

Control of Transport Processes

In this chapter we study control of transport phenomena. Transport processes could be used to model many physical systems such as traffic flow, chemical systems and cell rolling among many others. Fundamentally, such physical systems are in *non-equilibrium* and said to be operating in a *non-equilibrium steady state* (NESS). A system in non-equilibrium steady state is characterized by observables that do not change with time (steady), yet exhibit an *irreversible* exchange of heat, particles or volume with the environment. As opposed to systems that are in thermodynamic equilibrium with the environment, NESS systems are operating far from their equilibrium conditions.

In this chapter, we study a model for transport phenomena called the totally asymmetric simple exclusion process (TASEP), with applications to transportation networks. Similar to the role of the Ising model in equilibrium statistical physics, TASEP is a paradigmatic model for systems in non-equilibrium. The TASEP model, usually described on a one dimensional lattice, is a model for molecular transport that allows particles to jump stochastically and independently along a particular direction. The particles enter the system at one end of the lattice, and exit at the other end at specified entry and exit rates. These rates are the parameters of the TASEP model. In addition, the particles at a particular site experience hardcore repulsion; *i.e.* two particles cannot occupy a given site simultaneously. The global quantity that one is concerned with in the TASEP model is the *current* or the flux of the particles

through the system as a function of entry and exit rates. A key feature of the TASEP model is that it shows *phase transitions*: depending on the values of entry and exit rates, the current through the system exists is one of the three possible phases and at certain critical rates exhibits a sharp transition from one phase to another for minute variations about the rate. This thesis makes one of the first attempts to control TASEP based models. The aim of exerting control actions is to achieve one or more of the following behaviors - (i) maintain the system in a desired phase (ii) move the system from one phase to another (iii) change the boundaries of the phase diagram, and (iv) introduce new phases in the phase diagram. Such control strategies would improve the efficiency of existing systems, and might also aid in engineering new applications. For example, analysis and control of non-equilibrium phenomena in transportation networks might lead to better organization of urban transportation systems, thereby reducing delays and enhancing safety.

Towards this end, in this chapter, we study TASEP models of traffic flow to characterize and develop congestion control policies for transportation. The phase transition behavior of the TASEP model discussed before have been well studied in the statistical physics literature and exact solutions to the TASEP model have been calculated through a technique called Matrix Ansatz [96–98]. However, the key issue in applying control techniques directly to TASEP models is that they break the symmetry of the problem, thereby making exact formulations using Matrix Ansatz techniques intractable. As such, we use one form of mean field approximation that ignores long term correlation between random variables, but show that the approximate model recovers the results obtained from rigorous Ansatz techniques exactly. Furthermore, using this approximation we study routing policies for TASEP models of transportation networks.

In Section 5.1, we discuss the TASEP model for a single lane traffic flow. We characterize its behavior in non-equilibrium and identify phase transitions using mean field techniques. In Section 5.2, we consider feedback control policy for the single lane traffic and study the effect of an exit control policy on the traffic flow rate. We show the system achieves maximum possible current under feedback for all possible input

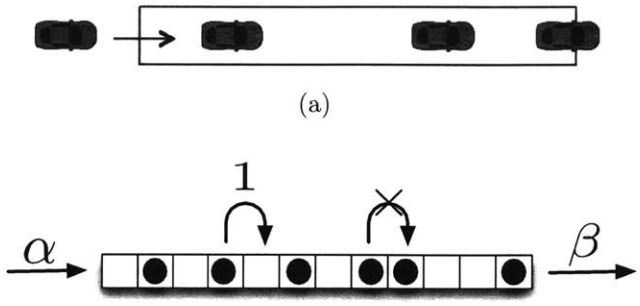

(a)

(b)

Figure 5-1: (a) Vehicles moving on a single lane, and (b) the equivalent Totally asymmetric simple exclusion process (TASEP) model with open boundaries. Particles attempt to enter from left at times that follow a Poisson process with parameter α. Particles move only towards right (totally asymmetric) if and only if the neighboring site is unoccupied (simple exclusion) at times that are form a Poisson process with parameter 1. If last site is occupied, particles leave the system at times that form a Poisson process with parameter β.

rates. In Section 5.3, we consider a road intersection with each road modeled as an independent TASEP. We derive technical conditions for exit control for individual roads in order to achieve maximum flow rate through the traffic junction.

5.1 The TASEP Model

This section provides a description of a one dimensional model of totally asymmetric simple exclusion process (TASEP) with open boundaries (Figure 5-1). Consider a one dimensional lattice consisting of L sites. Each of these cites is either occupied by a particle or is empty. If a site is occupied, then the particle tries to jump to its neighboring site with rate p, only if the neighboring site is unoccupied, independent of all other particles. That is during every infinitesimal time dt, a particle attempts to jump to a neighboring site immediately right to itself with probability $p \cdot dt$, if the neighboring site is empty. If the neighboring site is occupied, the particle cannot jump. In addition, a new particle can enter the system with rate α if site $i = 1$ is unoccupied, and a particle at site $i = L$ can leave the system with rate β. Let τ_i be a Bernoulli random variable that denotes occupation probability of a particular

site i, i.e. $\tau_i = 1$ if site i is occupied and $\tau_i = 0$ otherwise. Let the system be in configuration $(\tau_1, \tau_2, \cdots, \tau_N)$ at time instant t, then the system configuration at time $t + dt$ (when $p = 1$) can be described by probability update equations,

$$\tau_1(t+dt) = \begin{cases} 1, & p_1 = \tau_1 + [\alpha(1-\tau_1) - \tau_1(1-\tau_2)]dt \\ 0, & 1 - p_1 \end{cases} \tag{5.1}$$

$$\tau_i(t+dt) = \begin{cases} 1, & p_i = \tau_i + [\tau_{i-1}(1-\tau_i) - \tau_i(1-\tau_{i+1})]dt \\ 0, & 1 - p_i \quad \forall i,\ 1 < i < L \end{cases} \tag{5.2}$$

$$\tau_L(t+dt) = \begin{cases} 1, & p_L = \tau_L + [\tau_{L-1}(1-\tau_L) - \beta\tau_L]dt \\ 0, & 1 - p_L \end{cases} \tag{5.3}$$

The update equations count the number of possible ways a particle can enter a site and subsequently leave a site. We define the *current* J_i and *density* ρ_i at site i as the following,

$$J_i = E[\tau_i(1 - \tau_{i+1})] \tag{5.4}$$

$$\rho_i = E[\tau_i] \tag{5.5}$$

The current J_i can be interpreted as the average flux of particles between site i and i+1. The density ρ_i represents the average occupancy of site i. We are interested in computing the current and density profile for every site of the lattice in steady state, i.e. when the transients have died out. It should be noted that even though the system is in steady state, it is not in equilibrium as there is a non-zero current or flux of particles flowing from site $i = 1$ to site $i = L$.

5.1.1 Non-equilibrium Steady State

As $\tau_i(t)$ is a random variable, from (5.2) and by using law of iterated expectations we get,

$$E[\tau_i(t+dt)] = E[\tau_i(t)] + E[\tau_{i-1}(1-\tau_i)]\ dt - E[\tau_i(1-\tau_{i+1})]\ dt, \quad 1 < i < L$$

$$\implies E[\frac{\partial \tau_i}{\partial t}] = E[\tau_{i-1}(1-\tau_i)] - E[\tau_i(1-\tau_{i+1})] \tag{5.6}$$

Similarly, using (5.1) and (5.3) we have at the boundaries,

$$E[\frac{\partial \tau_1}{\partial t}] = E[\alpha(1-\tau_1)] - E[\tau_1(1-\tau_2)], \quad i = 1 \tag{5.7}$$

$$E[\frac{\partial \tau_L}{\partial t}] = E[\tau_{L-1}(1-\tau_L)] - E[\beta\tau_L], \quad i = L \tag{5.8}$$

In steady state, the quantities $\tau_i(t)$ do not change with time. Thus, by equating $\frac{\partial(\cdot)}{\partial t}$ to 0, we obtain the following,

$$E[\alpha(1-\tau_1)] = \ldots = E[\tau_i(1-\tau_{i+1})] = \ldots = E[\beta\tau_L] \tag{5.9}$$

$$\implies J_1 = J_2 = \ldots = J_i = \ldots = J_{L-1} = J_L \tag{5.10}$$

This result states that the current through the system is a constant in steady state, which is a feature of a system in NESS.

5.1.2 Open Loop Behavior

In this section, we use an approximation known as mean field technique, to compute the current and the density profile for the one dimensional lattice. Fundamentally, the mean field approximation ignores correlations between random variables τ_i, τ_j and assumes,

$$E[\tau_i\ \tau_j] = E[\tau_i]\ E[\tau_j], \quad \forall i \neq j$$

Recall that ρ_i denotes average occupancy of site i, $\rho_i = E[\tau_i]$. Let J denote the constant current in steady state. From equation (5.9) and by using mean field ap-

proximation, we get the following recurrence relationship for the average occupancies,

$$\rho_1 = 1 - \frac{J}{\alpha} \tag{5.11}$$

$$\rho_{i+1} = 1 - \frac{J}{\rho_i}, \quad 1 < i < L \tag{5.12}$$

$$\rho_L = \frac{J}{\beta} \tag{5.13}$$

The recurrence relationship (5.12) is known as a homographic function in analysis. We state the following theorem from theory of homographic functions which we then use to compute density and current profiles for the TASEP model.

Theorem 5.1. *Let (a_n) be a sequence defined by a_0 and a recurrence relation, $a_{n+1} = f(a_n), \forall n \in \mathbb{N}$.*

1. *If $f(x)$ is a homographic function, then let x^+ and x^- be the two real roots of the fixed point equation $f(x) = x$,*
   (a) *If $x^\pm$ is a double root, then the sequence (b_n) defined by $b_n = \dfrac{1}{a_n - x^\pm}$ is arithmetic.*
   (b) *If the fixed point equation has distinct roots, then the sequence (b_n) defined by $b_n = \dfrac{a_n - x^+}{a_n - x^-}$ is geometric, irrespective of the choice of x^+ and x^-*
2. *If $f(x)$ is an affine function, then there exists a real number γ, such that the sequence (b_n) defined by $b_n = a_n + \gamma$ is geometric.*

Theorem 5.2. *For large L, the steady state current J shows phase transitions and exists in one of the following three phases,*

(a) (Low density phase) If $\alpha < \beta, \alpha < \dfrac{1}{2}$, then $J \to \alpha(1-\alpha)$

(b) (High density phase) If $\beta < \alpha, \beta < \dfrac{1}{2}$, then $J \to \beta(1-\beta)$

(c) (Maximum current phase) If $\alpha, \beta \geq \dfrac{1}{2}$, then $J \to \dfrac{1}{4}$

Proof. We note that (5.12) can be written as $\rho_{i+1} = f(\rho_i)$, where $f(x) = 1 - \dfrac{J}{x}$.

(a) Let x^+ and x^- be two roots of fixed point equation $f(x) = x$, then $x^+ = \dfrac{1+\sqrt{1-4J}}{2}$ and $x^- = \dfrac{1-\sqrt{1-4J}}{2}$ when $J < 1/4$. Define sequence (b_n) as,

$$b_n = \frac{\rho_n - x^+}{\rho_n - x^-}, \quad \rho_0 = \alpha \tag{5.14}$$

$$\text{Then, } b_{n+1} = \frac{\rho_{n+1} - x^+}{\rho_{n+1} - x^-} \tag{5.15}$$

$$= \frac{1 - J/\rho_n - x^+}{1 - J/\rho_n - x^-} = \frac{x^-\rho_n - J}{x^+\rho_n - J} \tag{5.16}$$

$$= \frac{x^- \frac{x^+ - x^- b_n}{1-b_n} - J}{x^+ \frac{x^+ - x^- b_n}{1-b_n} - J} = -\frac{x^- - 2J}{x^+ - 2J}\, b_n \tag{5.17}$$

$$= \left(\frac{x^-}{x^+}\right) b_n \tag{5.18}$$

where we have used the following relations to simplify expressions,

$$x^+ x^- = J, \quad x^+ + x^- = 1, \tag{5.19}$$

$$(x^+)^2 = x^+ - J, \quad (x^-)^2 = x^- - J, \tag{5.20}$$

$$(x^+ - 2J) = \sqrt{1-4J}\; x^+, \quad (x^- - 2J) = -\sqrt{1-4J}\; x^- \tag{5.21}$$

As the sequence (b_n) is geometric, it follows that,

$$b_n = \left(\frac{x^-}{x^+}\right)^n b_0 = \left(\frac{x^-}{x^+}\right)^n \frac{\alpha - x^+}{\alpha - x^-} \tag{5.22}$$

When $n = L$, using (5.13) and (5.14) we have,

$$b_L = \left(\frac{x^-}{x^+}\right)^L \frac{\alpha - x^+}{\alpha - x^-} = \frac{J - \beta x^+}{J - \beta x^-} \tag{5.23}$$

$$\text{Then, } \frac{(J - \beta x^+)(\alpha - x^-)}{(J - \beta x^-)(\alpha - x^+)} = \left(\frac{x^-}{x^+}\right)^L \tag{5.24}$$

When $J < 1/4$, $\left(\dfrac{x^-}{x^+}\right) < 1$, and thus for large L,

$$\text{Either } x^- \to \alpha \implies J = \alpha(1-\alpha), \tag{5.25}$$

$$\text{or } x^+ \to \frac{J}{\beta} \implies J = \beta(1-\beta) \tag{5.26}$$

We note that as $b_L \geq 0$ as $L \to \infty$ and $x^- < x^+$,

$$\text{If } \alpha < \beta, \text{and } \alpha < 1/2, \text{then } \; x^- \uparrow \alpha, \tag{5.27}$$

$$\text{If } \beta < \alpha, \text{and } \beta < 1/2, \text{then } \; x^+ \downarrow \frac{J}{\beta} \tag{5.28}$$

(b) When $J = 1/4$, the fixed point equation has double root $x^{\pm} = 1/2$. Define sequence (b_n) as,

$$b_n = \frac{1}{\rho_n - 1/2}, \quad \rho_0 = \alpha \tag{5.29}$$

$$\implies b_{n+1} = \frac{1}{1 - \frac{J}{\rho_n} - 1/2} = \frac{1}{\frac{1}{2} - \frac{1}{4\rho_n}} = \frac{4\rho_n}{2\rho_n - 1} = \frac{4(1/b_n + 1/2)}{2(1/b_n + 1/2) - 1} \tag{5.30}$$

$$= b_n + 2 \tag{5.31}$$

As the sequence (b_n) is arithmetic, it follows that,

$$b_n = 2n + b_0 = 2n + \frac{2}{2\alpha - 1} \tag{5.32}$$

When $J = 1/4$, $n = L$,

$$b_L = \frac{1}{\frac{1}{4\beta} - \frac{1}{2}} = 2L + \frac{2}{2\alpha - 1} \implies \frac{(1/2 - \beta)(\alpha - 1/2)}{(\alpha\beta - 1/4)} = \frac{1}{L} \tag{5.33}$$

Thus for large L, as $\frac{1}{L} \downarrow 0$,

$$\text{Either } \alpha \to \frac{1}{2}, \text{ or } \beta \to \frac{1}{2} \tag{5.34}$$

$$\text{If } \alpha > \beta, \; \beta \downarrow \frac{1}{2}, \quad \text{or if } \beta > \alpha, \; \alpha \uparrow \frac{1}{2} \tag{5.35}$$

□

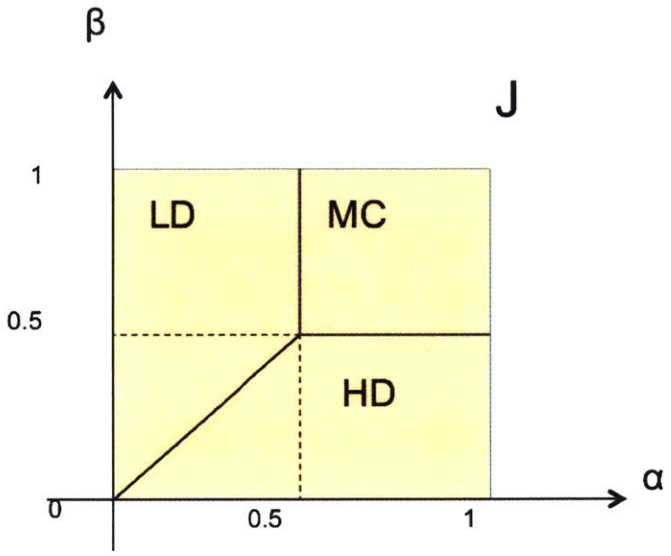

Figure 5-2: Phase transition diagram for the TASEP model where current J is shown as a function of entry rate α and exit rate β. The system can exist in three different phases - low density (LD), high density (HD) and maximum current (MC) phase. At the intersection of these phases, the system shows phase transitions. In the LD phase, the current is completely determined by the entry rate α. In HD phase, the current depends only on the exit rate β. In the MC phase, system achieves its maximum current of $J = 1/4$, and the current is independent of both α and β.

Theorem 5.2 proves the existence a phase transition diagram for the TASEP model. Depending on the entry rate α and exit rate β, the system can exist in three different phases - (i) a low density (LD) phase in which $\alpha < \beta$, (ii) a high density (HD) phase in which $\alpha > \beta$, and (iii) a maximum current (MC) phase in which $\alpha, \beta > 1/2$. At the intersection of these phases, the model shows phase transitions. In the LD phase, the current is completely determined by the entry rate α. Similarly, in HD phase, the current depends only on the exit rate β. In contrast, in the MC phase, the system achieves its maximum possible flow rate of $J = 1/4$, and the current is independent of both entry and exit rates. Once the current profile in various regimes are known, the density profiles ρ_i can be calculated from (5.12). The density profile ρ_i is a continuous function and depends on the location of particle i. However three main quantities are of interest - (i) the entry density ρ_1, (ii) the bulk density ρ_{bulk}, which is the density for large part of model away from the ends, and (iii) the exit

Table 5.1: A summary of key quantities of interest in the three phases of the TASEP model as a function of input rate α and exit rate β

	Low Density (LD)	High Density (HD)	Max Current (MC)
(α, β)	$\alpha < \beta, \alpha < 1/2$	$\beta < \alpha, \beta < 1/2$	$\alpha, \beta > 1/2$
J	$\alpha(1-\alpha)$	$\beta(1-\beta)$	$1/4$
ρ_1	α	$1 - \frac{\beta(1-\beta)}{\alpha}$	$1 - \frac{1}{4\alpha}$
ρ_{bulk}	α	$1-\beta$	$1/2$
ρ_L	$\frac{\alpha(1-\alpha)}{\beta}$	$1-\beta$	$\frac{1}{4\beta}$

density ρ_L. These quantities can be computed easily from (5.12) once the current is known. Table 5.1 summarizes the relevant quantities of interest for various regimes in phase diagram.

5.2 Control of TASEP on 1D Lattice

In this section we develop an exit control feedback policy for the TASEP model on 1D lattice. Specifically, we choose the exit rate β to be the average over the occupancy probability of all L sites as follows,

$$\beta = \frac{1}{L} \sum_{i=1}^{L} \rho_i \tag{5.36}$$

Recall that ρ_i is the expected occupancy of site i, $\rho_i = E[\tau_i]$. We assume that sensors are available on various sections of the road that measure the average occupancy of sites. In the following theorem we show that the control policy results in the system

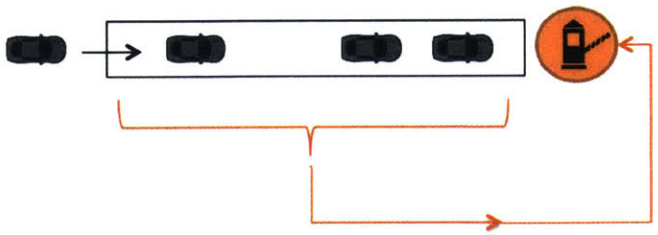

Figure 5-3: Exit control strategy in which the exit rate β is changed based on average occupation probability of the entire road

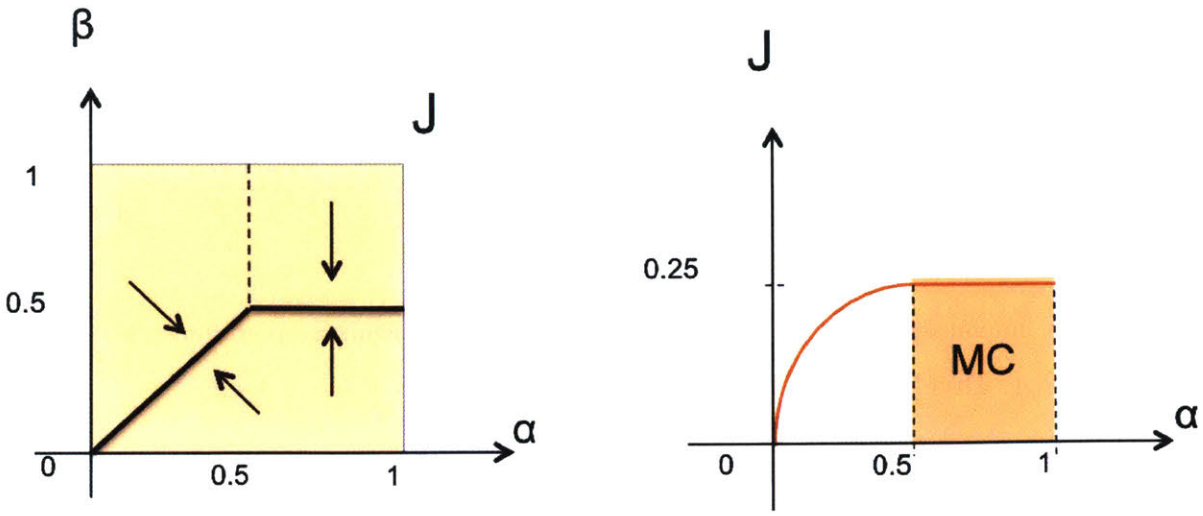

Figure 5-4: The exit control strategy changes the phase diagram by collapsing the phase diagram onto the thick line as shown. This results in the system operating at MC phase even in HD regime

achieving maximum flow rate whenever possible.

Theorem 5.3. *For large L, under control policy* (5.36)*, current J exists in one of the two possible phases,*

(a) If $\alpha < 1/2$, then $J \to \alpha(1-\alpha)$

(b) If $\alpha > 1/2$, then $J \to 1/4$

Proof. We show the convergence of current to the two possible cases for LD, HD, and MC phases. From (5.12), it follows that,

$$\begin{aligned}\sum_{i=1}^{L} \rho_i &= \rho_1 + \sum_{i=2}^{L-1} \rho_i + \rho_L \\ &= 1 - \frac{J}{\alpha} + \sum_{i=1}^{L-2}(1 - \frac{J}{\rho_i}) + \frac{J}{\beta} \\ &= L + (\frac{J}{\beta} - \frac{J}{\alpha} - 1) - \sum_{i=1}^{L-2} \frac{J}{\rho_i}\end{aligned}$$

We note that in a summation of ρ_i in any phase, the bulk density ρ_{bulk} dominates

Table 5.2: The effect of exit rate control policy on a single lane traffic model.

Low Density (LD) $\alpha < \beta, \alpha < 1/2$	High Density (HD) $\beta < \alpha, \beta < 1/2$	Max Current (MC) $\alpha, \beta > 1/2$
$\beta \to \alpha$	$\beta \to 1/2$	$\beta \to 1/2$
$J = \alpha(1-\alpha)$	$J = 1/4$	J = 1/4

over the values at the end points, and as such in the limit average densities converge to ρ_{bulk}. Dividing both sides by L and taking limit as $L \to \infty$ yields,

$$\beta = 1 - \frac{J}{\rho_{bulk}} \tag{5.37}$$

From Table 5.1, in LD phase, $\frac{J}{\rho_{bulk}} = 1 - \alpha$, which implies that $\beta = \alpha$. In the HD phase, $\frac{J}{\rho_{bulk}} = \beta$, which implies $\beta = 1/2$, and in the MC phase $\frac{J}{\rho_{bulk}} = 1/2$ which again results in $\beta = 1/2$. □

Thus the effect of exit control policy is a collapse of the phase transition diagram (Figure 5-4), onto the phase transition line as shown. The current is independent of exit rate β and adjusts based on α. When the road is relatively free and in the low density traffic regime ($\alpha < 1/2$), the exit rate reduces its value, and for all other regimes maintains itself at $\beta = 1/2$ to achieve maximum flow rate of traffic. Table 5.2 summarizes this behavior.

5.3 Control of TASEP on Intersections

In this section, we consider a two-road intersection controlled by an automated gated exit that can reduce or increase flow rate of traffic into the traffic junction. Figure 5-6 shows a TASEP equivalent model of a road intersection (Figure 5-5). The roads have been modeled as two TASEPs connected by a single site which is a traffic junction. We assume that the traffic at the junction are controlled by two gate controllers u_1 and u_2, that can regulate the flow of traffic into the junction. The parameters of two road model are entry rates for individual roads α_1, α_2 and the exit rate through junction β_3.

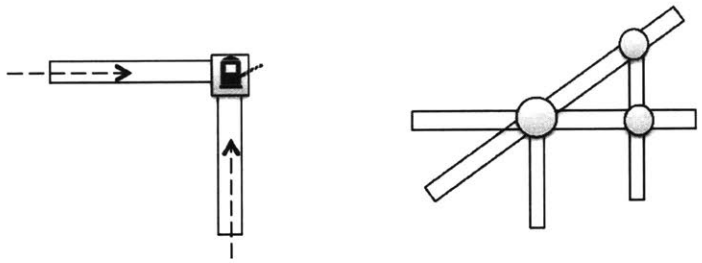

Figure 5-5: TASEP models on generic road networks and intersections

To analyze the coupled TASEP model, we construct an equivalent model (Figure 5-6) which consists of three independent one dimensional TASEP models. Both models should operate at same currents, and this constraint gives us the effective exit rates $\beta_{1,\text{eff}}, \beta_{2,\text{eff}}$ for two roads, and effective entry rate $\alpha_{3,\text{eff}}$ for the traffic junction.

$$J_1 = u_1\rho_1(1-\rho), \qquad J_2 = u_2\rho_2(1-\rho), \qquad J = \beta_3\rho \tag{5.38}$$

$$J_1 = \rho_1\beta_{1,\text{eff}}, \qquad J_2 = \rho_2\beta_{2,\text{eff}}, \qquad J = \alpha_{3,\text{eff}}(1-\rho) \tag{5.39}$$

Equating (5.38) to (5.39) results in,

$$\beta_1 = u_1(1-\rho), \qquad \beta_2 = u_2(1-\rho), \qquad \rho = \frac{\alpha_3}{\alpha_3+\beta_3} \tag{5.40}$$

where we have dropped $()_{\text{eff}}$ for notational ease. In addition, we have traffic (or current) conservation at the junction,

$$J = J_1 + J_2 \tag{5.41}$$

Equations (5.40) and (5.41) result in following conditions,

$$\beta_1 = \frac{\beta_3 u_1}{\alpha_3+\beta_3} \tag{5.42}$$

$$\beta_2 = \frac{\beta_3 u_2}{\alpha_3+\beta_3} \tag{5.43}$$

$$\alpha_3 = u_1\rho_1 + u_2\rho_2 \tag{5.44}$$

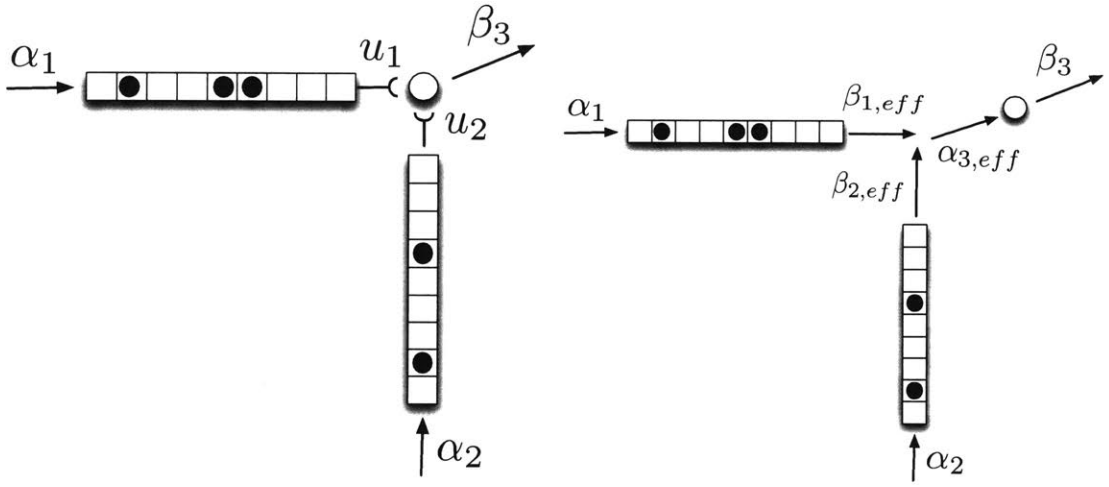

(a) (b)

Figure 5-6: (a) Coupled TASEP model for a road intersection with a junction. At the exit of each road there is a gate (u_1, u_2 respectively) that can regulate the flow of traffic (b) An equivalent model of (a) obtained by decoupling the system to three independent 1D TASEP models with effective entry and exit rates. The traffic flow rates in both (a) and (b) are the same.

The system can exist, in principle, in up to nine phases depending on individual phases of each road (LD, HD, or MC) combined with that of the other. However, an intersection reduces the overall capacity of the road and thus reduces the junction exit rate β_3. If β_3 is below certain threshold, certain phases among the nine phases would cease to exist. Furthermore, we note that the current through the junction, $J = \dfrac{\alpha_3\beta_3}{\alpha_3 + \beta_3}$, is an increasing function of α_3. Therefore, for a given exit rate $0 \leq \beta_3 \leq 1$, the current through the junction is maximized when $\alpha_3 = 1$.

Even though it is possible to analyze system behavior for all possible values of exit rate β_3, we consider the most likely scenario in a traffic intersection when individual roads are operating in the congested HD regimes. We consider the case when $\beta_3 = 1/4$. This choice models an eight lane traffic junction (with left and straight turns only) in which the overall road capacity has been reduced to 25% of the maximum capacity due to the presence of the junction. Let ρ_1 and ρ_2 denote the occupation densities for individual roads at their exit sites respectively. Recall from Table 5.1 that in the HD regime, the exit occupation density is given by $\rho_L = 1 - \beta$. This observation along

with (5.42), (5.43), (5.44) yields,

$$\rho_1 = 1 - \beta_1, \qquad \rho_2 = 1 - \beta_2 \tag{5.45}$$

$$\frac{u_1}{u_2} = \frac{\beta_1}{\beta_2} \tag{5.46}$$

$$\implies u_1\beta_3 = u_1[\beta_1(1-\beta_1) + \beta_2(1-\beta_2)] + \beta_1\beta_3 \tag{5.47}$$

Let $C^* = \beta_1(1-\beta_1) + \beta_2(1-\beta_2)$, then (5.47) simplifies to,

$$u_1 = \frac{\beta_1\beta_3}{\beta_3 - C^*}, \qquad \text{or} \qquad \beta_3 = \frac{u_1 C^*}{u_1 - \beta_1} \tag{5.48}$$

The constraints $0 \leq u_1, \beta_3 \leq 1$ imply that for (HD-HD) phase to exist in the two-road intersection, a necessary condition is,

$$C^* \leq \beta_3 \tag{5.49}$$

It should be noted that if this equation is not satisfied, the phase (HD-HD) ceases to exist. From (5.42) and (5.43), if $\beta_3 = 1/4$, it can be easily seen that $u_1 = 5\beta_1$ and $u_2 = 5\beta_2$. Consequently from (5.49), the two individual roads are operating in the (HD-HD) regime if the parameters (β_1, β_2) lie inside the region bounded by,

$$(\beta_1 - 1/2)^2 + (\beta_2 - 1/2)^2 \leq 7/10, \qquad 0 \leq \beta_1, \beta_2 \leq 1/2, \tag{5.50}$$

and the optimal control rates (u_1, u_2) *for the exit gates lie on the manifold,*

$$u_1(1 - u_1/5) + u_2(1 - u_2/5) = 1. \tag{5.51}$$

The relation implies that any choice of (u_1, u_2) satisfying (5.51) achieves maximum flow rate of traffic through the junction. For the sake of completeness, if we assume $\beta_1 = \beta_2$, then optimal control rates $u_1 = u_2 = 0.56$.

5.4 Summary

In this chapter we considered control of systems in non-equilibrium using TASEP models for traffic flow. We first showed that the TASEP model shows phase transition in the current (or the rate of flow of traffic) depending on entry and exit rates. We then considered an exit control policy for traffic flow on a single road and showed that the system achieves its maximum possible flow rate under feedback. Finally, we considered interesting extensions of TASEP models to a two-road intersection and analyzed automated gated control policies that achieve maximum flow rate of traffic through the junction.

Chapter 6

Conclusions and Future Work

In this thesis we studied analysis and control of stochastically interacting systems on networks. Stochastically interacting systems are dynamic models of complex systems involving a large number of interconnected components with three essential features - (i) they are stochastic processes, (ii) their connectivity architecture has a networked structure, and (iii) the connected components influence one another through local interactions. The main goal of this thesis was to develop a control theoretic framework for analyzing, characterizing, and stabilizing these complex systems. Using three representative examples of such systems from the fields of spreading processes, smart manufacturing, and transport phenomena, this thesis (i) developed mathematically tractable yet realistic models, (ii) performed control theoretic analysis of these models and characterized their stability and open loop behavior, and (iii) developed control policies to stabilize unstable behaviors while optimizing desired performance objectives.

In the first part of the thesis, we considered control of spreading processes on lattices. Such processes could be used to model many phenomena such as spread of epidemic diseases, forest fires, opinion dynamic, crystal growth on surfaces, and financial markets. Analysis and control of spreading processes is difficult mainly due to high dimensionality of the state space of these processes. The most common approach to deal with this issue in the literature has been to use a broad class of approximate models known as the mean field approximations. Even though these approximations

allow one to consider complex network structures and heterogeneous interactions between nodes, these descriptions completely remove the stochasticity associated with these systems, which is one of their key features. Furthermore, approximate models do not characterize stability nor the behavior of the processes accurately. As such, in this thesis we analyzed exact formulations of spreading processes and considered models on lattices for mathematical tractability. Using recently developed tools from non-equilibrium statistical physics, we characterized stability of these processes accurately. This thesis develops the notion of stability of spreading processes using critical probability (p_c) of a given graph. This formulation allows one to derive accurate bounds on stability thresholds, as opposed to mean field approaches. Furthermore, we characterized open loop behavior of spreading processes in its stable, neutral and unstable regimes accurately; a characterization that is not possible using approximate models. Finally, for an unstable spreading process, we developed a randomized control policy that is optimal in both resource allocation and control effort.

In the second part of the thesis, we considered control of smart manufacturing processes. Due to increased product customization and rapidly changing demands, the recent trend in manufacturing is to shift towards a new industrial revolution which has been popularized as Industry 4.0. Such a manufacturing process envisions smart factories in which the shop floor is modular and is divided into many work stations (or machines) with multiple capabilities. Individual work stations are connected by automated guided vehicles (AGVs). Key issues in achieving this vision are effective modeling, monitoring and scheduling of individual work stations and AGVs while accounting for dynamically changing shop floor environment, that include machines failures, rapidly changing demands, multiple products on production lines, addition and removal of AGVs, among others. However, traditional methods of modeling and scheduling lead to formulations that are combinatorially hard to solve, thus making them difficult for real time implementation. To avoid this issue, in this thesis we developed a queuing theory framework for modeling job flow between work stations and AGVs. Using this framework, we showed that that the structure of the problem

can be expressed in terms of incidence matrix of the connectivity graph. Finally, we developed a stochastic scheduling algorithm, and showed that the optimal schedule can be solved as a linear program. The approach is amenable for fast implementation, and achieves a balanced load among operating agents in the case of failures.

In the last part of this thesis, we considered control of transport processes. Transport phenomena or processes are systems that are in *non-equilibrium*, *i.e.* even though the observables associated with the processes are time invariant, there is an irreversible transfer of heat, energy, or particles with the environment. For instance, such processes could be used to model traffic flow on transportation networks which is the main application considered in this thesis. Even though study and analysis of systems exhibiting non-equilibrium phenomena have been considered in the past, there are no effective ways to control or modify the behavior of these systems. Towards this end, in this thesis, we studied control theoretic formulations for systems in nonequilibrium aimed to achieve one or more of the following behaviors - (i) maintain the system in a desired phase (ii) move the system from one phase to another (iii) change the boundaries of the phase diagram, and (iv) introduce new phases in the phase diagram. Starting from a paradigmatic model of non-equilibrium phenomena known as totally asymmetric simple exclusion process (TASEP), we considered TASEP models for traffic flow on simple networks. We developed automated routing policies for traffic flow on a single road with a gated exit, that achieved maximum flow rate of traffic for all set of entry traffic conditions. We also extended this work and developed control policies for intersections and generic road networks to maximize flow rate of traffic. It was shown that the optimal control strategies could lie on nonlinear manifolds.

This work opens up opportunities to many further directions, few of which are listed below:

Characterization of spreading processes based on critical probability rather than eigenvalues of adjacency matrices: This thesis used the notion of critical probability to characterize behavior of spreading process on a graph. In majority of

literature on spreading processes, eigenvalues of adjacency matrices have been used to characterize stability of process. However, critical probability might be better suited for characterizing stability of spreading processes as they capture the essential structure of the graph inherently. Characterizations of spreading processes based on eigenvalues of adjacency matrices, could be insufficient at times, as many different graph topologies could have the same eigenvalue.

Accurate characterization of spreading processes on different lattices: The value of critical probability for percolation are accurately known for a variety of lattices including square, triangular, hexagonal, Archimedean, inhomogeneous and random lattices. The optimal policies developed in this work could be extended to spreading processes models on all such lattices

Characterization of spreading process on inhomogenous and heterogeneous models: Direction dependent spreading processes in which one direction is preferred over another or spatially and time varying models of spreading haven't been accurately characterized in the literature. This could be one possible direction for further study.

Throughput optimization for different job flows and on reconfigurable floors: Industry 4.0 also envisions a reconfigurable factory floor, on which machines self organize to maximize throughput depending on the product flow. A real time optimal algorithm that could achieve the same could be a possible future direction. In addition, there are many other types of job flows that could be considered in future work. For example, mating of products, and products produced by 3D printing are hard to model using traditional methods, and might need new modeling frameworks.

Analysis and control of TASEP models on generic networks: Analysis and control of TASEP problems on generic transportation networks is an open problem. The results from this thesis could also be extended to various networks that have a specific structure (for e.g. scale free networks).

Bibliography

[1] David G. Kendall. Stochastic processes and population growth. *Journal of the Royal Statistical Society. Series B (Methodological)*, 11(2):230–282, 1949.

[2] Rick Durrett. Stochastic spatial models. *SIAM review*, 41(4):677–718, 1999.

[3] Mark Newman. *Networks: an introduction.* Oxford university press, 2010.

[4] B Scholz-Reiter and M Freitag. Autonomous processes in assembly systems. *CIRP Annals-Manufacturing Technology*, 56(2):712–729, 2007.

[5] Klaus Schwab. The fourth industrial revolution. World Economic Forum Geneva, 2016.

[6] Daron Acemoglu and Asuman Ozdaglar. Opinion dynamics and learning in social networks. *Dynamic Games and Applications*, 1(1):3–49, 2011.

[7] David Easley and Jon Kleinberg. *Networks, crowds, and markets: Reasoning about a highly connected world.* Cambridge University Press, 2010.

[8] Debashish Chowdhury, Ludger Santen, and Andreas Schadschneider. Statistical physics of vehicular traffic and some related systems. *Physics Reports*, 329(4):199–329, 2000.

[9] Dirk Helbing. Traffic and related self-driven many-particle systems. *Reviews of modern physics*, 73(4):1067, 2001.

[10] Andreas Schadschneider. Traffic flow: a statistical physics point of view. *Physica A: Statistical Mechanics and its Applications*, 313(1):153–187, 2002.

[11] Andreas Schadschneider, Debashish Chowdhury, and Katsuhiro Nishinari. *Stochastic transport in complex systems: from molecules to vehicles.* Elsevier, 2010.

[12] Peter Mörters, Roger Moser, Mathew Penrose, Hartmut Schwetlick, and Johannes Zimmer. *Analysis and stochastics of growth processes and interface models.* OUP Oxford, 2008.

[13] Patrik L Ferrari and Herbert Spohn. Random growth models. *arXiv preprint arXiv:1003.0881*, 2010.

[14] Daron Acemoglu, Asuman Ozdaglar, and Alireza Tahbaz-Salehi. Systemic risk and stability in financial networks. Technical report, National Bureau of Economic Research, 2013.

[15] Leah B. Shaw, R.K.P Zia, and Kelvin H. Lee. Totally asymmetric exclusion process with extended objects: a model for protein synthesis. *Physical Review E*, 68(2):021910, 2003.

[16] Norman T.J. Bailey. *The mathematical theory of infectious diseases and its applications*. London, 1975.

[17] Stefano Boccaletti, Vito Latora, Yamir Moreno, Martin Chavez, and D-U Hwang. Complex networks: Structure and dynamics. *Physics reports*, 424(4):175–308, 2006.

[18] Norman T.J. Bailey. The mathematical theory of epidemics. 1957.

[19] Herbert W. Hethcote. The mathematics of infectious diseases. *SIAM review*, 42(4):599–653, 2000.

[20] Roy M Anderson, Robert M May, and B Anderson. *Infectious diseases of humans: dynamics and control*, volume 28. Wiley Online Library, 1992.

[21] Nicola Perra, Duygu Balcan, Bruno Gonçalves, and Alessandro Vespignani. Towards a characterization of behavior-disease models. *PloS one*, 6(8):e23084, 2011.

[22] Klaus Dietz. Epidemics and rumours: A survey. *Journal of the Royal Statistical Society. Series A (General)*, pages 505–528, 1967.

[23] Tom Britton. Stochastic epidemic models: A survey. *Mathematical biosciences*, 225(1):24–35, 2010.

[24] Cameron Nowzari, Victor M. Preciado, and George J Pappas. Analysis and control of epidemics: A survey of spreading processes on complex networks. *arXiv preprint arXiv:1505.00768*, 2015.

[25] Robert M. May and Roy M. Anderson. Population biology of infectious diseases. *Nature*, 280(5722):455–461, 1979.

[26] Fred Brauer, Carlos Castillo-Chavez, and Carlos Castillo-Chavez. *Mathematical models in population biology and epidemiology*, volume 40. Springer, 2001.

[27] Daryl J Daley, Joe Gani, and Joseph Mark Gani. *Epidemic modelling: an introduction*, volume 15. Cambridge University Press, 2001.

[28] J.A.P Heesterbeek. *Mathematical epidemiology of infectious diseases: model building, analysis and interpretation*, volume 5. John Wiley & Sons, 2000.

[29] Matt J. Keeling and Pejman Rohani. *Modeling infectious diseases in humans and animals.* Princeton University Press, 2008.

[30] Pierre Auger, Pierre Magal, and Shigui Ruan. *Structured population models in biology and epidemiology*, volume 1936. Springer, 2008.

[31] Odo Diekmann, Hans Heesterbeek, and Tom Britton. *Mathematical tools for understanding infectious disease dynamics.* Princeton University Press, 2012.

[32] Piet Van Mieghem, Jasmina Omic, and Robert Kooij. Virus spread in networks. *IEEE/ACM Transactions on Networking*, 17(1):1–14, 2009.

[33] Hyoung Jun Ahn and Babak Hassibi. Global dynamics of epidemic spread over complex networks. In *52nd IEEE Conference on Decision and Control*, pages 4579–4585. IEEE, 2013.

[34] Piet Van Mieghem. The n-intertwined sis epidemic network model. *Computing*, 93(2-4):147–169, 2011.

[35] Eric Cator and Piet Van Mieghem. Second-order mean-field susceptible-infected-susceptible epidemic threshold. *Physical review E*, 85(5):056111, 2012.

[36] Cong Li, Ruud van de Bovenkamp, and Piet Van Mieghem. Susceptible-infected-susceptible model: A comparison of n-intertwined and heterogeneous mean-field approximations. *Physical Review E*, 86(2):026116, 2012.

[37] Ali Khanafer, Tamer Başar, and Bahman Gharesifard. Stability properties of infected networks with low curing rates. In *American Control Conference*, 2014.

[38] Ali Khanafer, Tamer Başar, and Bahman Gharesifard. Stability properties of infection diffusion dynamics over directed networks. In *IEEE Conference on Decision and Control*, 2014.

[39] Piet Van Mieghem and Jasmina Omic. In-homogeneous virus spread in networks. *arXiv preprint arXiv:1306.2588*, 2013.

[40] Hal Caswell. *Matrix population models.* Wiley Online Library, 2001.

[41] Norman T.J. Bailey. Macro-modelling and prediction of epidemic spread at community level. *Mathematical Modelling*, 7(5):689–717, 1986.

[42] Victor M. Preciado and Michael Zargham. Traffic optimization to control epidemic outbreaks in metapopulation models. In *IEEE Global Conference on Signal and Information Processing*, 2013.

[43] Yang Wang, Deepayan Chakrabarti, Chenxi Wang, and Christos Faloutsos. Epidemic spreading in real networks: An eigenvalue viewpoint. In *Reliable Distributed Systems, 2003. Proceedings. 22nd International Symposium on*, pages 25–34. IEEE, 2003.

[44] Victor M. Preciado and Ali Jadbabaie. Spectral analysis of virus spreading in random geometric networks. In *Decision and Control, 2009 held jointly with the 2009 28th Chinese Control Conference. CDC/CCC 2009. Proceedings of the 48th IEEE Conference on*, pages 4802–4807. IEEE, 2009.

[45] S. Eshghi, M.H.R. Khouzani, S. Sarkar, and S.S. Venkatesh. Optimal patching in clustered epidemics of malware. *IEEE Transactions on Networking*, 2015.

[46] Richard Morton and Kenneth H Wickwire. On the optimal control of a deterministic epidemic. *Advances in Applied Probability*, pages 622–635, 1974.

[47] K.H. Wickwire. Optimal isolation policies for deterministic and stochastic epidemics. *Mathematical biosciences*, 26(3-4):325–346, 1975.

[48] Victor M Preciado, Michael Zargham, Chinwendu Enyioha, Ali Jadbabaie, and George Pappas. Optimal resource allocation for network protection: A geometric programming approach. *IEEE Transactions on Control of Network Systems*, 1(1):99–108, 2014.

[49] Cameron Nowzari, Victor M. Preciado, and George J. Pappas. Stability analysis of generalized epidemic models over directed networks. 2014.

[50] Cameron Nowzari, Victor Preciado, and George Pappas. Optimal resource allocation for control of networked epidemic models. *IEEE Transactions on Control of Network Systems*, 2015.

[51] Joel C Miller and James M Hyman. Effective vaccination strategies for realistic social networks. *Physica A: Statistical Mechanics and its Applications*, 386(2):780–785, 2007.

[52] Christian M Schneider, Tamara Mihaljev, Shlomo Havlin, and Hans J Herrmann. Suppressing epidemics with a limited amount of immunization units. *Physical Review E*, 84(6):061911, 2011.

[53] Michael Bloem, Tansu Alpcan, and Tamer Başar. Optimal and robust epidemic response for multiple networks. *Control Engineering Practice*, 17(5):525–533, 2009.

[54] Ali Khanafer and Tamer Basar. An optimal control problem over infected networks. In *Proceedings of the International Conference of Control, Dynamic Systems, and Robotics, Ottawa, Ontario, Canada*, 2014.

[55] Elsa Hansen and Troy Day. Optimal control of epidemics with limited resources. *Journal of mathematical biology*, 62(3):423–451, 2011.

[56] Horst Behncke. Optimal control of deterministic epidemics. *Optimal control applications and methods*, 21(6):269–285, 2000.

[57] Piet Van Mieghem. Decay towards the overall-healthy state in sis epidemics on networks. *arXiv preprint arXiv:1310.3980*, 2013.

[58] Piet Van Mieghemy, Faryad Darabi Sahnehz, and Caterina Scoglioz. An upper bound for the epidemic threshold in exact markovian sir and sis epidemics on networks. In *53rd IEEE Conference on Decision and Control*, pages 6228–6233. IEEE, 2014.

[59] Romualdo Pastor-Satorras and Alessandro Vespignani. Epidemic spreading in scale-free networks. *Physical review letters*, 86(14):3200, 2001.

[60] Murray Eden. A two-dimensional growth process. *Dynamics of fractal surfaces*, 4:223–239, 1961.

[61] A-L Barabási and Harry Eugene Stanley. *Fractal concepts in surface growth*. Cambridge university press, 1995.

[62] Mehran Kardar, Giorgio Parisi, and Yi-Cheng Zhang. Dynamic scaling of growing interfaces. *Physical Review Letters*, 56(9):889, 1986.

[63] Réka Albert and Albert-László Barabási. Statistical mechanics of complex networks. *Reviews of modern physics*, 74(1):47, 2002.

[64] Ryogo Kubo, Morikazu Toda, and Natsuki Hashitsume. *Statistical physics II: nonequilibrium statistical mechanics*, volume 31. Springer Science & Business Media, 2012.

[65] Krishna B Athreya and Peter E Ney. *Branching processes*, volume 196. Springer Science & Business Media, 2012.

[66] Russell Lyons and Yuval Peres. Probability on trees and networks, 2005.

[67] Malte Brettel, Niklas Friederichsen, Michael Keller, and Marius Rosenberg. How virtualization, decentralization and network building change the manufacturing landscape: An industry 4.0 perspective. *International Journal of Mechanical, Industrial Science and Engineering*, 8(1):37–44, 2014.

[68] Jay Lee, Behrad Bagheri, and Hung-An Kao. A cyber-physical systems architecture for industry 4.0-based manufacturing systems. *Manufacturing Letters*, 3:18–23, 2015.

[69] SJ Hu, Xian-wei Zhu, Hui Wang, and Yoram Koren. Product variety and manufacturing complexity in assembly systems and supply chains. *CIRP Annals-Manufacturing Technology*, 57(1):45–48, 2008.

[70] Mario Hermann, Tobias Pentek, and Boris Otto. Design principles for industrie 4.0 scenarios. In *2016 49th Hawaii International Conference on System Sciences (HICSS)*, pages 3928–3937. IEEE, 2016.

[71] Weiming Shen, Lihui Wang, and Qi Hao. Agent-based distributed manufacturing process planning and scheduling: a state-of-the-art survey. *IEEE Transactions on Systems, Man, and Cybernetics, Part C (Applications and Reviews)*, 36(4):563–577, 2006.

[72] Stefan Bussmann and Klaus Schild. An agent-based approach to the control of flexible production systems. In *Emerging Technologies and Factory Automation, 2001. Proceedings. 2001 8th IEEE International Conference on*, volume 2, pages 481–488. IEEE, 2001.

[73] Paulo Leitão. Agent-based distributed manufacturing control: A state-of-the-art survey. *Engineering Applications of Artificial Intelligence*, 22(7):979–991, 2009.

[74] Nadine Keddis, Gerd Kainz, Christian Buckl, and Alois Knoll. Towards adaptable manufacturing systems. In *Industrial Technology (ICIT), 2013 IEEE International Conference on*, pages 1410–1415. IEEE, 2013.

[75] Chun Wang, Hamada Ghenniwa, and Weiming Shen. Real time distributed shop floor scheduling using an agent-based service-oriented architecture. *International Journal of Production Research*, 46(9):2433–2452, 2008.

[76] Thomas Gabel and Martin Riedmiller. Adaptive reactive job-shop scheduling with reinforcement learning agents. *International Journal of Information Technology and Intelligent Computing*, 24(4), 2008.

[77] Munir Merdan, Mathieu Vallée, Thomas Moser, and Stefan Biffl. A layered manufacturing system architecture supported with semantic agent capabilities. In *Semantic Agent Systems*, pages 215–242. Springer, 2011.

[78] Farhad Ameri, Colin Urbanovsky, and Christian McArthur. A systematic approach to developing ontologies for manufacturing service modeling. In *Proc. 7th International Conference on Formal Ontology in Information Systems (FOIS 2012), Graz, Austria.* Citeseer, 2012.

[79] Mohsen Karimi Haghighi and Dirk J Pons. Ontological approach to new product development. *Journal of Industrial and Intelligent Information Vol*, 2(2), 2014.

[80] Nadine Keddis, Bilal Javed, Georgeta Igna, and Alois Zoitl. Optimizing schedules for adaptable manufacturing systems. In *2015 IEEE 20th Conference on Emerging Technologies & Factory Automation (ETFA)*, pages 1–8. IEEE, 2015.

[81] Nadine Keddis, Gerd Kainz, and Alois Zoitl. Capability-based planning and scheduling for adaptable manufacturing systems. In *Proceedings of the 2014 IEEE Emerging Technology and Factory Automation (ETFA)*, pages 1–8. IEEE, 2014.

[82] Soumya Banerjee and Joshua Hecker. A multi-agent system approach to load-balancing and resource allocation for distributed computing. *arXiv preprint arXiv:1509.06420*, 2015.

[83] Kleanthis Thramboulidis. An open distributed architecture for flexible hybrid assembly systems: a model-driven engineering approach. *The International Journal of Advanced Manufacturing Technology*, pages 1–12, 2014.

[84] Dazhong Wu. Cloud-based design and manufacturing: a network perspective. 2014.

[85] Gene F Mazenko. *Nonequilibrium statistical mechanics.* John Wiley & Sons, 2008.

[86] T. Chou, K. Mallick, and R.K.P. Zia. Non-equilibrium statistical mechanics: from a paradigmatic model to biological transport. *Reports on progress in physics*, 74(11):116601, 2011.

[87] Luca Peliti. *Statistical mechanics in a nutshell.* Princeton University Press, 2011.

[88] Graham R. Fleming and Mark A. Ratner. Grand challenges in basic energy sciences. *Physics Today*, 28, 2008.

[89] John Hemminger, Graham Fleming, and M. Ratner. Directing matter and energy: Five challenges for science and the imagination. *Department of Energy's Office of Science*, 2007.

[90] National Research Council Committee on CMMP. *Condensed-Matter and Materials Physics: The Science of the World Around Us*, Jan 2010.

[91] K. Mallick. Some recent developments in non-equilibrium statistical physics. *Pramana*, 73(3):417–451, 2009.

[92] Abigail Klopper. Topics in non-equilibrium physics. *Nature Physics*, 11(2):103–103, 2015.

[93] Michael J Lighthill and Gerald Beresford Whitham. On kinematic waves ii. a theory of traffic flow on long crowded roads. In *Proceedings of the Royal Society of London A: Mathematical, Physical and Engineering Sciences*, volume 229, pages 317–345. The Royal Society, 1955.

[94] Masako Bando, Katsuya Hasebe, Akihiro Nakayama, Akihiro Shibata, and Yuki Sugiyama. Dynamical model of traffic congestion and numerical simulation. *Physical Review E*, 51(2):1035, 1995.

[95] Takashi Nagatani. The physics of traffic jams. *Reports on progress in physics*, 65(9):1331, 2002.

[96] Bernard Derrida, Eytan Domany, and David Mukamel. An exact solution of a one-dimensional asymmetric exclusion model with open boundaries. *Journal of Statistical Physics*, 69(3-4):667–687, 1992.

[97] Bernard Derrida, Martin R. Evans, Vincent Hakim, and Vincent Pasquier. Exact solution of a 1d asymmetric exclusion model using a matrix formulation. *Journal of Physics A: Mathematical and General*, 26(7):1493, 1993.

[98] G Schütz and E Domany. Phase transitions in an exactly soluble one-dimensional exclusion process. *Journal of statistical physics*, 72(1-2):277–296, 1993.

[99] National emergency fire center, http://www.nifc.gov/fireinfo.html.

[100] Michelle Nijhuis. Forest fires : Burn out. *Nature, 489, 352-354*, 2012.

[101] A. Ollero and L. Merino. Unmanned aerial vehicles as tools for forest-fire fighting. *Forest Ecology and Management*, 234(1):263, 2006.

[102] Luis Merino, Fernando Caballero, J Ramiro Martínez-de Dios, Joaquin Ferruz, and Aníbal Ollero. A cooperative perception system for multiple UAVs: Application to automatic detection of forest fires. *Journal of Field Robotics*, 23(3-4):165–184, 2006.

[103] David W. Casbeer, Derek B. Kingston, Randal W. Beard, and Timothy W. McLain. Cooperative forest fire surveillance using a team of small unmanned air vehicles. *International Journal of Systems Science*, 37(6):351–360, 2006.

[104] Harry Kesten. The critical probability of bond percolation on the square lattice equals 1/2. *Communications in mathematical physics*, 74(1):41–59, 1980.

[105] Geoffrey Grimmett. *Percolation*. Springer, 1999.

[106] Wendelin Werner. Part ii: Random planar curves and schramm-loewner evolutions. In *Lectures on probability theory and statistics*, pages 107–195. Springer, 2004.

[107] Gregory F Lawler. *Conformally invariant processes in the plane*. Number 114. American Mathematical Soc., 2008.

[108] Steffen Rohde and Oded Schramm. Basic properties of SLE. In *Selected Works of Oded Schramm*, pages 989–1030. Springer, 2011.

[109] Vincent Beffara. The dimension of the SLE curves. *The Annals of Probability*, pages 1421–1452, 2008.

[110] Stanislav Smirnov and Wendelin Werner. Critical exponents for two-dimensional percolation. *arXiv preprint math/0109120*, 2001.

[111] International Mathematical Union. List of fields medallists.

[112] Vincent Beffara. Hausdorff dimensions for SLE6. *Annals of probability*, pages 2606–2629, 2004.

[113] Gregory F Lawler, Oded Schramm, and Wendelin Werner. The dimension of the planar brownian frontier is 4/3. *arXiv preprint math/0010165*, 2000.

[114] J.M. Hammersley and D.J.A. Welsh. First-passage percolation, subadditive processes, stochastic networks, and generalized renewal theory. pages 61–110. Springer Berlin Heidelberg, 1965.

[115] Nathaniel D Blair-Stahn. First passage percolation and competition models. *arXiv preprint arXiv:1005.0649*, 2010.

[116] J.F.C. Kingman. The ergodic theory of subadditive stochastic processes. *Journal of the Royal Statistical Society. Series B (Methodological)*, 30(3):499–510, 1968.

[117] Robert Thomas Smythe and John C. Wierman. *First-passage percolation on the square lattice*, volume 671. Springer, 2006.

[118] Harry Kesten. Aspects of first passage percolation. Springer Berlin Heidelberg, 1986.

[119] Charles M. Newman and Marcelo S. T. Piza. Divergence of shape fluctuations in two dimensions. *Ann. Probab.*, 23(3):977–1005, 07 1995.

[120] Robin Pemantle and Yuval Peres. Planar first-passage percolation times are not tight. In *Probability and phase transition*, pages 261–264. Springer, 1994.

[121] J.T. Cox and Richard Durrett. Limit theorems for the spread of epidemics and forest fires. *Stochastic processes and their applications*, 30(2):171–191, 1988.

[122] Martin Hairer. Solving the KPZ equation. *arXiv preprint arXiv:1109.6811*, 2011.

[123] Jeremy Quastel. Introduction to KPZ. *Current developments in mathematics*, 2011:125–194, 2011.

[124] Ivan Corwin. The Kardar-Parisi-Zhang equation and universality class. *Random matrices: Theory and applications*, 1(01):1130001, 2012.

[125] Ivan Corwin, Jeremy Quastel, and Daniel Remenik. Renormalization fixed point of the KPZ universality class. *Journal of Statistical Physics*, 160(4):815–834, 2015.

[126] Russell Lyons. Random walks and percolation on trees. *The annals of Probability*, pages 931–958, 1990.